INTERNATIONAL SCIENTIFIC JOURNAL

MECHANIZATION IN AGRICULTURE & CONSERVING OF THE RESOURCES



Issue 2
2021

Year LXVII, ISSN print2603-3704, ISSN web 2603-3712

SCIENTIFIC TECHNICAL UNION OF MECHANICAL ENGINEERING
BULGARIAN ASSOCIATION OF MECHANIZATION IN AGRICULTURE

PUBLISHERS

SCIENTIFIC-TECHNICAL UNION OF MECHANICAL ENGINEERING "INDUSTRY-4.0"
BUGLARINA ASSOTIOATION OF AGRICULTURAL MACHINERY

ISSN (PRINT) 2603-3704, ISSN (ONLINE) 2603-3712

YEAR LXVII ISSUE 2 / 2021

EDITORIAL BOARD

Chief Editor: Prof. Dr. eng Miho Mihov
Responsible secretary: Corresp. Memb. Prof. D.Sc. Hristo Beloev

MEMBERS:
Acad. D.Sc. Jemal Katsitadze – Georgia
Acad. D.Sc. Sayakhat Nukeshev - Kazakhstan
Acad. D.Sc. Volodymyr Bulgakov – Ukraine
Acad. D.Sc.Valeriy Adamchuk – Ukraine
Prof. Abdullah Sessiz - Turkey
Prof. Abdulrahman Al-soqeer - Saudi Arabia
Prof. Alexander Tokarev - Russia
Prof. Alexey Vassilev - Russia
Assoc.Prof. Angel Trifonov - Bulgaria
Prof. Anupam Kumar Nema - India
Prof. Ayrat Valiev - Russia
Prof. Barbro Ulén - Sweden
Prof. Carmen Puia - Romania
Prof. Cheslav Vashkievich - Poland
Prof.Cumhur Aydinalp - Turkey
Prof. Daisuke Higaki - Japan
Prof. Davor Romic - Croatia
Prof. Domenico Pessina - Italy
Dr. Finn Plauborg - Denmark
Assoc.Prof. Ganka Baeva - Bulgaria
Assoc.Prof. Georgi Mitev - Bulgaria
Prof. Georgi Tassev - Bulgaria
Prof. Haiyan Huang - China
Prof. Hoang Thai Dai - Vietnam

MEMBERS:
Prof. Iliya Malinov - Bulgaria
Prof. PhD Iurie Melnic - Moldova
Assoc.Prof. Ivan Ivanov - Bulgaria
Prof. Jan Szczepaniak - Poland
Prof. Komil Muminov - Uzbekistan
Prof. Krassimira Georgieva - Bulgaria
Prof. Maja Manojlović - Serbia
Prof. Mihail Iliev - Bulgaria
Prof. Mohammad Salem Al-Hwaiti - Jordan
Prof. Papamichail Dimitris - Greece
Prof. Pavel Tlustos - Czech Republic
Prof. Plamen Kangalov - Bulgaria
Prof. Ralph Meissner - Germany
Prof. Rossen Ivanov - Bulgaria
Prof. Svetla Rousseva - Bulgaria
Prof. Tadeusz Pawłowski - Poland
Prof. Tamara Persikova - Belarus
Prof. Valentina Kundius - Russia
Prof. Wojciech Tanaś - Poland
Prof. Yerbol Sarkynov - Kazakhstan
Prof. Zdenko Tkach - Slovakia
Prof. Zinta Gaile - Latvia
Prof. Zivko Davchev - Macedonia

The journal "MECHANIZATION IN AGRICULTURE & CONSERVING OF THE RESOURCES " is continuer of the journals "Mechanized farming" (1948-1957), "Mechanization and electrification of agriculture" (1959-1980) and "Mechanization of agriculture " (1981-1991)

108, Rakovski Str., 1000 Sofia, Bulgaria
tel. (+359 2) 987 72 90, tel./fax (+359 2) 986 22 40,
office@stumejournals.com
WWW.STUMEJOURNALS.COM

C O N T E N T S

MECHANIZATION IN AGRICULTURE

Theory of vertical oscillations of a frontally mounted tops harvesting machine
Volodymyr Bulgakov, Yevhen Ihnatiev, Valerii Adamchuk, Vasil Mitkov, Vitaliy Movchan, Viktor Karapetrov 41

Research on reducing the impact of sloshing on the walls of a liquid manure tank of partially filled in a braking manoeuver
Gabriela Milian, Sorin-Ștefan Biriș, George Ipate, Valentin Vlăduț, Mihai Matache 47

Digital agriculture: the experience of ukraine
Derkach O.D., Mykhaylichenko Y.M., Makarenko D.O. 52

Evaluation of effects of biofuels blends on performance and emissions of diesel engine
Tomas Mickevič ius 57

Operational properties of diesel fuel with the addition of rapeseed oil esters
V. Tkachuk, Iu. Melnic, O. Rechun 61

Evaluation of the tire cross-section shape in relation with the traction force and traction efficiency of an agricultural tire
Radu Rosca, Petru Cârlescu, Ioan Țenu 64

CONSERVING OF THE RESOURCES

Study of the influence of the irrigation regime on the yield of short-fruited cucumbers grown in open areas under drip irrigation
Rumiana Kireva, Miho Mihov 68

Energy consumption and emissions of agricultural machinery for different arable land types
Ńimun Lončarević, Petar Ilinčić, Goran Ńagi, Zoran Lulić 71

Balkan endemic plants of Shutman Strict Nature Reserve in Kosovo - an inventory with chorological and life-form analyses
Haxhi Halilaj, Lirika Kupe, Xhavit Mala 75

Theory of vertical oscillations of a frontally mounted tops harvesting machine

Volodymyr Bulgakov[1], Yevhen Ihnatiev[2], Valerii Adamchuk[3], Vasil Mitkov[2], Vitaliy Movchan[2], Viktor Karapetrov[2]
[1]National University of Life and Environmental Sciences of Ukraine, 15, Heroyiv Oborony Str., Kyiv, 03041, Ukraine;
[2]Dmytro Motornyi Tavria State Agrotechnological University, 18, Khmelnytsky av., Melitopol, 72312, Zaporizhia region, Ukraine;
[3]National Scientific Centre "Institute for Agricultural Engineering and Electrification", Ukraine,
E-mail:vbugakov@meta.ua, yevhen.ihnatiev@tsatu.edu.ua

Abstract: *To establish influence of kinematic and constructive parameters of tops-harvesting machine on quality of a continuous cut of the massif of tops at oscillations in the longitudinal-vertical plane of its tops-cutting device at frontally mounted machine on a wheeled row-crop aggregate tractor. Used modeling methods based on higher mathematics, theoretical mechanics, solving a system of differential equations and compiling programs and numerical solutions on a PC. An equivalent scheme has been developed for a tops-harvester mounted on a wheeled tractor in front of it on its oscillations in the longitudinal-vertical plane, considering all the forces that arise, taking into account the kinematic excitation that occurs when moving along soil surface definitions also due to the elastic-damping properties of its support-copying wheels. For the specified equivalent scheme, on the basis of application of initial equations in the form of Lagrange of the 2nd kind, on the chosen generalized coordinates, the system of two nonlinear differential equations of oscillatory motion of the tops-harvesting machine is received. According to the analytical transformations, the solution of this system was obtained, which made it possible to obtain the final expressions for determining the amplitude and circular frequency of natural and forced oscillations of the tops-harvesting machine. Numerical calculations of the received expressions on the made program on the personal computer are carried out. According to the results of numerical simulation, the final expression was obtained, which allowed to determine the vertical displacements of the end of the rotary cutting unit during the oscillations of the topping machine in the longitudinal-vertical plane. Numerical calculations on the PC of the received expression gave the chance to construct graphic dependences which establish dependences of amplitude of the specified oscillations depending on constructive parameters of the tops-harvesting machine, and also characteristics of roughnesses of a soil surface and elastic-damping properties of copying wheels.*

KEY WORDS: SUGAR BEET, BEET TOPS, HARVESTING, ROTARY CUTTER, OSCILLATIONS, DIFFERENTIAL EQUATIONS, AMPLITUDE, FREQUENCY.

1. Introduction

High-performance and high-quality harvesting of sugar beet tops remains a very complex and urgent task of the beet industry. Recently, the most common in the world is a multi-stage method of tops harvesting, which is based on a continuous main cutting of the entire tops array (the width of the harvesting machine), its collection and transportation to a vehicle moving nearby, and then using individual copies of each heads of a root crop in a line, additional cleaning or additional pruning (or at the same time: and additional cleaning and additional cutting by various working bodies) of heads of root crops from the remains of a top is provided. Since these operations are carried out sequentially for sugar beet roots in the soil (ie on the root) and harvesting of the beet precedes the operation of digging beet roots from the soil, in the front position relative to the power tool (to the tractor - in the case of trailed tops harvesters or to the front of the frame of self-propelled beet harvesters). However, our studies show that in the process of work, front-mounted on the tractor topper makes movements in space, which are determined by the relief of the field surface, the translational speed of the tractor, the location of the copy wheels, the hitch system of the machine, etc., which significantly affects on the quality of this technological process. The use of pneumatic wheels as copiers - causes oscillations of the tops-harvesting machine in the vertical plane, which will have the greatest impact on the quality of the process - uniform cutting of the hitch from the root heads across the width, the most complete collection and transportation without loss.

2. Preconditions and means for resolving the problem

Analysis of recent research and publications. Despite the widespread use of front-mounted tops-harvesting modules of Western-made beet harvesters, as well as some designs of domestic front-mounted tops-harvesting machines, analytical studies of their oscillating motion have not yet been conducted. However, using the method described in [1], it is possible to build a calculated mathematical model of this machine, which will allow to study the influence of its design parameters on the movement of rows of sugar beet roots and soil surface irregularities.

The aim of the study. Determine the influence of the kinematic and structural parameters of the tops-harvesting machine mounted on the front of the wheeled tractor on the magnitude of the amplitude of oscillations in the longitudinal-vertical plane of the tops-cutting machine.

Research methods. This study used methods for constructing computational mathematical models of agricultural machines and machine units, based on the theoretical mechanics of higher mathematics and methods of compiling programs and numerical solutions of systems of differential equations on the PC.

3. Results and discussion

We have developed a new universal hitch harvester that performs the technological process on the principle of a mower-shredder, which is frontally mounted on a wheeled tractor. This machine uses a rotary tops cutter, in which the cutting knives are hinged on the drive drum, have an arcuate shape and rotating in the longitudinal-vertical plane, provide an non-supported, non-sensing cut of the main array of tops across the working width [9-11]. In Fig. 1 shows a structural and technological scheme of this machine, which cuts bundles and leaves of the bud, and plants that are in the beet field, and transports the cut mass into the basket of a vehicle moving nearby.

The technological process of collecting sugar beet tops takes place as follows. When moving a wheeled tractor (with narrow tires) on the rows of roots of sugar beets copy wheels 2, located in front of the movable frames 1, set the rotor 3 with knives to the desired height of cut. The knives have an arcuate shape, and are hinged on a cylindrical forming along the length of the rotor 3 in such a way as to ensure the overlap of the entire width of the grip. Knives rotate with high frequency thanks to what the cut of all array of a top is provided. The absolute speed of the ends of the blades of arcuate knives for cutting tops reaches 20...25 m/s, and for mowing other, in particular thick-stemmed crops - 40...50 m/s [11]. Cutted by arcuate knives moves to the upper part of the casing, where it falls on the auger conveyor, which moves the cut mass to the end part of the machine, after which the thrower 4 through the pipe 5 unloads it into the basket of the vehicle moving next to the impeller. The drive 6 of the tops harvester is carried out from the front shaft of the power take-off of the power tools (tractor). Finally, the technological process of tops harvesting occurs when cleaning the heads of the roots from the tops remnants installed behind tractor cleaner with a vertical drive shaft.

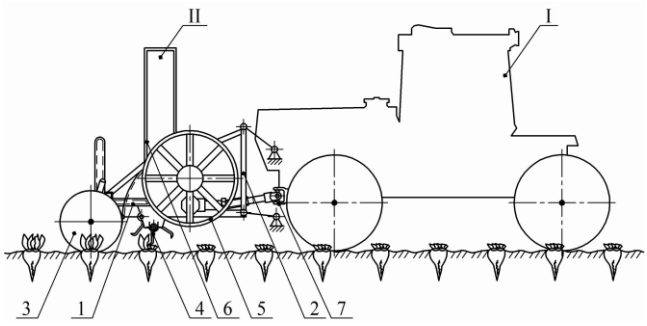


Fig. 1. *Structural and technological scheme of the machine-tractor unit for harvesting sugar beet tops:*
I - wheeled, arable and row-crop integrated tractor; II - front-mounted tops-harvesting machine: 1 - frame; 2 - hitch; 3 - the basic pneumatic copying wheel; 4 - rotary tops-cutting device; 5 - transporting working body; 6 - loading device; 7 - drive from a forward power take-off shaft

The main advantage of the rotary type tops-harvester is that, having only one working body - a rotor with knives, it provides a quality cut of the bulk of the tops and transporting it to a vehicle moving nearby, or can scatter the crushed tops on the harvested part of the beet field. The tops harvester is universal and has high reliability and can be used as a rotary mower (ie it can qualitatively cut various grasses up to 1 m high) [11]. The disadvantages of the rotary-type tops harvester include excessive grinding of the tops in the case of its collection in the basket of the vehicle, some contamination of the harvested tops with soil impurities, especially when working on dry soil and when adjusting the hitch cutter to a lower cutting height. When removing arcuate knives for sharpening, replacement, etc.).

To determine the influence of structural and kinematic parameters of the tops-harvesting machine mounted on the aggregate wheeled tractor on the magnitude of the amplitude of oscillations in the longitudinal-vertical plane of the tops-cutting apparatus, it is necessary to build its mathematical model.

To do this, we will analytically consider the motion of the tops-harvesting machine only in the longitudinal-vertical plane, ie we will build a mathematical model of oscillations of the tops-harvesting machine when moving along the irregularities of the soil surface in only one plane. On the basis of [1] we will first make an equivalent scheme of movement of a tops-harvesting machine mounted on a wheeled aggregate tractor in the longitudinal-vertical plane (Fig. 2).

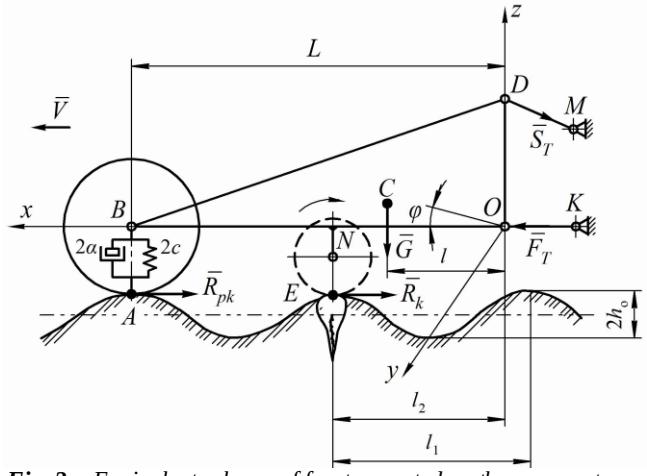


Fig. 2. *- Equivalent scheme of front-mounted on the aggregate integrated tractor topper*

As can be seen from Fig. 2, the tops harvester is connected to the tractor unit by means of two lower rods OK and one upper rod DM having hinges at points O, D, M and K. The radiuses of the copying wheels and the cutting device are denoted by R and R_1. The mass of the whole hitch-harvesting machine is denoted by M; the mass of the two copying wheels - through $m = m_1 + m_2$ (where m_1 - the mass of the first copying wheel m_2 - the mass of the second copying wheel). The mass m of both copy wheels is concentrated at a point B. The force of gravity of the hitch-harvesting machine applied in its center of mass (point C) is through G.

We attribute this dynamic system to a fixed Cartesian coordinate system $XOYZ$. The plane XOZ coincides with the longitudinal plane of the tops-harvesting machine and is a vertical plane to the field surface.

Pneumatic copying wheels are presented in the form of elastic damping models, which have a total stiffness factor $2c$ and a total damping factor 2α.

We believe that the wheels in general, when moving between rows of sugar beet crops crumple the upper (looser) layer of the soil surface, but move on irregularities that have a longitudinal profile close to the sinusoidal type.

In the first approximation, we can assume that the pneumatic copying wheel, moving between the rows of sugar beet crops and crumpling the upper loose layer of soil, is in contact with the unevenness of the field surface at a point A. The irregularities of the soil surface (in a smoothed form) can be represented as a harmonic function, ie an analytical expression of the following form [2]:

$$h = h_o\left(1 - \cos\frac{2\pi x}{l_1}\right), \qquad (1)$$

where h - the ordinate of the height of the unevenness of the soil surface, m, h_o - half the height of the unevenness of the soil surface, m, l_1 - the step of the unevenness of the soil surface, m; $x = V \cdot t$ - current coordinate, m; V - movement speed of the tops-harvesting machine, m/s.

Due to its weight, the tractor, when moving on the unevenness of the soil surface, even more significantly crumples the upper layer of soil with its running wheels, thus smoothing the existing irregularities, which reduces the amplitude of vertical oscillations of the center of mass of the tractor.

It is obvious that for these reasons, the vertical oscillations of the wheeled aggregate tractor are significantly reduced, however, do not disappear. Therefore, the hinges at points K and M (Fig. 2), as belonging to the tractor, also carry out vertical oscillations.

However, due to the presence of hinges at the points O and D the significant mass of the hitch, these oscillations are practically not transmitted to the hitch. The oscillations of the aggregate tractor cause only angular oscillations of the rods OK and DM connecting the topper to the tractor. Thus practically it is possible to consider that hinges O and D also do not carry out vertical oscillations, and drafts OK and DM also turn around points O and D accordingly, and other ends (hinges K and M) fluctuate independently together with a tractor. Due to the above, we can assume that the suspension points of the tops-harvesting machine (hinges O and D) move in the first approximation in a straight line and evenly.

Since the hitch is mounted in front of the aggregate tractor, its copy wheels are the first to perceive the existing irregularities of the field surface profile, which causes vertical angular oscillations of the frame of the topper around the point O. It is obvious that the angle φ of rotation of the frame of the hitch-picking machine around the point O significantly depends on the magnitude h of the roughness at the point A at which the copy wheel is at this time. Therefore, this angle in some approximation can be determined from the following expression:

$$h = L \cdot \varphi, \qquad (2)$$

where L is the distance from the point B of the axis of the copying wheel to the point O of suspension of the frame to the lower rod OK (Fig. 2).

From expression (2) we find the value of this angle φ:

$$\varphi = \frac{h}{L}, \tag{3}$$

or, given expression (1), we obtain the final expression for the angle φ:

$$\varphi = \frac{h_o}{L}\left(1 - \cos\frac{2\pi x}{l_1}\right). \tag{4}$$

Thus, the irregularities of the field surface are the kinematic exciter of the angular oscillations of the frame of the tops-harvester. However, the rotation of the machine frame around the point O can only make a moment of some force, the line of action of which does not pass through the point O. Such a force in this case is the force generated by these irregularities of the soil surface, which will obviously also change according to the same sinusoidal law as the inequalities of the field surface profile, ie, according to the following expression:

$$H = H_o\left(1 - \cos\frac{2\pi x}{l_1}\right), \tag{5}$$

where H_o is the amplitude of the specified force.

Obviously, this force is applied at a point A directed along the axis OZ, and its moment relative to the point O will be equal to:

$$M_o(H) = H_o L\left(1 - \cos\frac{2\pi x}{l_1}\right). \tag{6}$$

This force is an external active force acting on the frame of the topper from the surface of the field.

In addition to this main force, a horizontal reaction $\bar{R}_{pk}$ is applied at the point A, which is also, in general, variable and is more important when moving the wheel up the sinusoid of type (1) and less - when moving the copy wheel down the specified sinusoid. Also at the point E there is a reaction $\bar{R}_k$ of resistance to tops cutting by a rotary cutting device. Obviously, these two forces play an insignificant role in creating the angular oscillations of the machine frame compared to the force $\bar{H}$ and weight $\bar{G}$ of the topping machine itself.

The forces $\bar{R}_{pk}$ and $\bar{R}_k$ primarily create resistance to the movement of the topping machine on the field, and are directed opposite to the driving force $\bar{F}_T$ of the aggregate tractor. The force $\bar{S}_T$ also does not play a significant role in creating angular oscillations of the frame of the tops-harvesting machine due to its small size. The driving force $\bar{F}_T$ generally crosses the point O, and therefore only pushes forward the machine, without creating any moment of rotation of the frame of the topper around poin O.

Thus, only the force $\bar{H}$ (kinematic excitation) arising from the presence of surface irregularities and the force of gravity $\bar{G}$ of the tops-harvester play a significant role in creating angular oscillations of the frame of the topping machine. It should be noted that the line of action of these forces coincide with the direction of movement of their points of application, ie points A and C, accordingly.

However, it should be noted that the amplitude H_o of the force $\bar{H}$, as well as the reaction $\bar{R}_{pk}$ and $\bar{R}_k$ are unknown quantities. Therefore, it is not possible to use the basic law of dynamics to compile differential equations of motion of a tops-harvesting machine mounted on a wheeled aggregate tractor, taking into account the irregularities of the field surface profile. To solve this problem, it is advisable to use differential equations of motion in the form of Lagrange of the second kind [1].

To do this, we determine, first of all, the generalized coordinates of this dynamic system. The position of the center of mass of the topping machine (point C) in the longitudinal-vertical plane is completely determined by the independent coordinate φ. Since the center of mass of pneumatic copying wheels (point B) performs independent oscillating motions due to the elastic damping properties of copying wheels and the ordinates of the heights h of the unevenness of the soil surface is much smaller than the length L, we can assume that these oscillations can be determined by independent coordinates Z. Thus, the considered oscillating system can be reduced to two generalized coordinates:

$$\begin{aligned} q_1 &= \varphi, \\ q_2 &= Z. \end{aligned} \tag{7}$$

From the above it follows that the main influence on the vertical oscillations of the topping machine is exerted by the elastic-viscous resistance of the tires of the copying wheels, the weight of the topping machine and the magnitude of the surface irregularities. Thus, there is every reason to believe that the investigated mechanical system is affected only by potential forces and forces of viscous resistance. We use this circumstance when compiling differential equations of motion of the considered dynamic system on the basis of equations in the form of Lagrange of the II kind.

According to [12], if the considered dynamic system is affected only by potential forces and forces of viscous resistance, then the generalized force Q_i included in the Lagrange equation of the second kind are from the following expression:

$$Q_i = -\frac{\partial P}{\partial q_i} - \frac{\partial R}{\partial \dot{q}_i}, \tag{8}$$

where P is the potential energy of the dynamic system; R - dissipative function (Rayleigh function), q_i - generalized coordinate, $\dot{q}_i$ - generalized velocity.

The differential equations of Lagrange of the second kind in this case have the following form:

$$\frac{d}{dt}\left(\frac{\partial T}{\partial \dot{q}_i}\right) - \frac{\partial T}{\partial q_i} = -\frac{\partial P}{\partial q_i} - \frac{\partial R}{\partial \dot{q}_i}, \tag{9}$$

where T – kinetic energy of this dynamic system.

The dynamic system considered in this paper has two degrees of freedom, and hence, as noted above, two generalized coordinates $q_1 = \varphi$ and $q_2 = Z$. Therefore, as a result, we obtain a system of two differential equations in the form of Lagrange of the second kind:

$$\left.\begin{aligned} \frac{d}{dt}\left(\frac{\partial T}{\partial \dot{\varphi}}\right) - \frac{\partial T}{\partial \varphi} &= -\frac{\partial P}{\partial \varphi} - \frac{\partial R}{\partial \dot{\varphi}}, \\ \frac{d}{dt}\left(\frac{\partial T}{\partial \dot{Z}}\right) - \frac{\partial T}{\partial Z} &= -\frac{\partial P}{\partial Z} - \frac{\partial R}{\partial \dot{Z}}. \end{aligned}\right\} \tag{10}$$

Next, we define the components that are part of the system of equations (10). Thus, the kinetic energy T of this mechanical system consists of the kinetic energy of the translational motion of the tops-harvesting machine, the angular displacement of the machine frame around a point O and the kinetic energy of the vertical oscillations of its copying wheels. Therefore, it will be equal to

$$T = \frac{MV^2}{2} + \frac{I_{oy}\dot{\varphi}^2}{2} + \frac{m\dot{Z}^2}{2}, \tag{11}$$

where M is the mass of the hitch harvester, kg; V - speed of translational movement of the car, m / s; I_{oy} - moment of inertia of the machine about the axis OY, kg · m^2; m - weight of copying wheels, kg.

The potential energy P of this dynamic system will be equal to the work of the elastic forces of deformation of the pneumatic tires of both copy wheels and is therefore determined by the following expression:

$$P = c\left(L\varphi - Z\right)^2, \tag{12}$$

where c is the stiffness coefficient of the pneumatic tires of the wheels of the copying system, N / m; L - distance from the axis

of the suspension of harvesting machines (point O) to the axis of its copying wheels (point B), m.

The dissipative function R of this dynamic system is determined by the forces of viscous resistance, which are proportional to the speed of movement, and therefore equal to:

$$R = \alpha\left(L\dot{\varphi} - \dot{Z}\right)^2, \tag{13}$$

where α – damping factor of copying wheels, N · s / m.

These resistance forces are also due to the tires of the copying wheels of the hitchhiking machine.

We perform the necessary transformations due to the application of the equations of dynamics in the form of Lagrange of the II kind. To do this, we first find the necessary derivatives that are included in expression (10). For the first generalized coordinate φ, they will be equal:

$$\frac{\partial T}{\partial \dot{\varphi}} = I_{oy}\dot{\varphi}, \tag{14}$$

then

$$\frac{d}{dt}\left(\frac{\partial T}{\partial \dot{\varphi}}\right) = I_{oy}\ddot{\varphi}. \tag{15}$$

Given that:

$$\frac{\partial T}{\partial \varphi} = 0, \tag{16}$$

then

$$\frac{d}{dt}\left(\frac{\partial T}{\partial \dot{\varphi}}\right) - \frac{\partial T}{\partial \varphi} = I_{oy}\ddot{\varphi}. \tag{17}$$

Similarly:

$$\frac{\partial P}{\partial \varphi} = 2cL\left(L\varphi - Z\right), \tag{18}$$

and

$$\frac{\partial R}{\partial \dot{\varphi}} = 2\alpha L\left(L\dot{\varphi} - \dot{Z}\right). \tag{19}$$

For the second generalized coordinate Z we find similar expressions. They will be equal:

$$\frac{\partial T}{\partial \dot{Z}} = m\dot{Z}, \tag{20}$$

then

$$\frac{d}{dt}\left(\frac{\partial T}{\partial \dot{Z}}\right) = m\ddot{Z}. \tag{21}$$

Further:

$$\frac{\partial T}{\partial Z} = 0, \tag{22}$$

and

$$\frac{\partial P}{\partial Z} = 2c\left(Z - L\varphi\right), \tag{23}$$

in accordance:

$$\frac{\partial R}{\partial \dot{Z}} = -2\alpha\left(L\dot{\varphi} - \dot{Z}\right). \tag{24}$$

Substitute the values of expressions (14) - (24) into the system of equations (10), we obtain:

$$\left.\begin{aligned} I_{oy}\ddot{\varphi} + 2cL\left(L\varphi - Z\right) + 2\alpha L\left(L\dot{\varphi} - \dot{Z}\right) = 0, \\ m\ddot{Z} + 2c\left(Z - L\varphi\right) - 2\alpha\left(L\dot{\varphi} - \dot{Z}\right) = 0. \end{aligned}\right\} \tag{25}$$

The obtained system (25), consisting of two differential equations, simulates the oscillations of the center of mass of the toping machine (point C) in the longitudinal-vertical plane and the oscillations of the center of the copying wheel (point B).

Let's convert system (25) to this form:

$$\left.\begin{aligned} I_{oy}\ddot{\varphi} + 2cL^2\varphi - 2cLZ + 2\alpha L^2\dot{\varphi} - 2\alpha L\dot{Z} = 0, \\ m\ddot{Z} + 2cZ - 2cL\varphi - 2\alpha L\dot{\varphi} + 2\alpha\dot{Z} = 0, \end{aligned}\right\} \tag{26}$$

or finally:

$$\left.\begin{aligned} \ddot{\varphi} + \frac{2cL^2}{I_{oy}}\varphi - \frac{2cL}{I_{oy}}Z + \frac{2\alpha L^2}{I_{oy}}\dot{\varphi} - \frac{2\alpha L}{I_{oy}}\dot{Z} = 0, \\ \ddot{Z} + \frac{2c}{m}Z - \frac{2cL}{m}\varphi - \frac{2\alpha L}{m}\dot{\varphi} + \frac{2\alpha}{m}\dot{Z} = 0. \end{aligned}\right\} \tag{27}$$

Thus, a system of nonlinear differential equations (27) with respect to unknown generalized coordinates φ and Z is obtained, which is a calculated mathematical model of the motion of a tops-harvester mounted on an aggregate wheel integrated tractor.

The system of differential equations (27) with initial conditions can be solved by a program compiled for this purpose on a PC by the adapted Runge-Kutta method in the MathCAD system.

However, the obtained mathematical model is quite general. It is suitable for the description of vertical oscillations of the tops-harvesting machine mounted on a tractor in front when the law of change of a profile of roughnesses of a surface of a field is unknown.

In this case, the law of change of the profile of irregularities of the soil surface is known and is given by expression (1). Based on it, the above expression (4), which describes the law of change of the angular coordinate φ during the translational movement of the tops-harvesting machine. Therefore, in this particular case, expression (4) is a solution of the system of differential equations (27). Substituting this expression into one of the equations of system (27), we obtain a differential equation to determine the law of change of coordinates Z.

Substitute expression (4) into the second differential equation of system (27). To do this, write expression (4) as follows:

$$\varphi = \frac{h_o}{L}\left(1 - \cos\frac{2\pi Vt}{l_1}\right). \tag{28}$$

Differentiating expression (28) over time t we obtain:

$$\dot{\varphi} = \frac{2\pi h_o V}{L \cdot l_1} \cdot \sin\frac{2\pi Vt}{l_1}. \tag{29}$$

Substituting expressions (28) and (29) into the second equation of system (27), we obtain the following differential equation with respect to the unknown function $Z(t)$:

$$\begin{aligned} &\ddot{Z} + \frac{2\alpha}{m}\dot{Z} + \frac{2c}{m}Z = \\ &= \frac{4\pi\alpha h_o V}{m l_1}\sin\frac{2\pi Vt}{l_1} - \frac{2ch_o}{m}\cos\frac{2\pi Vt}{l_1} + \frac{2ch_o}{m} \end{aligned}. \tag{30}$$

Equation (30) is a linear differential equation of the second order with constant coefficients with the right part.

Its general solution is known to consist of a general solution of a linear homogeneous equation and a partial solution of an inhomogeneous equation, the form of which is determined by the form of the right-hand side of equation (30).:

$$Z = Z_{adn.} + Z^*. \tag{31}$$

We first find the general solution $Z_{odn.}$ of the homogeneous equation:

$$\ddot{Z} + \frac{2\alpha}{m}\dot{Z} + \frac{2c}{m}Z = 0. \tag{32}$$

The characteristic equation of homogeneous equation (32) has the following form:

$$k^2 + \frac{2\alpha}{m}k + \frac{2c}{m} = 0. \tag{33}$$

The roots of this characteristic equation will take the following value:

$$\begin{aligned} k_1 &= -\frac{\alpha}{m} + \sqrt{\frac{\alpha^2}{m^2} - \frac{2c}{m}}, \\ k_2 &= -\frac{\alpha}{m} - \sqrt{\frac{\alpha^2}{m^2} - \frac{2c}{m}}. \end{aligned} \tag{34}$$

Since in a real dynamic system, ie in our particular case, the values under the roots in expressions (34) must be:

$$\frac{\alpha^2}{m^2}-\frac{2c}{m}<0,$$

then the roots k_1 and k_2 will be complex numbers, and therefore the general solution of the homogeneous differential equation (32) will look like this:

$$Z_{odn.}=e^{-\frac{\alpha}{m}t}\left(C_1\sin\sqrt{\frac{\alpha^2}{m^2}-\frac{2c}{m}}\cdot t+C_2\cos\sqrt{\frac{\alpha^2}{m^2}-\frac{2c}{m}}\cdot t\right), \quad (35)$$

where C_1 and C_2 – arbitrary constants.

We will look for the partial solution Z^* of the inhomogeneous differential equation (30) in the following form:

$$Z^*=M\cdot\sin\frac{2\pi Vt}{l_1}+N\cdot\cos\frac{2\pi Vt}{l_1}+R, \quad (36)$$

where M, N, R – unknown coefficients.

These coefficients are found by the method of indeterminate coefficients. To do this, we perform a twofold differentiation of expression (36). We have:

$$\dot{Z}^*=M\frac{2\pi V}{l_1}\cdot\cos\frac{2\pi V}{l_1}t-N\frac{2\pi V}{l_1}\cdot\sin\frac{2\pi V}{l_1}t, \quad (37)$$

$$\ddot{Z}^*=-M\frac{4\pi^2V^2}{l_1^2}\cdot\sin\frac{2\pi V}{l_1}t-N\frac{4\pi^2V^2}{l_1^2}\cdot\cos\frac{2\pi V}{l_1}t. \quad (38)$$

Substituting expressions (36), (37) and (38) into the differential equation (30), we obtain:

$$\begin{aligned}&-M\frac{4\pi^2V^2}{l_1^2}\cdot\sin\frac{2\pi V}{l_1}t-N\frac{4\pi^2V^2}{l_1^2}\cdot\cos\frac{2\pi V}{l_1}t+\\&+\frac{2\alpha}{m}\left(M\frac{2\pi V}{l_1}\cdot\cos\frac{2\pi V}{l_1}t-N\frac{2\pi V}{l_1}\cdot\sin\frac{2\pi V}{l_1}t\right)+\\&+\frac{2c}{m}\left(M\cdot\sin\frac{2\pi Vt}{l_1}+N\cdot\cos\frac{2\pi Vt}{l_1}+R\right)=\\&=\frac{4\pi\alpha h_oV}{ml_1}\cdot\sin\frac{2\pi V}{l_1}t-\frac{2ch_o}{m}\cdot\cos\frac{2\pi V}{l_1}t+\frac{2ch_o}{m}.\end{aligned} \quad (39)$$

In expression (39) we equate the coefficients for the same functions in the left and right parts of the specified expression.

As a result, we obtain the following system of three algebraic linear equations with respect to unknowns M, N and R:

$$\left.\begin{aligned}&\left(\frac{2c}{m}-\frac{4\pi^2V^2}{l_1^2}\right)\cdot M-\frac{4\pi\alpha V}{ml_1}\cdot N=\frac{4\pi\alpha h_oV}{ml_1},\\&\frac{4\pi\alpha V}{ml_1}\cdot M+\left(\frac{2c}{m}-\frac{4\pi^2V^2}{l_1^2}\right)\cdot N=-\frac{2ch_o}{m},\\&\frac{2c}{m}\cdot R=\frac{2c}{m}h_o.\end{aligned}\right\} \quad (40)$$

From the last equation of system (40) we find:

$$R=h_o. \quad (41)$$

We find the main determinant of the system, consisting of coefficients for the unknowns M and N the first two equations of the system (40). We have:

$$\begin{aligned}\Delta&=\begin{vmatrix}\frac{2c}{m}-\frac{4\pi^2V^2}{l_1^2} & -\frac{4\pi\alpha V}{ml_1}\\ \frac{4\pi\alpha V}{ml_1} & \frac{2c}{m}-\frac{4\pi^2V^2}{l_1^2}\end{vmatrix}=\\&=\left(\frac{2c}{m}-\frac{4\pi^2V^2}{l_1^2}\right)^2+\left(\frac{4\pi\alpha V}{ml_1}\right)^2\end{aligned}. \quad (42)$$

Next, calculate the determinant Δ_M. It will be equal to:

$$\Delta_M=\begin{vmatrix}\frac{4\pi\alpha h_oV}{ml_1} & -\frac{4\alpha\pi V}{ml_1}\\ -\frac{2ch_o}{m} & \frac{2c}{m}-\frac{4\pi^2V^2}{l_1^2}\end{vmatrix}=-\frac{16\pi^3\alpha V^3h_o}{ml_1^3}. \quad (43)$$

After that we find the determinant Δ_N. It will be equal to:

$$\begin{aligned}\Delta_N&=\begin{vmatrix}\frac{2c}{m}-\frac{4\pi^2V^2}{l_1^2} & \frac{4\pi\alpha h_oV}{ml_1}\\ \frac{4\alpha\pi V}{ml_1} & -\frac{2ch_o}{m}\end{vmatrix}=\\&=-\frac{2ch_o}{m}\left(\frac{2c}{m}-\frac{4\pi^2V^2}{l_1^2}\right)-\frac{16\pi^2\alpha^2V^2h_o}{m^2l_1^2}\end{aligned}. \quad (44)$$

The coefficients M and N can be found using Cramer's rule. Then, given expressions (31), (35) and (36), we write the general solution of the differential equation (30):

$$\begin{aligned}Z=&e^{-\frac{\alpha}{m}t}\left(C_1\sin\sqrt{\frac{\alpha^2}{m^2}-\frac{2c}{m}}\cdot t+C_2\cos\sqrt{\frac{\alpha^2}{m^2}-\frac{2c}{m}}\cdot t\right)+\\&+M\cdot\sin\frac{2\pi V}{l_1}t+N\cdot\cos\frac{2\pi V}{l_1}t+R.\end{aligned} \quad (45)$$

Arbitrary constant integrations C_1 and C_2 are defined from the following initial conditions:

at $t=0$: $z=0$, $\dot{z}=0$. (46)

To do this, we differentiate expression (45) over time. We have:

$$\begin{aligned}\dot{Z}=&-\frac{\alpha}{m}e^{-\frac{\alpha}{m}t}\left(C_1\sin\sqrt{\frac{\alpha^2}{m^2}-\frac{2c}{m}}\cdot t+C_2\cos\sqrt{\frac{\alpha^2}{m^2}-\frac{2c}{m}}\cdot t\right)+\\&+e^{-\frac{\alpha}{m}t}\cdot\left(C_1\sqrt{\frac{\alpha^2}{m^2}-\frac{2c}{m}}\cdot\cos\sqrt{\frac{\alpha^2}{m^2}-\frac{2c}{m}}\cdot t\right.\\&\left.-C_2\sqrt{\frac{\alpha^2}{m^2}-\frac{2c}{m}}\cdot\sin\sqrt{\frac{\alpha^2}{m^2}-\frac{2c}{m}}\cdot t\right)+\\&+M\cdot\frac{2\pi V}{l_1}\cos\frac{2\pi V}{l_1}t-N\cdot\frac{2\pi V}{l_1}\sin\frac{2\pi V}{l_1}t.\end{aligned} \quad (47)$$

Substitute the values of the initial conditions (46) into expressions (45) and (47), we obtain the following system of linear equations for unknowns C_1 and C_2:

$$\left.\begin{aligned}&C_2+N+R=0,\\&-\frac{\alpha}{m}C_2+C_1\sqrt{\frac{\alpha^2}{m^2}-\frac{2c}{m}}+\frac{2\pi V}{l_1}M=0.\end{aligned}\right\} \quad (48)$$

From the system of equations (51) we find:

$$\begin{aligned}C_1&=-\frac{\frac{\alpha}{m}(N+R)+\frac{2\pi V}{l_1}M}{\sqrt{\frac{\alpha^2}{m^2}-\frac{2c}{m}}},\\C_2&=-(N+R).\end{aligned} \quad (49)$$

Substituting the values of arbitrary constants (49) into expression (47), we finally find the general solution of the differential equation (30):

$$\begin{aligned}z=&e^{-\frac{\alpha}{m}t}\left(-\frac{\frac{\alpha}{m}(N+R)+\frac{2\pi V}{l_1}M}{\sqrt{\frac{\alpha^2}{m^2}-\frac{2c}{m}}}\cdot\sin\sqrt{\frac{\alpha^2}{m^2}-\frac{2c}{m}}\cdot t-\right.\\&\left.-(N+R)\cdot\cos\sqrt{\frac{\alpha^2}{m^2}-\frac{2c}{m}}\cdot t\right)+M\cdot\sin\frac{2\pi V}{l_1}t+\\&+N\cdot\cos\frac{2\pi V}{l_1}t+R.\end{aligned} \quad (50)$$

Expression (50) determines the law of translational vertical oscillations of the center of mass of the copying wheels (point B) during the movement of the tops harvesting machine on the irregularities of the soil surface, given by analytical expression (1).

4. Conclusions

1. A new machine-tractor unit has been developed, in which a tops-harvesting machine, front-mounted on a wheeled integrated tractor, performs a continuous sensingless cut of the main massif of tops along the entire working width.

2. Front-mounted on the aggregating tractor, the tops-harvesting machine performs, in the process of work, angular oscillations in the longitudinal-vertical plane when moving along the unevenness of the soil surface, which are kinematic perturbings, as well as independent oscillating movements due to elastic-damping properties of beets and have the corresponding coefficients of rigidity and damping.

3. For the considered dynamic system the equivalent scheme of movement in the longitudinal-vertical plane with designation of all forces operating on it, the constructive sizes and the set coordinate system, and also a choice of the generalized coordinates is constructed.

4. Based on the initial equations of dynamics in the form of Lagrange of the 2nd kind, a system of two nonlinear differential equations of oscillations of a tops-harvesting machine mounted on an wheeled integrated tractor with respect to unknown generalized coordinates φ and Z is obtained, which is a calculated mathematical model of its motion.

5. Analytical transformations made it possible to obtain a general solution of the differential equation, to find the law of translational vertical oscillations of the center of mass of copying wheels during the movement of the tops harvesting machine on the surface irregularities, to find finite expressions of the amplitude of natural and forced oscillations of mass center of copying wheels. oscillations.

5. References

1. Vasilenko P.M. Vvedenie v zemledelcheskuju mekhaniku. – Kiev: Selkhozobrazovanie, 1996. – 252 p. (in Russian)

2. Morozov B.I., Gringauz N.M. Calculation of the movement of a wheeled vehicle on an uneven road. – Mechanization and electrification of socialist agriculture. – 1969. – № 7. – C. 11-14. (In Russian)

3. Vasilenko I.F. Theory of cutting devices of reaping machines. Proceedings of VISKHOM. – Moscow: 1937, №5. – pp.7-14. (In Russian)

4. Reznik N.E. The theory of cutting with a blade and the basics of calculating cutting devices. – Moscow: Mashinostroyeniye, 1975. – 311 p. (In Russian)

5. Bosoy E.S. Cutting devices of harvesting machines. Theory and calculation. - Moscow: Mashinostroyeniye, 1967. – 167 p. (In Russian)

6. Tatyanko N.V. Calculation of working bodies for cutting sugar tops. Tractors and agricultural machinery. – 1962, №11. – pp. 18-21. (In Russian)

7. Ihnatiev Y. Theoretical substantiation of topping parameters without sugar beet head copying. IV International scientific Congress "Agricultural machinery". – Varna. – Issue 18 (181). Vol. 1, 22-25 june 2016. – P. 55 – 58.

8. Bulgakov V., Adamchuk V., Nozdrovicky L., Ihnatiev Ye.Theory of vibrations of sugar beet leaf harvester front-mounted on universal tractor. Acta Technologica Agriculturae. – 2017. – Issue 4. – pp. 96 – 103.

9. Adamchuk V., Bulgakov V., Korenko M., Boris A., Boris M. Laboratory and field equipment workingout and the results of experimental studies of pre-harvesting sugar beet field conditions. Mechanization in agriculture. – Sofia, Bulgaria, 2016. – Issue 1. – pp. 3 – 5.

10. Bulgakov V., Pascuzzi S., Arak M., Santoro F., Anifantis A.S., Ihnatiev Y., Olt J. An experimental investigation of performance levels in a new root crown cleaner. Agronomy Research. 2019. Vol. 17. No 2. p.p. 358–370.

11. Bulgakov V.M. Sveklouborochnye mashiny. Monografija. – Kiev: Agrarna nauka, 2011. – 351 p (in Ukrainian)

12. Butenin N.V., Lunc Ja.L., Merkin D.R. Kurs teoreticheskoj mekhaniky. Tom II. Dynamika. – Moskva: Nauka, 1985. – 496 p. (in Russian)

Research on reducing the impact of sloshing on the walls of a liquid manure tank of partially filled in a braking manoeuver

Gabriela Milian[1,*], Sorin-Ștefan Biriș[2] , George Ipate[2], Valentin Vlăduț[1], Mihai Matache[2]

[1]INMA Bucharest, Testing Department, 013813, Romania
[2]University "Politehnica" Bucharest, Biotechnical System Department, 060042, Romania
gabrielamilian44@gmail.com*

Abstract: *The appearance of violent liquid sloshing on the walls of the tank can cause great problems to those who handle these liquid manure tank that spread coarse residues from animal farms. This violent sloshing occurs when the tank is partially filled with liquid product. This movement of the liquid inside the tank imposes pressure along the walls when the tank is not full, thus causing instability on the entire structure during its movement on agricultural land. In this work was used a tanker that transports and spreads on the ground animal manure from a cattle farm. The modelling of the tank was done with the Solidworks program and the numerical analysis of the impact of the liquid tension distributions on the tank through with Ansys-CFX. The tanker moves at a constant speed (v=5m/s), after which it is subjected to a braking manoeuver. In this paper is analyzed behaviour and effect the impact of tensions distribution on the walls of the tank, when it has or does not have baffles.*

Keywords*: STRESS DISTRIBUTION, ANSYS CFX, BAFFLE, SLOSHING LIQUID*

1. Introduction

The appearance of violent liquid sloshing on the walls of the tank can cause great problems to those who handle these liquid manure tank that spread coarse residues from animal farms. This violent sloshing occurs when the tank is partially filled with liquid product. This movement of the liquid inside the tank imposes pressure along the walls when the tank is not full, thus causing instability on the entire structure during its movement on agricultural land. So when the sloshing of the liquid in the tank is strong there is an increase in the roll moment which can cause to rollover the vehicle, leading to the instability and safety of the vehicle as well as that of the operator.[1] Further research shows that containers carrying liquid products (eg: liquid manure, etc.), partially filled that are subject to accelerated excitations present the phenomenon of sloshing, which have a negative effect on the stability and safety of these vehicles. Therefore, the movement of liquids in rigid containers has been the subject of many studies in recent decades. Horizontal excitations (eg deceleration) of the contained liquids can lead to substantial slosh-induced loads, which can affect the dynamic behaviour of the structures due to the strength of the liquid. [2] For example, Ranganathan, Ying, and Miles analyzed liquid sloshing in partially filled tanks as the motion of an equivalent mechanical pendulum system that occurs during a given steering manoeuvre. Making this analogy to be able to determine the dynamic behaviour of the vehicle during an imposed manoeuvre [3]. When a fluid moves and interacts with its wall tank, the dynamic pressures of such an interaction can cause large deformations in the container wall as well as in the supporting structure. In studies using the equivalent mechanical model to simulate liquid sloshing, the system parameters are determined so that the natural frequency of the equivalent model is equal to the first natural frequency of the original system, as in our case. There are two major issues that arise in a sloshing calculation approach. These are the limit conditions in motion at the interface of the fluid tank and the nonlinear motion of the free surface. Alternatively, the quasi-static method was used to determine the forces and moments of the fluids up to the tank walls due to liquid sloshing. For example, Rakheja, Sankar and Ranganathan, using the steady-state model for fluid movement, developed a quasi-steady state yaw/roll model, in order to find out the effects of tank design parameters on the rollover threshold of partially filled tank vehicles [4]. And Wu and Lin, taking their studies, continued to investigate what happens if the vehicle is multi-axle-steering, in order to identify the directional response at a constant forward speed in a constant direction [5]. Using this method, steady-state load shift, and directional responses of the tank vehicle can be achieved, but the effect of transient liquid slosh on vehicle dynamics cannot be predicted. Saeedi, Kazemi, and Azadi they researched the dynamic interaction of the liquid cargo with the vehicle was investigated in this research by integrating a quasi-static liquid sloshing model [6]. Over the years, the problem of sloshing has been studied by an impressive number of researchers, using different methods and techniques. Salemet et al. investigated that partially filled tanks that undergo turns or lane change maneuvers have a lower overturning threshold than any other type of vehicle [7] Celebi et al. investigated nonlinear liquid sloshing inside a partially filled rectangular tank assuming that the fluid is homogeneous, isotropic, viscous, Newtonian, and has limited compressibility [7]. Frandsen studied a completely nonlinear differential finite element model based on viscous flow equations [7]. The inherent liquid viscosity reduces the sloshing height in the liquid storage tanks. Scarci, Chiba and collaborators studied the effects of liquid viscosity from different points of view. In practice, the viscosity of the liquid does not have a significant effect on the dynamic characteristics of the liquid storage tanks. Therefore, other methods should be introduced to suppress dynamic sloshing tasks. In this regard, several devices, such as circular tankers, floating plates, etc., have been studied and used primarily to reduce the effects of sloshing. Baffles installed in tanks can also play the role of sloshing suppression devices, which can produce additional nonlinear damping due to cross-flow, resulting in either a separation of the flow or a flow in the form of a jet. Recently, using the sloshing linearization theory and the domain decomposition method, Faltinsen and Timokha made an analytical approximation of the natural ways of producing sloshing in a rectangular tank with a lamella-type baffle in the middle of the tank. Kyoung et al observed that a nonlinear sloshing problem can be simulated numerically [2]. Akyildiz et al. analuzed pressure variations and three-dimensional effects of sloshing forces in a partially filled rectangular tank moving both numerically and experimentally. Liu et al. used a numerical model to study the three-dimensional (3D) model of liquid sloshing in a tank with baffles. Eswaran et al. studied sloshing waves (sloshing waves) for tanks with and without droughts. Panigrahy et al. conducted a series of experiments in a liquid sloshing system developed to estimate the pressure developed on the tank walls and the free movement of water from the static static level. Khezzar et al. designed a test facility to study the phenomenon of water sloshing from a rectangular tank subjected to a sudden impact. Zheng et al. studied a two-phase internal fluid flow model by solving the Navier-Stokes equations using this study to investigate the phenomena of liquid sloshing in a cubic tank with different baffle configurations under harmonic-motion excitation. Hasheminejad et al. studied transient two-dimensional sloshing in non-deformable horizontal circular cylindrical vessels, filled with invisibly incompressible fluids at variable depths and subjected to subsequent time-dependent variable accelerations [2].

In addition to all these studies on the production and effects on vehicle dynamics of liquid sloshing while moving the vehicle, there are also the characteristics of manure that changes by processing, including anaerobic digestion.

The main objective of this paper is to determine the effects of the sloshing load (sloshing stresses) on the fluid tank using or not baffle.

2. Materials and Methods

The design of equipment that transports and stores liquid manure requires a detailed understanding of the movement of the liquid during sloshing.

The pressure distribution on the tank wall is a special concern because the local temporal peaks of the sloshing, which can reach the same as the road tank twice the value of the rigid load. In road tanks, the free surface of the liquid can experience large displacements even for very small movements of the tank, leading to stability problems. [1]

The literature review reveals that many studies have been conducted mainly on rectangular tanks both by numerical and experimental approach, and very few scale models of cylindrical tanks, which carry liquids. So, in this paper, the effect of mounting a baffle configuration or removing it has been studied. The fluid structure interface was analyzed using two-dimensional nonlinear CFD analysis of a scale model of a tank carrying liquid manure from farmers.

The real model of the simulated tank carrying liquid manure is found in Fig.1, also represented in 3D after being modeled in Solidworks software in Fig.2



***Fig.1**. The real model of the liquid manure tank simulate*

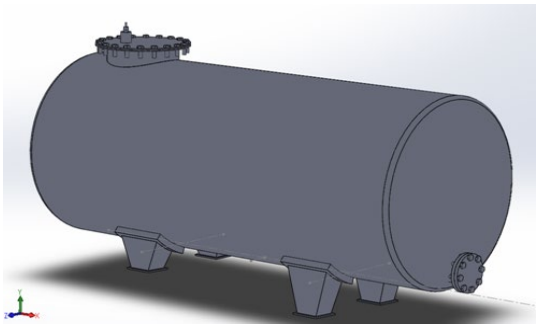


***Fig.2**. The real model of the liquid manure tank simulate in Solidworks*

The research was carried out on a tank with a volume of 4000l, with a circular section with a diameter of d = 1420mm and a length L = 3400mm, subjected to two numerical simulations, once a tank with a random configuration was mounted inside the tank (see Fig.3) and in second without it . The thickness of the tank wall and the baffle was 3 mm, made of cold rolled steel, with standardized characteristics resistant to traction and corrosion. The real-scale constructive parameters of the numerically simulated tank model (geometric shape of the tank) were shown in Fig.4. The dimensions and configuration of the boiler mounted in the middle of the tank were highlighted in Fig.3. From the sketch in Fig.3, it appears that the baffle has a circular shape, with a diameter equal to that of the tank. Being welded on the wall of the vessel and perforated in the vertical direction, having two holes of different sizes, thus dividing the tank into two equal compartments. In order to study the effects of stresses on the tank walls due to sloshing, the interface between the liquid and the structure using the Ansys-CFX numerical simulation software was considered, after the three-dimensional model with Solidworks was made in the first stage.

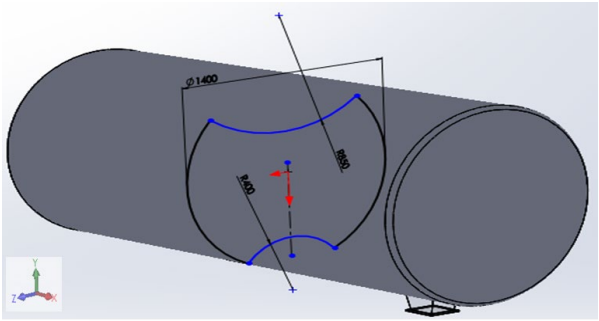


***Fig.3** The configuration of the baffle mounted inside the tank*

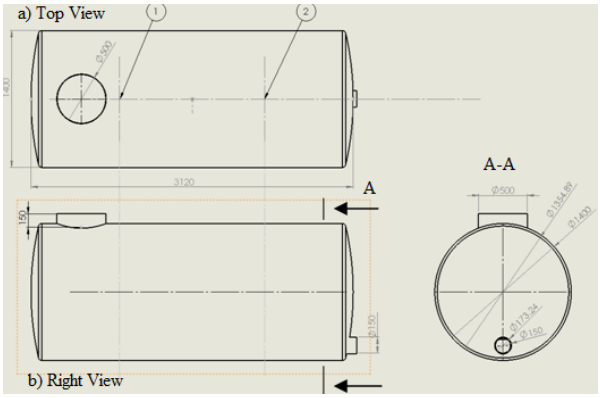


***Fig.4** The real-scale constructive parameters of the numerically simulated tank model; a)- top view; b)-right view (A-A section view);1- front axle support;2- back axle support.*

The first simulation is done without baffles and the fluid can move freely, so as to find the maximum pressure exerted by the fluid. A sudden force is applied to the tank due to the braking maneuver and takes 6 seconds to stop completely. When a tank is subjected to linear instability, a series of waves are formed in the liquid and thus the liquid moves and therefore wield pressure on the walls of the tank. For the second simulation, a vertical baffle is used, perforated at the top and bottom of the tank (see fig.3). The movement of the fluid during the braking maneuver was shown in Fig.4.

The sloshing liquid inside the partially filled tank is considered rigid, with an oxyz cartesian coordinate system as shown in Fig 5.

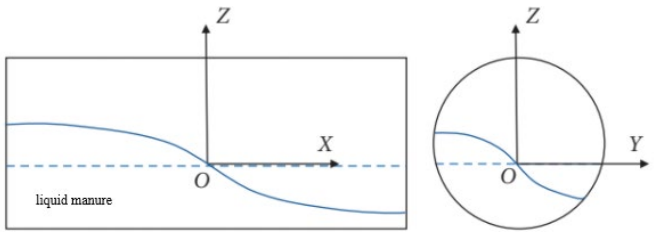


***Fig.5** Coordinate system of liniar sloshing liquid manure of the tank with baffle or unbaffle during the braking maneuver*

For the numerical simulation of the two cases with or without baffles, the liquid was considered incompressible, inviscid and irrational, according to the linear flow potential theory, thus the velocity field of the fluid in the whole fluid range can be described by a velocity potential φ which satisfies the conditions of the continuity equation, i.e.:

$$\frac{\partial \varphi^2}{\partial x^2} + \frac{\partial \varphi^2}{\partial y^2} + \frac{\partial \varphi^2}{\partial z^2} = 0 \qquad (1)$$

And free surface y = η, the kinematic (2) and dynamic free surface boundary conditions have to be satisfied:

$$\frac{\partial \varphi^2}{\partial n} - \nabla\eta \cdot \nabla\varphi = \frac{\partial \eta}{\partial t}, \quad (2)$$

$$\frac{\partial \varphi}{\partial t} + g\eta + \frac{1}{2}(\nabla\varphi^2) = 0 \quad (3)$$

The above boundary conditions are nonlinear. Higher-order terms come from the convective derivatives in equation (2) and the kinetic energy term in equation (3). For linear sloshing problems, the free surface elevation is considered to be small. Thus, the higher-order terms in the above equations are neglected. The boundary conditions are linearized as below at the mean water level as η⟶0:

$$\frac{\partial \varphi}{\partial y} = \frac{\partial \varphi}{\partial t} \quad (4)$$

$$\frac{\partial \varphi}{\partial t} + g\eta = 0 \quad (5)$$

When violent sloshing takes place, the contribution of the higher-order terms should not be neglected. Further, the solid-wall boundary condition is satisfied on the rigid tank wall:

$$\frac{\partial \varphi}{\partial n} = v_n \quad (6)$$

where η is the free surface elevation and v_n is the velocity of rigid body motion on body surface.

In addition, since the fluid domain in the sloshing problem is a confined space and the free surface is non-breaking in potential flow problems, the fluid in the tank should satisfy overall fluid volume conservation, which requires the integration of free surface elevation on the mean water level to be zero:

$$\int \eta dx dy = 0 \quad (7)$$

The boundary value problem (1) and (4)–(7) is solved analytically by separating the total velocity potential into three parts, namely, the rigid body motion, the liquid velocity induced by free surface elevation applying the Navier-Stokes and mass equilibrium equations.

By integrating both sides of the equation and utilizing the orthogonality property, the sloshing in liquid tank can be expressed by a series of modal equations as [8].

$$\ddot{\beta}_j + \omega_j^2 \beta_j = K_j(t), \quad (8)$$

$$K_j(t) = -\frac{\lambda_{1j}}{\mu_j}(\ddot{\eta}_1(t) - g\eta_5(t)) - \frac{\lambda_{2j}}{\mu_j}(\ddot{\eta}_2(t) + g\eta_4(t)) - \sum_{k=4}^{6}\frac{\ddot{\eta}_k(t)\lambda_{kj}}{\mu_j}, \quad (9)$$

where β_j is a generalized coordinate, ω_j is the circular natural frequency of the j-th sloshing mode (note that j can be an integer for 2D sloshing or an integer pair j= (a, b) for 3D sloshing), and η_1, η_2, η_4, η_5, and η_6 denote the prescribed surge, sway, roll, pitch, and yaw motions of the sloshing tank, respectively. Equations (8) and (9) show that η3, which denotes the heave motion of the tank, does not show up in $K_j(t)$, which means a pure heave motion will not induce liquid sloshing. However, in the coupled fluid-vehicle problems, if there is a coupling of heave motion with other DOFs in the vehicle motion equation, the heave motion still has to be considered and a 6-DOF equation of motion needs to be established. λ_i and μ_i are the hydrodynamic coefficients corresponding to the j-th sloshing mode; $K_j(t)$ is jointly determined by external excitation and hydrodynamic properties of the fluid.

The hydrodynamic parameters corresponding to the j-th sloshing mode are given by [8]:

$$\mu_j = \frac{\rho g}{\omega_j^2}\int_{\sum 0} f_j^2 dx\, dy, \quad (10)$$

$$\lambda_{1j} = \rho\int_{\sum 0} f_j x\, dx\, dy, \quad (11)$$

$$\lambda_{2j} = \rho\int_{\sum 0} f_j y\, dx\, dy, \quad (12)$$

$$\lambda_{4j} = \rho\int_{\sum 0} f_j \Omega_4 dx\, dy, \quad (13)$$

$$\lambda_{5j} = \rho\int_{\sum 0} f_j \Omega_5 dx\, dy. \quad (14)$$

The hydrodynamic parameters are derived from the free surface shape function fj and the Stokes–Joukowski potential Ω_{ij}, with the same scale of mass. The sloshing force and moment are calculated by solving the modal equation (equations (8) and (9)), given that all the prescribed motion and hydrodynamic parameters are known. Neglecting the sloshing moment induced purely by Stokes–Joukowski potential and considering only the effect of free surface vibration, the sloshing force and moment components can be written as [8].

$$F_1(t) = -\sum_{j=1}^{\infty}\lambda_{1j}\ddot{\beta}_j, \quad (15)$$

$$F_2(t) = -\sum_{j=1}^{\infty}\lambda_{2j}\ddot{\beta}_j, \quad (16)$$

$$F_3(t) = 0, \quad (17)$$

$$M_4(t) = -\sum_{j=1}^{\infty}(g\lambda_{2j}\beta_j + \lambda_{4j}\ddot{\beta}_j), \quad (18)$$

$$M_5(t) = -\sum_{j=1}^{\infty}(-g\lambda_{1j}\beta_j + \lambda_{5j}\ddot{\beta}_j), \quad (19)$$

$$M_6(t) = -\sum_{j=1}^{\infty}\lambda_{6j}\ddot{\beta}_j. \quad (20)$$

Therefore, the fluid-induced force and moment can be decomposed into an inertial term that is equivalent to a solid mass, and a sloshing term induced by liquid vibration inside the tank.

Calculation, solving and interpretation of equations were quickly rendered using Ansys-CFX software. The characteristics of the simulated fluid can be found in the table below (Tab.1)

3. Results and discussions

The numerical simulations of the tank give the characteristics of the realization of a braking manoeuvre, after 6s, at a speed of 5m/s. In the simulation, the real phenomenon of producing the braking manoeuvre was shown. The tank starts at a speed of 0m/s, which then moves at a speed of 5m/s, for 6s, after which the braking occurs. The movement of the liquid in the tank has the shape shown in the graph, from figure 4. The same methodology was performed for the tank with or without baffle, partially filled (85%) with liquid manure, having the characteristics in Tabel 1.

***Tabel 1**. The parameter characteristics used of the simulated fluid*

Fluid name	Manure liquid
Density [kg/m^3]	1017
Velocity [m/s]	5
Gravity [m/s^2]	9.814
Time taken by the truck to stop [sec]	6
Frequency [Hz]	1

In order to obtain an efficiency of the desired solution in a short time, in the stage of 3D numerical simulation, in the Ansys-CFX program, a simplified model was used. The tank carrying liquid manure was modelled and simulated by the method of similarity, having a compact and uniform geometric shape (see Fig 6 a), b)). Thus, in the case when the tank did not have a baffle mounted, 728017 elements and 133963 nodes were obtained, and when they were mounted 386262 elements and 95874 nodes, as can be seen in Fig.6(a), b)). Fig 7 shows the captured screenshots, revealing the pressure of the fluid (sloshing fluid) on the walls of the tank during the braking manoeuvre when the vertical baffle with the two holes was not mounted. Fig.8 shows the captured screenshots, revealing the pressure of the fluid over the mounted baffle at different times.

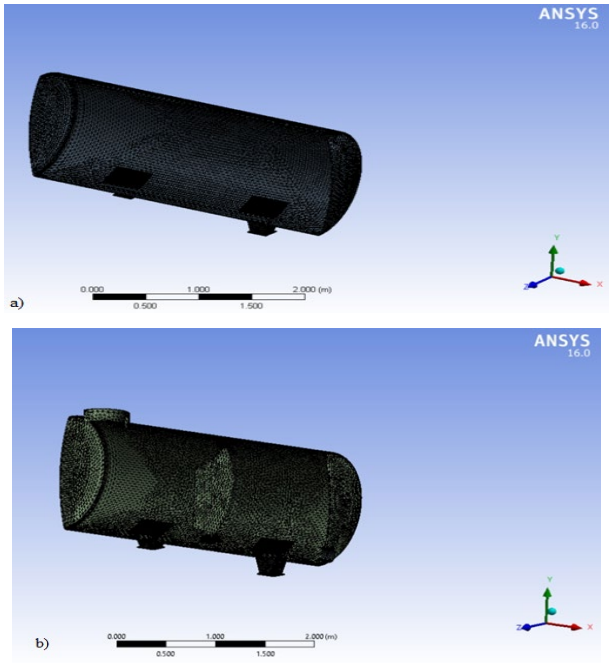


***Fig.6** The mesh model of the liquid manure tank simulate without/with baffle, a) without baffle;b) with baffle*

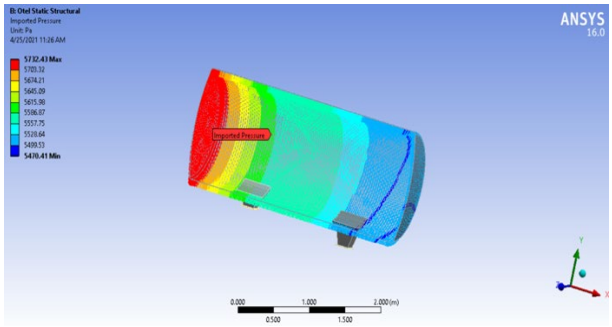


***Fig.7**. The sloshing of the liquid manure tank simulate without baffle-*screenshots

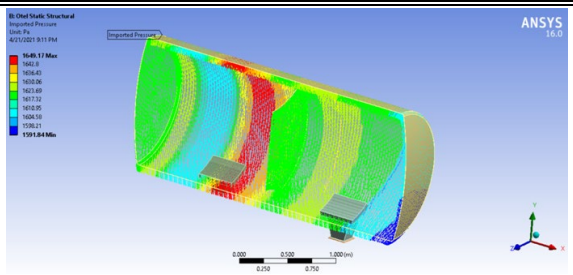


***Fig.8**. The sloshing of the liquid manure tank simulate with baffle-screenshots*

It has been found that the severity of the sloshing load depends on various factors such as fluid depth, excitation frequency, tank movement. In Fig. 9 and Fig.10 were represented the values of the maximum pressure when a single vertical baffle is used. In conclusion, in Fig.11 it is possible to observe the variation of the liquid tensions on the wall of the tank that was subjected to a braking manoeuvre for both cases. It can be seen that the stresses of the liquid sloshing on the walls of the tank are much higher, compared to those in which a tank was placed inside the tank. as a result, the use of baffles has an important role in the dynamic behaviour of the liquid on the tank structure.

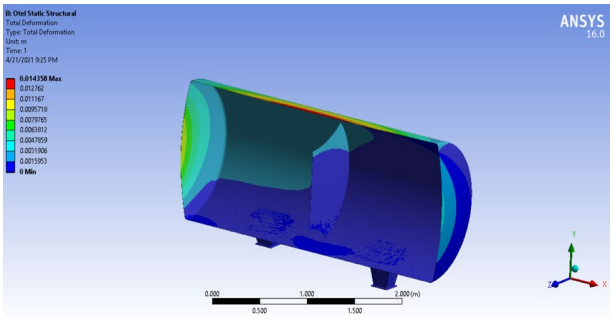


***Fig.9**. The sloshing of the liquid manure tank simulate with baffle-screenshots*

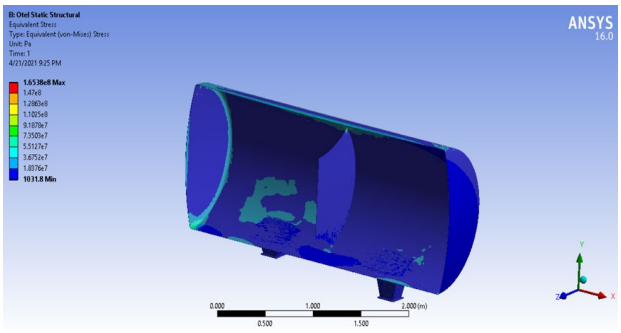


***Fig.10**. The sloshing of the liquid manure tank simulate with baffle-screenshots*

4. Conclusions

✓ From the present study, it was found that the maximum fluid pressure in the CFD analysis of the tank without baffles is 5732, 43 N / m2, and with a single baffle is 1649.17 N / m2. From the study it can be concluded that the configuration of the baffles affects the average and maximum pressure developed in the tank walls. The reduction of the fluid pressure on the walls of the container is 4.27 % without baffle and it is observed that in case of a vertical baffle it is 8.84 %. It can also be concluded that a vertical baffles is more effective in sloshing control.

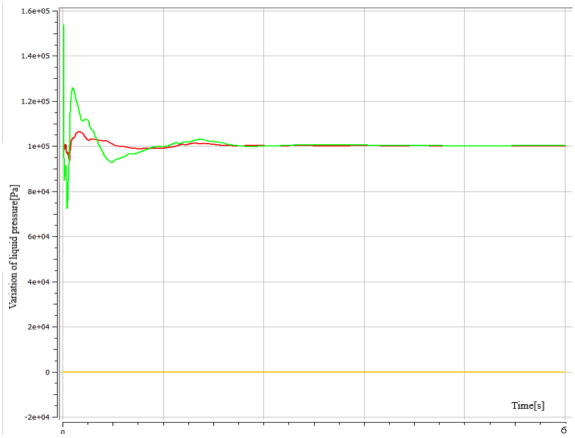


***Fig.11**. The impact sloshing on the wall of a manure tank simulate without/with baffle, the green color - represents the variation of the tensions in the tank without baffles, and the red color - represents the variation of the tensions with baffles.*

✓ The design of equipment that transports and stores liquid manure requires a detailed understanding of the movement of the liquid during sloshing.

✓ In addition to all these studies on the production and effects on vehicle dynamics of liquid sloshing while moving the vehicle, there are also the characteristics of manure that changes by processing, including anaerobic digestion.

5. References

1. M.M.Jalili, M. Sefied, M. Motavasselolhagh, J. Mech. Based Struct. Mech., DOI:10.101080, (2020)
2. M.A. Goudarzi, S.R. Sabbagh-Yazdi, Ocean Eng.,**42,** 205-217, (2012)
3. R. Ranganathan, Y. Ying,J. B. Miles, SAE Transactions **102**, 502–505, (1993)
4. S. Rakheja, S. Sankar, R. Ranganathan, SAE Transactions, **98**, 536–547,(1989)
5. D. H. Wu, Y. H. Lin, SAE Technical Paper, 01–0415, (2005)
6. M. A. Saeedi, R. Kazemi, S. Azadi, Proc. Inst. Mech. Eng., **231** (2), 295-315, (2017)
7. G.S.Brar, S.Singh, *Procedia Technology*, **14**, 490-496, (2014)
8. O. M. Faltinsen, A. N. Timokha, Sloshing, Cambridge University Press, (2009)

Digital agriculture: the experience of ukraine

Derkach O.D., Mykhaylichenko Y.M., Makarenko D.O.
Dnipro State Agrarian and Economics University, Ukraine
e-mail: derkach_dsau@i.ua, flymakd@gmail.com

Abstract: *For example of the implementation of an educational project to train students in the field of digital agriculture technologies is given. The project was implemented at the Dnipro State Agrarian and Economic University. The equipment was provided by LLC "Agro KMR" for information. An overview of software of Ukrainian and foreign production working in the field of digital agriculture is given. The advantages of using digital agriculture are shown. As an example, the implementation of the functions of differentiated sowing of sunflower by the unit Case IH Magnum 380 + Horsch Maestro 36.50SW, for which sowing maps were developed by students, is given. Sowing was performed in real conditions*

It is shown that farmers and owners of agricultural holdings should be more interested in the functioning of such a project than universities - because it significantly optimizes and automates production. Without such technologies in the coming years, agricultural enterprises will begin to lose competitiveness.

Keywords: DIGITAL FARMING, AGRICULTURAL, EQUIPMENT, STUDING

1. Introduction

The development of the agricultural sector of Ukraine will be constantly accompanied by modern agricultural machines [1-2] and technologies, which will provide: intensive introduction of energy-saving technologies for agricultural, reducing the cost of using machinery, total control and accounting of soils, crops, resources, production, etc. Today, Ukraine is a leader in the pace of implementation of modern technologies in agriculture in the world. However, Digital Farming is not being implemented so rapidly. Large agricultural holdings and medium-sized farmers have high-tech foreign equipment from the world's leading manufacturers.

It should be noted that in general, there are no problems with the provision of agriculture with machinery today. All technological operations are performed, as a rule, in due time. The struggle and competition for the cost of work began. At the same time, the coefficient of use of machinery is still at a non-high (and sometimes low) level, which reaches 65… 80%. Although the tractors and harvesters is equipped with advanced means of diagnostics and automatic control. And few farmers know that they already have many free options in the purchased equipment, but due to ignorance of how to use them, unreasonably overpay dealers.

Why is this happening? There are several reasons, but one of them is the lack of understanding of the owner of the agricultural enterprise about the algorithm of introduction of Digital Farming technologies and qualified machinery operators.

However, today we can conclude that the first to master the technology of the Digital Farming, he will ensure the colossal competitiveness of his enterprise.

2. Analysis of the state of the issue

So, what are the bonuses that the introduction of Digital Farming technologies will bring to the agribusiness owner? Where and when to start?



Figure 1 *- A fragment of the use of machinery in the field with digital farming.*

Who and how will support the functionality? Are there enough qualified specialists in this sector?

The bonuses are obvious: the practice of farmers in the US, Canada, Australia, innovative agricultural enterprises of Ukraine (Fig. 1) shows, that the introduction of Digital Farming technologies not only provides a high level of planning, control, cost reduction, but also increases profits by 10% . At the same time, a significant problem faced by Ukrainian farmers is the lack of a flexible algorithm for managing the Digital Farming. Dealers who sell equipment and software are not ready to fully provide qualified support to the company, to organize the necessary and sufficient training of consumers of the product. On the contrary, they charge for consultations, thus increasing the cost of implementing and maintaining Digital Farming, and thus, the latter becomes cumbersome and incomprehensible to the farmer. We also found that today agricultural universities do not train full-fledged specialists in Precision Farming or Digital Farming (even if it is advertised on university websites). Thus, a large proportion of graduates, for example, specialty 208 "Agroengineering" are not competitive and do not fully meet the modern requirements of the agricultural labor market. The fact that it is necessary to thoroughly and immediately update the quality of education, to rejuvenate the scientific and pedagogical staff in agricultural education is evidenced, for example, by the fact that the Center for Distance Testing and Education "Agroosvita" [1] offers in tests the knowledge of agricultural machines, which are obsolete and are not used today. Who prepares these tests? Do the questions correspond to the level of the modern fleet of machines and technologies of their use?

It is obvious that students who study new modifications of combine harvesters, for example, John Deere - series W, T, S, telematic systems like JD Link, control and management of them - do not know the structure of combines ККП-3 "Херсонець-9" and similar combines! Because, they are obsolete and are no longer used today. Thus, there is an imbalance in the assessment of students' knowledge: the student has knowledge and skills in relation to modern technology, but does not have them in relation to outdated technology and "Agroosvita" assesses his knowledge as "unsatisfactory". Does this correspond to the objective reality?

The purpose of the work is to bring the quality of training of engineering and technical workers to the real needs of production, taking into account the introduction of Digital Farming!

Today, there are definitions of "precision farming" and "smart farming" (they can be found in free access on the Internet), the implementation of which allows you to collect a significant amount of various production data in real time and store them. Digital Farming integrates both concepts of Precision and Smart Farming. It can be defined as "the consistent application of methods of Precision and Smart Farming, internal and external interconnections of the economy, as well as the use of both web platforms containing

data and big data analysis" - according to the definition of DLG (Deutsche Landwirtschafts-Gessellschaft).

Thus, at the Dnipro State Agrarian and Economic University, the implementation of an experimental project to train specialists in the field of Digital Farming technologies has been launched.

It should be noted that we have already started a similar project before with one of the John Deere dealers, but this project has not been developed. The analysis showed that for the full and, most importantly, the actual functioning of such a project requires the following:

- systematic interest of the dealer and the university in the implementation of such a project through continuous operation without interruption of the production process and training;
- motivation of students and teachers-participants of the project;
- constant and stable access of project participants to the digital data of the enterprise, which is already working with the technologies of the Digital Farming or is at the stage of their implementation.

Taking note of the reasons for the failures, we launched a new project on Digital Farming, which should solve the following tasks:

- to give a clear explanation to the Project participants of the essence, purpose and tasks of Digital Farming, advantages and problems on the way of their implementation;
- to teach practical skills of students in the use of equipment, software, obtaining accurate data of production activities;
- to study the algorithm of introduction of Digital Farming in the enterprise;
- learn to make the right decisions based on the data obtained;
- be able to make forecasts, identify risks and implement flexibility of decisions in production activities;
- to exchange students between DSAEU and Olds College (Canada).
- to get full-fledged ready specialists in the field of Digital Farming.

Eleven AFS (Advanced Farming System) licensed programs provided by My Agro Canada were installed for the implementation of the Project at the Department of Machine and Tractor Operations (DSAEU). The management of LLC "Agro KMR", represented by the director Clement Coussens, provided access to the databases of the headed enterprise. Thus, students worked online, designing production tasks for the company.

Most farmers and dealers today make the same mistake: they try to buy equipment without delving into the software, violating the sequential algorithm. In addition, not everyone understands the need to introduce an additional staffing unit for a person who would be directly involved in Digital Farming in the enterprise. As a rule, it is an IT specialist.

In the first lectures, students were able to get a detailed analysis of the digital platform Cropio, which is widely used in Ukraine (Fig. 3): what are its functions, how to start working, what to look for and much more. For example, on these maps we see that you can simultaneously observe on some relief what is the state of vegetation of crops on specific dates. And hundreds of such data can be collected. Ukraine (Fig. 2): what are its functions, how to start working, what to look for and much more. For example, on these maps we see that you can simultaneously observe on some relief what is the state of vegetation of crops on specific dates. And hundreds of such data can be collected.

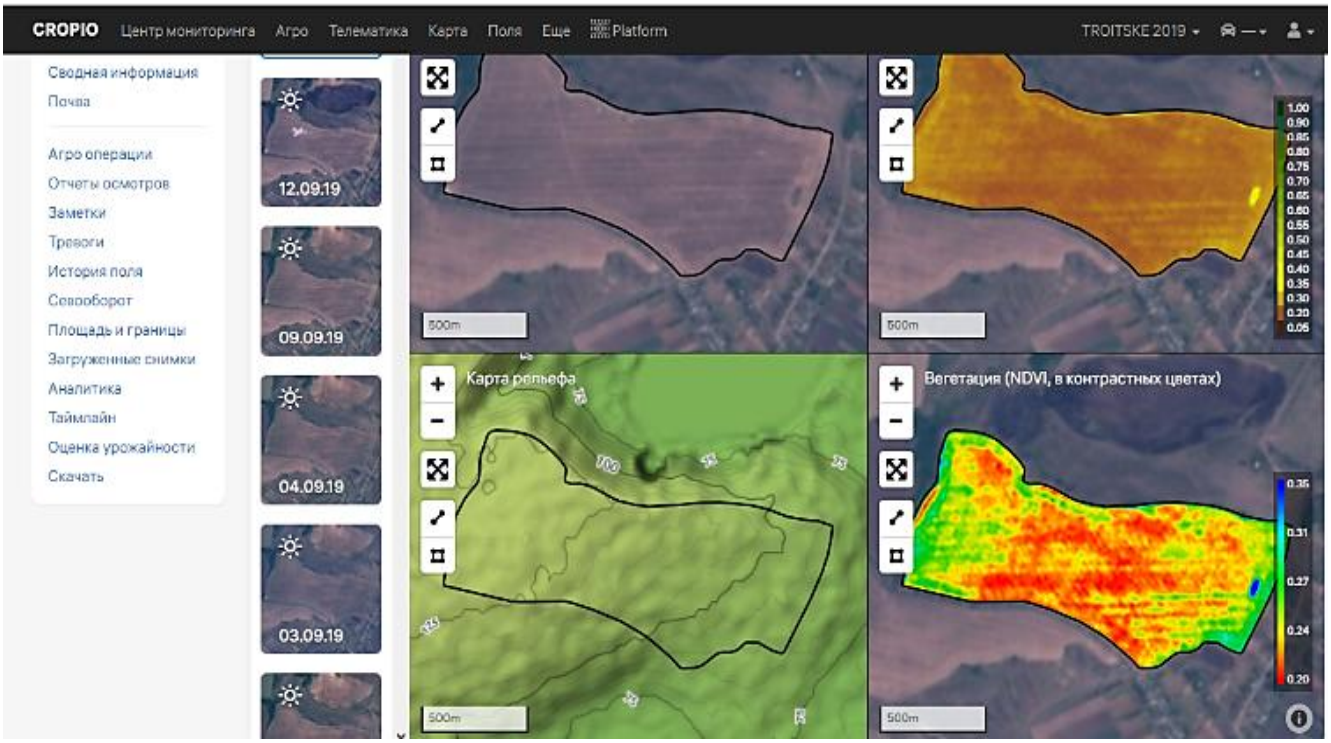


Figure 2 - *Characteristics of one of the fields of the enterprise on the Cropio platform.*

In fact, only in one figure 3 you can see a lot of collected data, showing a complete picture of the current state of production and on the basis of which you can make the right and effective decisions.

A comparative analysis of different platforms, their similarities and differences was conducted. For many it was a surprise that there are similar platforms of domestic manufacturers, such as the platform from AgroOnline (Fig. 4), which has a similar platform to Cropio functionality.

The digital penetrometer developed by domestic manufacturers is shown, which transmits soil hardness data to the SkokAgro platform (Fig. 5) – another Ukrainian product of digital technologies, online.

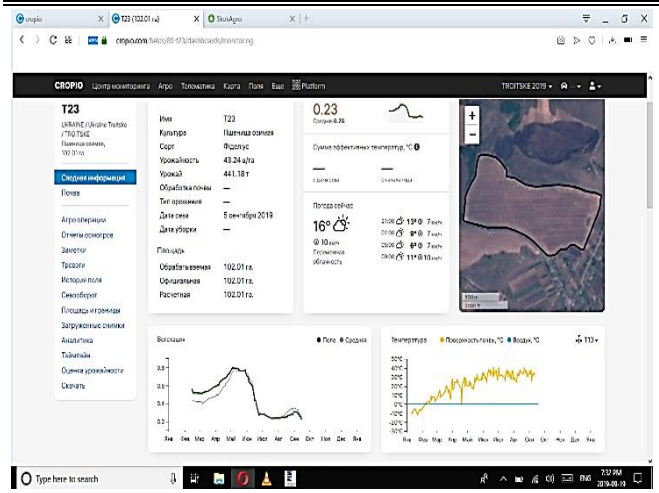


Figure 3 *- Characteristics of one of the fields of the enterprise on the Cropio platform.*



Figure 4 *- AgroOnline software interface*

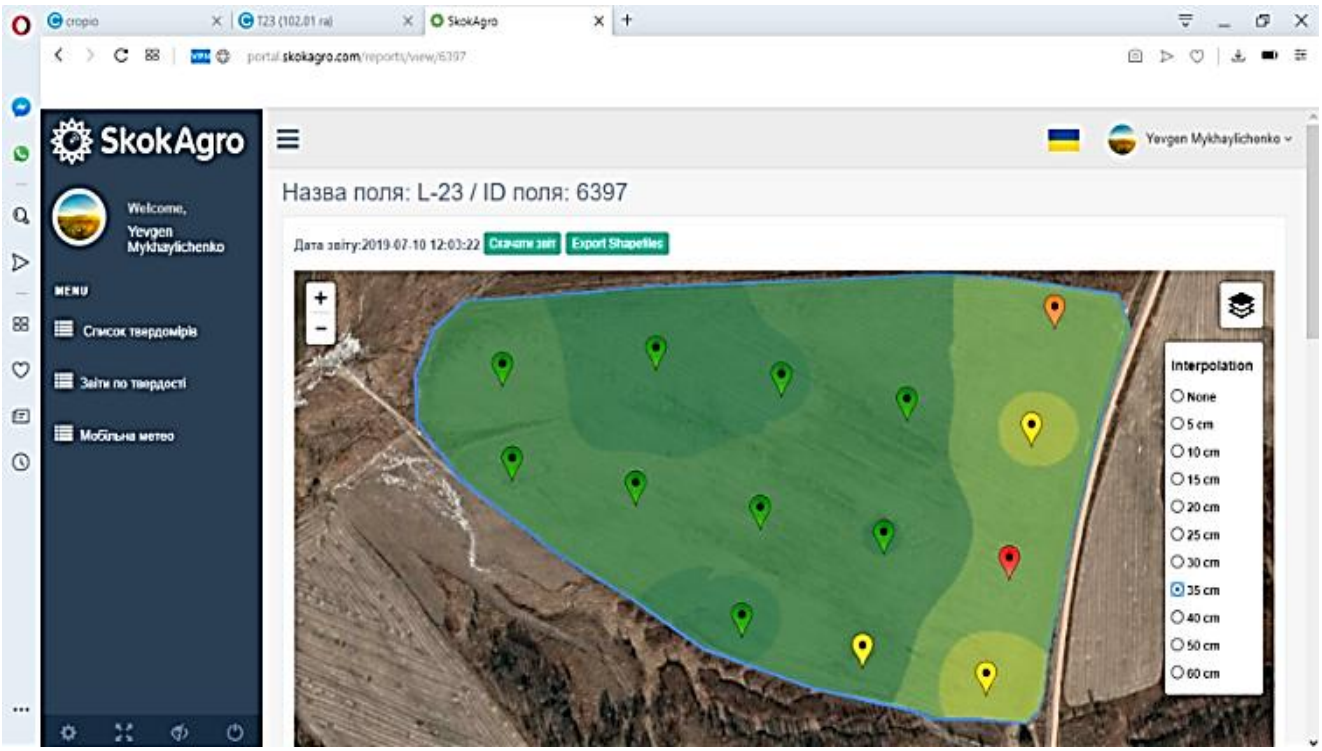


Figure 5 *- Fragment of the map of soil hardness measurement digital penetrometer S 600*

After finishing the first block of classes, 12 students who participated in the project for 2 years were selected into a separate group. They have gone step by step all the way that ensured the full start and functioning of Digital Farming. The next classes took place in a computer classroom, where students with the help of AFS software learned to operate data obtained from LLC "Agro KMR". And the next step was practical training in the selected fields of this enterprise: from hardness measurement to the technology of soil analysis and much more.

In general, after two years of intensive and systematic classes, we should exchange between students of one of Canada's colleges and show the ability of students (at that time already specialists in Digital Farming) to resist the change of situational production activities and the ability to perform tasks in other conditions, in this case - in another country.

After receiving positive results of this project, it should be implemented in other agricultural universities of Ukraine, in order to train competitive specialists who would not only meet the requirements of time and level of agricultural production, but also were generators of ideas and innovations of the agro-industrial complex.

3. Example

Here is one example of how and what you can save, increase the productivity of the unit. So, in one of the enterprises by means of a drone the operative control of a condition of a field is carried out and it is found out that long rains promoted formation on the field of a certain number of small lakes that completely destroyed crops. The dimensions and coordinates of these lakes were entered into a digital map, which was uploaded to the sprayer map. The agronomist decided: to carry out treatment with chemicals with a rate of 150 l / ha (blue color) and to stop processing (red color) in case of passage of the sprayer over the sites destroyed by water (fig 6).

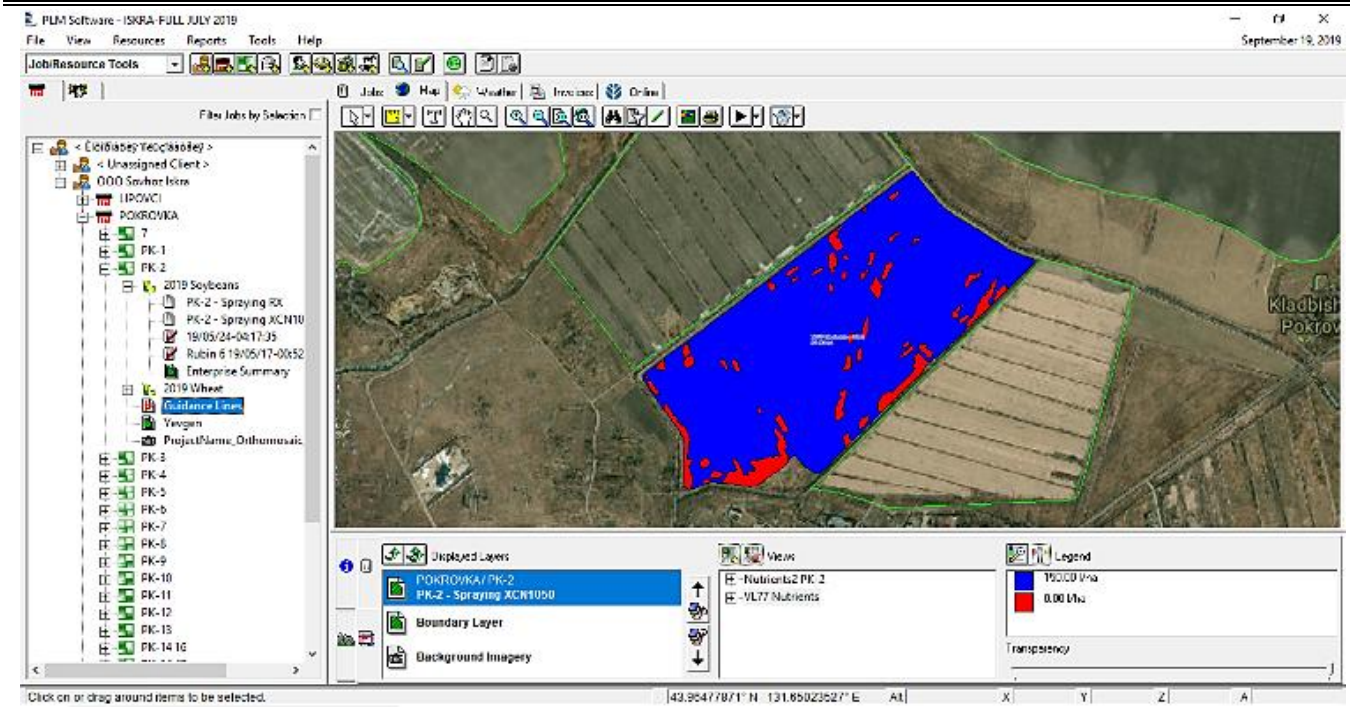


Figure 6 *- Operational map for differential application of chemicals*

What did this give the company? Disabling sprayers on the machine in the case of passage over the area of the field, where crops are destroyed by water, provided a reduction in the cost of chemicals by 9.5%. The volume of the working solution and the cost of transporting and preparing the working solution of chemicals were saved. That is, reduced energy consumption, and hence the cost of this technological operation. Similarly, adjustments are made at all stages of production: in the main and ancillary operations, in the process of production coordination (for example, coordination of the multiplicity of the width of the units, their productivity and more).

As a result of the block of studies, students based on a map of differentiated sunflower sowing. The task provided for differential sowing of sunflower seeds in three zones of the field with a sowing rate of 65, 70 and 75 thousand seeds per 1 ha.

The unit was part of a Case IH Magnum 380 tractor with a Horsch Maestro 36.50SW sowing complex. The unit is equipped with the Trimble TMX-2050 monitor. The process of uploading the task took place directly in the field and was completely filmed on video (Fig. 7, a), which readers can view by using the QR-code and following the link.

Figure 7 *- a) Video formation of the task. It starts from the moment after downloading the file from the flash drive. The duration of the operation is 6 minutes.*
b) start of sowing

The map of tasks (Fig. 8) with three seeding zones looked like this.

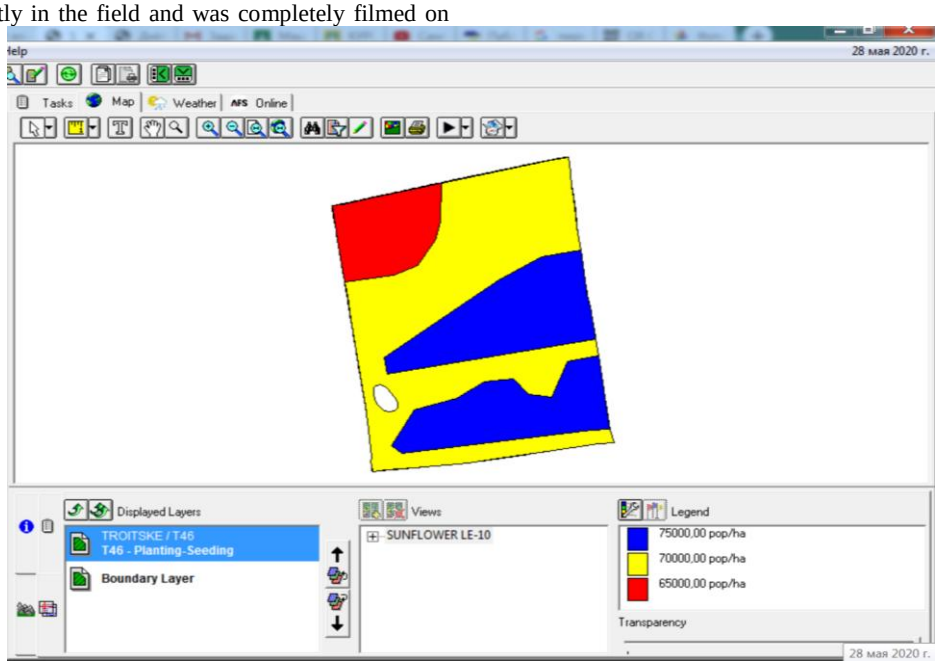


Figure 8 *- General view of the task map, built in AFS software, with three seeding zones.*

The map of the performed differentiated sowing is shown in Fig.9.

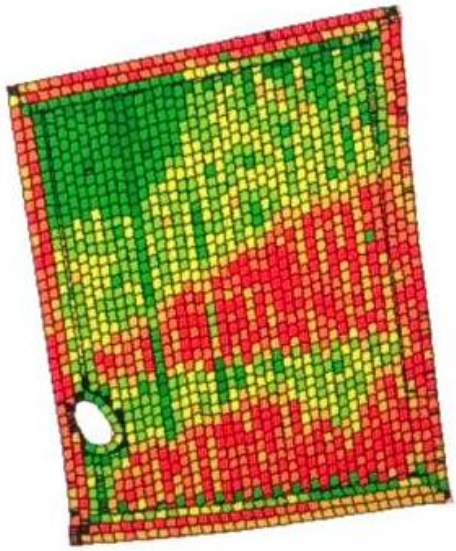


Figure 9 *- Map of differentiated sowing.*

Conclusion

The creation of the Project on Digital Farming at the Dnipro State Agrarian and Economic University is due to the lack of training of specialists in this field on the market of educational services.

Such a project is currently the first and only in Ukraine and its graduates must solve the problem of stable implementation of Digital Farming in agricultural companies of Ukraine.

In our opinion, farmers and owners of agricultural holdings should be even more interested in the functioning of such a project than universities - because it significantly optimizes and automates production. Without such technologies in the coming years, agricultural enterprises will begin to lose competitiveness.

ACKNOWLEDGEMENTS

Realization of this project would be impossible without owners of LLC “Agro KMR” in the person of Floran Renar, director of LLC “Agro KMR” Clement Coussenss, IT specialist Oleh Plakhin, agronomist Oleksandr Shipilo, assistant agronomist Vitalii Trotsenko.

REFERENCES

[1] Derkach O.D., Burya O.I. PIdvischennya tehnIchnogo rIvnya elektro-, avtomobIlnogo tran-sportu ta sIlskogospodarskoYi tehnIki za rahunok vikoristannya novih materIalIv. NaukovI rekomendatsIYi: DnIpropetrovsk: DDAU. – 2011. – 71 s.(Ukr)

[2] Derkach A., Makarenko D., Naumenko N. Primenenie ugleplastikov v shirokozahvatnyh posevnykh mashinakh. Mechanization in agriculture / International scientific, scientific applied and informational journal.YearLXI, 2/2015, Sofia, c. 3-6. (Rus)

[3] Tsentr dystantsiynogo testuvannya ta osvity. URL: http://test.smcae.com/

Evaluation of effects of biofuels blends on performance and emissions of diesel engine

Tomas Mickevičius
University of Applied Engineering Sciences, Lithuania
tomas.mickevicius@edu.ktk.lt

Abstract: *Growth of the economy and living standards of the population increase the need of people's and goods transportation by sea, railroads, the air, and highways. As a result, increases the need to use more ships, trains, airplanes, heavy-duty trucks, self-powered machines, city busses, and light-duty passenger cars. Unavoidably increases the demand of the fuel to be consumed, however the natural oil-resources are largely exhausted over hundreds of years. Moreover, the increased consumption of a fossil-origin fuel creates the urgent environment pollution problems and climate change. The automotive air-pollution problem emerged already aim of this article was to investigate the influence of three-component fuel on the efficiency and emission performance of a diesel engine. The results obtained during the research are presented, which are investigated with a single-cylinder diesel engine "ORUVA F1L511". The study examines diesel fuel and fuel blends J5Bu5, J5Bu10 and J5Bu15. The results obtained in the study are comparable. Engine load characteristics were recorded at n = 2000 rpm. The study found that the lowest carbon monoxide (CO) emissions (163ppm) were obtained by using J5Bu5 fuel blend. Maximum nitrogen oxide (NOx) emissions were obtained with the engine running on diesel fuel (1839ppm). The lowest NOx emission was obtained with the engine running on a three-component J5Bu15 fuel blend (1643ppm). The highest opacity was obtained when the engine was fuelled with 100% diesel fuel and at full load.*

KEYWORDS: DIESEL ENGINE, RAPESEED OIL BIODIESEL, AVIATION FUEL, BUTANOL, PERFORMANCE, EMISSIONS, SMOKE OPACITY

1. Introduction

In 1988, the North Atlantic Treaty Organization (NATO) countries decided to simplify the delivery of petroleum products to the combat zone and improve the interoperability of aircraft and land equipment with JP-8 (F-34) military kerosene. In order to put this decision into practice, the NATO Pipeline Committee (NPC) adopted the Single Fuel Policy (SFP) in 2004. The US legislation on the "One Fuel Delivery Policy" stipulates that US military ground vehicles used must be able to work with aviation fuel (JP-8). JP-8 petroleum-based fuel is very similar in specification to the commercially available Jet A-1 fuel. Jet A1 fuel is a light distillate of complex hydrocarbons such as 50-65% paraffins, 10-20% aromatics and 20-30% naphthenes [1]. Jet (JP-8) fuel is a military kerosene turbine fuel made from civilian (Jet A-1) fuel and widely used by the United States Air Force and Europe. Aviation turbine fuel is extracted almost exclusively from the kerosene fraction of crude oil, the distillation points of which are between the gasoline fraction and the diesel fraction.

The cetane number of a fuel is one of the most important factorsvaffecting the autoignition quality in diesel engines. It was foundvthat the JP-8 and ULSD with similar CN have highly comparable combustion characteristics in a DI compression ignition engine and CN is the paramount characteristic in comparing these fuels.

Authors investigate effects of diesel fuel (B5), turbine type JP-8 fuel and its 5 vol%, 10 vol%, 20 vol%, and 30 vol% blends with rapeseed oil methyl ester (RME) on the start of injection, ignition delay, combustion history, heat release, engine performance, and exhaust emissions. The engine performance parameters were examined at light 15% (1400 rpm) and 10% (2200 rpm), medium 50%, and high 100% loads and the two speeds. They found that the autoignition delay and maximum heat release rate decreased, maximum cylinder pressure, and pressure gradients increased, whereas brake specific fuel consumption changed little and brake thermal efficiency was 1.0–3.6% higher when running with fuel blends J5 to J30 at rated speed compared with the data measured with neat jet fuel. The NOx emissions increased slightly, but the CO, THC emissions, and smoke opacity boosted up significantly when using jet fuel blend J10 with a smooth reduction of unburned hydrocarbons for jet-biodiesel fuel blends with higher CN ratings. Operation at a full (100%) load with fuel blend J10 produced more CO and exhaust smoke, whereas the combustion of identical fuel blend B10 showed the reverse trends reducing both pollutants at both engine speeds [2].

Using fuel blends with the higher content of biodiesel changes the technical properties of the fuel: increase density, viscosity, decrease calorific value, cetane number, freezing temperature, etc. These indicators have the impact on the biofuel supply and injection characteristics, the quality of the combustible mixture that, in turn, has influence on diesel engine performance and ecological indicators [3].

Ethanol, methanol, and butanol are currently the most popular alcoholic fuels used in internal combustion engines around the world. Higher oxygen content in alcoholic fuels than that in mineral fuels may result in lower calorific value of the biofuels. However, these fuels need less air-borne oxygen to burn to burn the fuel completely and thus can contribute better quality of the environment. The elemental composition of alcoholic fuels makes it possible to reduce the amount of smoke (soot), carbon monoxide CO, carbon dioxide CO2 and aldehydes emitted from diesel engine [4]. A study conducted a comparative analysis of performance and emissions characteristics of aviation fuel (Jet A-1) and butanol/Jet A-1 fuel (B10) blend. Authors found that the fuel consumption and specific fuel consumption is slightly higher for blend with butanol, compared to Jet A-1 fuel. This is due to the fact, that lower calorific value for fuel blend. The values of carbon monoxide (CO), carbon dioxide (CO2) and nitrogen oxides (NOx) emissions for fuel B10 blend were slightly lower, compared to the cases of using Jet A-1 fuel [5]. Normal butanol (C4H9OH – 74.0 g/mol) is an alcoholic-origin colourless liquid with a harsh fusel with banana odour, which possess 21.58 wt% of fuel-bound oxygen and differs as having low flash point of 28.9 °C and the boiling point of 117.7 °C at 760 mm Hg. On the one part, n-butanol added to commercial diesel fuel reduces density, viscosity, C/H atoms ratio and provides fuel-bound oxygen that along with good evaporative properties improves both the air and fuel vapours mixing rate and the combustion of fuel blend leading to more environment friendly exhaust. On the other part, the presence of a lighter and oxygenated n-butanol reduces the cetane number, net heating value and thus mass of the fuel consumed per unit of energy developed by an engine. The sensitive interaction between advantages and disadvantages properties of n-butanol added to diesel fuel may lead to ambiguous development trends combustion, heat release rate and engine out emissions [6]. Moreover, the use of bio-based products in fuels is a strategic government resolution in most European countries [7]. The analysis of other works investigations of fuel chemical parameters shows, that from an engine-critical characteristics perspective butanol – hydrogenated vegetable oil – diesel blends are a potential solution [4].

Authors investigate and compare effects of biodiesel-ethanol (BE) and biodiesel-n-butanol (BBu) blends on combustion, performance and emissions of a direct-injection diesel engine. Experiments were conducted on BE5 (5% ethanol and 95% biodiesel, v/v), BE10, BE15, BBu5, BBu10 and BBu15, at five

engine loads and at 1800 rpm. They found that blended fuels have adverse effects on engine performance especially at low load, with the BE blends having more adverse effects than the BBu blends. Moreover, on average of the five engine loads, the BBu and BE blends increase CO emission by 13.7% and 22.8% and HC emission by 5.6% and 29.2%, respectively; but reduce NOx emission by 6.5% and 28.0%, particle mass concentration by 20.7% and 20.6% and particle number concentration by 22% and 21%, respectively. Overall, the BE blends are more effective in reducing particulate and NOx emissions but the BBu blends would lead to less increase in CO and HC emissions [8].

A study conducted a comparative analysis of fuel properties, performance, emissions and combustion characteristics of biodiesel produced from waste cooking oil (B100), along with a binary blend of biodiesel–diesel (B20) and ternary blends of biodiesel–diesel–butanol as substitutions to diesel fuel. Although biodiesel and n-butanol have some negative impacts on engine performance parameters, they generally positively affect exhaust emission parameters compared to euro diesel. Addition of n-butanol decreased some of the fuel thermo-physical properties such as density, viscosity and flash point. The average decreases in brake power when n-butanol was added were 6.17%, 7.49% and 11%, respectively, coupled with increases in specific fuel consumption of 6.25%, 8.96% and 14.29%, respectively. The addition of n-butanol decreased exhaust gas temperatures, CO, HC, NO and smoke emissions [9].

The purpose was to study the effects of three-component fuel blends on performance, and exhaust emissions of a diesel engine.

2. Preconditions and means for resolving the problem

Experimental research was carried out in the fuel equipment testing laboratory of the Power and Transport Machinery Engineering Institute at the Faculty of Agricultural Engineering of Vytautas Magnus University − Agricultural Academy. For stroke, one cylinder, direct injection, air cooled ,,ORUVA FL 511" diesel engine was used for these experiments.

At first, engine tests have been conducted by using jet-biodiesel fuel blend were prepared by mixing RME and JP-A1 fuel in the following proportion by volume 5/95 (J5). After all load characteristics were taken of the engine performance on jet-biodiesel fuel (J5), three blends with jet-biodiesel fuel (J5) and n−butanol (Bu) were prepared by mixing in various volumetric ratios 95% J5 and 5% Bu (J5Bu5), 90% J5 and 10% Bu (JBu10) and 85% J5 and 15% Bu (J5Bu15). The properties of the tested fuels and its blends are presented in Table 2.

The engine torque was measured with an eddy current dynamometer with a definition rate of ±0.1 Nm and the rotation speed with the mechanical meter with a definition rate of ±2 rpm.

The amounts of nitric oxide NO (ppm), nitrogen dioxide NO_2 (ppm), carbon monoxide CO (ppm) and total unburned hydrocarbons HC (ppm) in the exhausts were measured with the Testo 350 XL gas analyser. Total emissions of nitrogen oxides NOx were determined as a sum of both NO and NO_2 gases. Total NOx emissions were determined as a sum of both NO and NO_2 pollutants with an accuracy of ±5 ppm.

The exhaust opacity (%) was measured with a Bosch RTT 100/RTT 110 opacity-meter with an accuracy of ±0.1°.

Table 1. *Properties of JP-A1 fuel, rapeseed oil methyl ester (RME) and n-butanol*

Property parameters	**JP-A1**	**RME**	**n-butanol**
Density at 15°C, kg/m3	797.2	884.7	802
Kinematic viscosity at 40 °C, mm^2/s	4.0	4.8	2.63
Lubricity, corrected wsd, 1.4 lm at 60 °C	611	205	591
Cetane number	42,3	53.4	25
Oxygen content, max wt. %	–	10.9	21,58
Carbon-to-hydrogen ratio (C/H)	6.13	6.48	4.80
Net heating value, MJ/kg	43.30	37.23	33.08
Stoichiometric air/fuel ratio, kg/kg	14.84	12.62	11.2

The engine characteristics were determined when it was driven by a gradually increasing load and a constant engine speed of 2000 rpm. To improve reliability of the measured data the tests have been repeated no less than three times.

3. Solution of the examined problem

Fig. 1 shows the fuel consumption per hour and brake specific fuel consumption (bsfc) variations as a function of engine load. Alterations of the combustion process has effect on engine economy Under the same operating conditions, the fuel consumption, when the engine has been operating on jet-biodiesel fuel and its blend with n−butanol, has been little higher compared to the engine operating on jet-biodiesel fuel (J5) blend. It has to be noted, that the change of bsfc has been decreasing while the engine load was increasing (Fig.1). It is seen, when engine running on oxygenated biofuel blends J5Bu5, J5Bu10 and J5Bu15, at low load, the brake specific fuel consumption slightly increased by 1.1 %, 2.3 % and 4.5 %, respectively. When operating on biofuel J5Bu15 blend, the brake thermal efficiency of the diesel engine, decreases by 1 % (Fig.2).

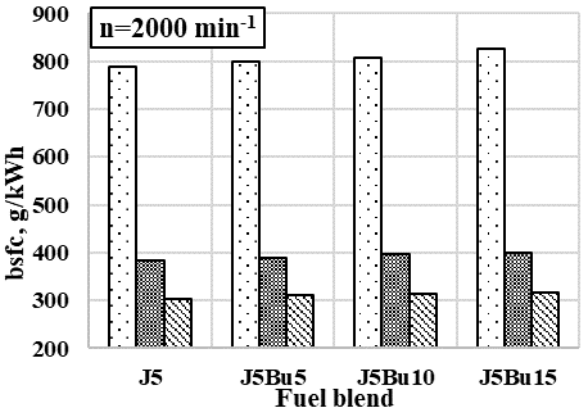


Fig. 1. *The fuel consumption per hour (B_d) and brake specific fuel consumption (bsfc) as a function of engine load at 2000 min^{-1}*

At full engine load, the brake specific fuel consumption changing tendencies remain similar. When operating on the three-component biofuel J5Bu5 – J5Bu15 blends, bsfc increased by 2.4–4.1 %, respectively, in comparison with engine running on fuel J5 blend. The increased fuel consumption of biofuel J5Bu5 – J5Bu15 blends may be attributed reasonably to the lower net heating value of oxygen blends. In case of using the three-component biofuel J5Bu5 – J5Bu15 blends, the brake thermal efficiency decreased by 0.4–1 % in comparison to the engine running on fuel J5 blend. The decrease of the brake thermal efficiency in this case can be explained by the fact that is the mostly affected by their reduced cetane number and the larger latent heat of vaporization of butanol as the latter suppresses the auto ignition and combustion processes in the cylinder.

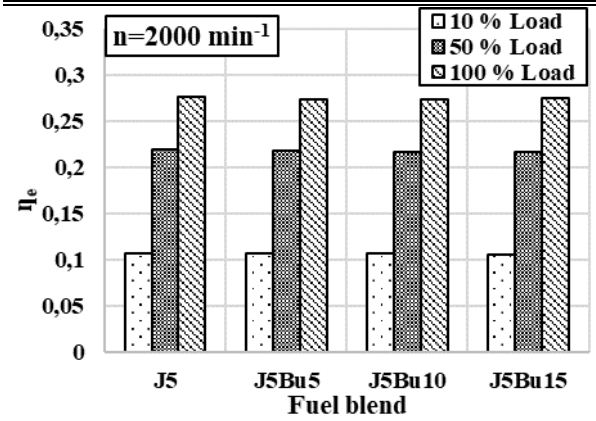


Fig. 2. *Brake thermal efficiency (η_e) and nitrogen oxide (NO_x) as a function of engine load at 2000 min^{-1}*

The nitrogen oxides are formed outside the flame front at high temperatures, with free nitrogen atoms reacting with excess oxygen in the combustion chamber by a complex chain reaction. The total emissions of nitrogen oxides amount in the combustion depends more on the maximum process temperature, because the reaction is endothermic and not directly related to the combustion processes of the mixture. The variation of total emissions of nitrogen oxides (NO_x) with as a function of engine load and different fuel blends is presented in Fig. 2. When the engine is running at the average engine load, using of oxygenated biofuel blends J5Bu5, J5Bu10 and J5Bu15, the total emissions of nitrogen oxides reduces by 7.9 %, 5.6 % and 15.8, respectively.

The total emission of nitrogen oxides scales up when load of the engine increases. In case at full engine load and use biofuel J5Bu5, J5Bu10 and J5Bu15 blends, the total emission of NO_x decreased by 3.5 %, 9.2 % and 10.6 %, respectively, in comparison with engine running on fuel J5 blend. The decrease in total emission of nitrogen oxides can be explained by the lower gas pressure and temperature in the cylinder as the combustion and heat release processes moved towards the direction of the expansion stroke. The pressure and temperature of the gas burning in a large volume of the cylinder are lower which in turn conditions the lower degree of nitrogen oxides emission. Butanol–diesel blends also show this behaviour, as butanol concentration increased, the NOx, and CO emissions decreased, while unburned HC emissions, BSFC, and BTE increased as compared to diesel [10].

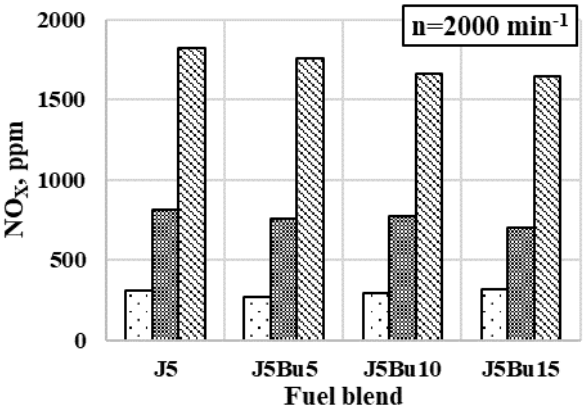


Fig. 2. *Brake thermal efficiency (η_e) and nitrogen oxide (NO_x) as a function of engine load at 2000 min^{-1}*

Carbon monoxide is formed at local locations in the combustion chamber where oxygen is completely lacking for the combustion reaction. Incompletely burned carbon atoms reduce the thermal energy conversion efficiency of fuels and increase carbon monoxide emissions. Ineffective combustion and low chamber temperatures release the carbon monoxide and the unburned hydrocarbons emissions.

The dependencies of carbon monoxide (CO) emission of engine load is shown in Fig. 3. When the engine is running at low load and using the three-component biofuel J5Bu5, J5Bu10 and J5Bu15 blends, the (CO) emission increases by 19–26 %, respectively, compared to the engine running on fuel J5 blend. In case at full engine load and using rich oxygenated blends J5Bu10 and J5Bu15, the carbon monoxide emission decreased by 13.3 % and 14.5 % in comparison to the engine running on fuel J5 blend. When operating on biofuel blend J5Bu5, the CO emission increases by 3 %. Similar trends were obtained using n-butanol as an additive in a heavy-duty diesel engine with 5%, 10%, 15% of n-butanol content using multiple injections. Similar results showed that n-butanol addition decreased soot and CO emissions, but did not have a serious impact on BSFC [11].

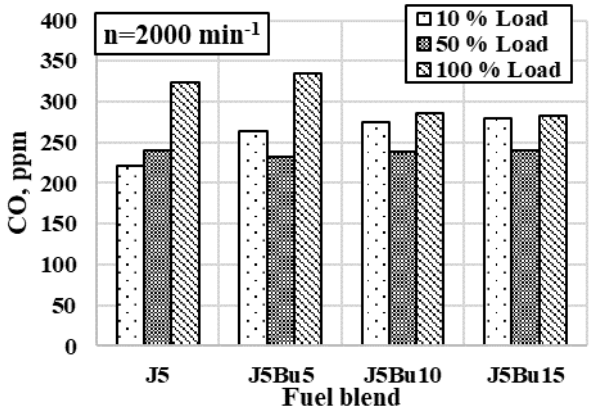


Fig. 3. *Dependencies of carbon monoxide (CO) and smoke opacity of the exhaust on engine load at 2000 min^{-1}*

The soot formation be able to progress at local locations in the fuel-saturated combustion chamber during pyrolysis of hydrocarbons. The smoke opacity of diesel engines depends on the cetane number of the fuel, the chemical composition, the amount of aromatic hydrocarbons, the fuel injection and the quality of the combustible mixture, the diffusion process in the chamber and the complex mechanism of soot particle formation and their combustion burn reaction rate. Fig. 3 shows dependencies of smoke opacity of the exhaust of engine load.

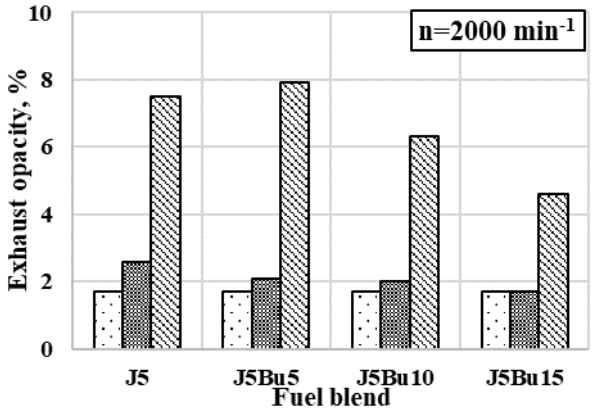


Fig. 3. *Dependencies of carbon monoxide (CO) and smoke opacity of the exhaust on engine load at 2000 min^{-1}*

At low engine load, the smoke opacity remained lower in case of using all J5, J5Bu5, J5Bu10 and J5Bu15 fuel blends. The smoke opacity produced from biofuels J5Bu5, J5Bu10 and J5Bu15 fuel blends sustained at lower levels over the average engine load. When running the engine on biofuel blends J5Bu10 and J5Bu15 at full load, the smoke opacity decreased by 19 % and 63 %, respectively, compared to the cases of using J5 fuel blend. The lower smoke matches well with the test results findings of other researchers [12]. The effects of oxygenated fuel blends on the auto-ignition delay,

combustion reactions, engine efficiency, smoke and exhaust emissions depend on the composition of the tested fuel blends, their chemical and physical properties as well as on engine load, speed, availability of air-born oxygen and temperature conditions inside the cylinder

Conclusions

1. The brake mean fuel consumption using three-component fuel blends increased across at over the whole load range. At full engine load, the three-component fuel J5Bu5, J5Bu10, and J5Bu15 blends, the break mean fuel consumption increased by 2.4 %, 3.5 %, and 4.1 %, respectively, compared to fuel J5 blend.
2. Using a three-component biofuel J5Bu15 blend, the break thermal efficiency was 1 % lower, compared to the engine running on fuel J5 blend, at full engine load.
3. The jet-biodiesel fuel (J5) blend developed the highest (1817 ppm) total emissions of nitrogen oxides. At full engine load and using different biofuel J5Bu5, J5Bu10 and J5Bu15 blends, the most environmentally and human harmful total emissions of nitrogen oxides decreased by 3.5 %, 9.2 % and 10.6 %, respectively.
4. When the engine running at low load, the highest the carbon monoxide emissions were obtained with the engine running on biofuel J5Bu15 blend (279 ppm) and the lowest using the fuel J5 blend (221 ppm).
5. At the medium engine load using the three-component fuel J5Bu5, J5Bu10 and J5Bu15 blends, the smoke opacity was 23 %, 30 % and 52.9 % lower, compared to the engine running on fuel J5 blend.

References

1. Labeckas, Gvidonas; Slavinskas, Stasys; Vilutienė, Valentina. The effect of aviation fuel JP-8 and diesel fuel blends on engine performance and exhaust emissions. Journal of KONES, 2015, 22.
2. Labeckas, Gvidonas; Slavinskas, Stasys. Combustion phenomenon, performance and emissions of a diesel engine with aviation turbine JP-8 fuel and rapeseed biodiesel blends. Energy Conversion and Management, 2015, 105: 216-229.
3. Labeckas G., Slavinskas S. The effect of rapeseed oil methyl ester on direct injection Diesel engine performance and exhaust emissions. Energy Conversion and Management, 2006, Vol. 47, Nr. 13–14, p. 1954–1967.
4. Labeckas, G., Slavinskas, S., & Mažeika, M. The effect of ethanol–diesel–biodiesel blends on combustion, performance and emissions of a direct injection diesel engine. Energy Conversion and Management, 2014, 79, 698-720.
5. Gawron, Bartosz, et al. Performance and emission characteristic of miniature turbojet engine FED Jet A-1/alcohol blend. Journal of KONES, 2016, 23.
6. H. Solmaz, H. Yamık, Y. İçingür , A. Calam Investigation of the effects of civil aviation fuel Jet A1 blends on diesel engine performance and emission characteristics, Indian Journal of Engineering & Materials Science Vol. 21, April 2014, pp. 200-206
7. EC, E. C. WHITE PAPER roadmap to a single European transport area towards a competitive and resource efficient transport system. COM (2011) 144 final [online], 2011.
8. Wei L., Cheung C.S., Ning Z. Effects of biodiesel-ethanol and biodiesel-butanol blends on the combustion, performance and emissions of a diesel engine. Energy, 2018-07-15, Vol. 155, Issue 3, p. 957-970, doi.org/10.1016/j.energy.2018.05.049.
9. YILMAZ, Nadir, et al. Effect of biodiesel–butanol fuel blends on emissions and performance characteristics of a diesel engine. Fuel, 2014, 135: 46-50. 15.
10. Dogan O. The influence of n-butanol/diesel fuel blends utilization on a small diesel engine performance and emissions. Fuel 2011;90:2467–72.
11. Yao M, Wang H, Zheng Z, Yue Y. Experimental study of n-butanol additive and multi-injection on HD diesel engine performance and emissions. Fuel 2010;89:2191–201.
12. Rakopoulos DC, Rakopoulos CD, Giakoumis EG, Papagiannakis RG, Kyritsis DC. Influence of properties of various common bio-fuels on the combustion and emission characteristics of high-speed DI (direct injection) diesel engine: vegetable oil, bio-diesel, ethanol, n-butanol, diethyl ether. Energy 2014;73:354–66. 14 August.

Operational properties of diesel fuel with the addition of rapeseed oil esters

Ass. Prof., PhD, V. Tkachuk[1], Ass. Prof., PhD, Iu. Melnic[2], Ass. Prof., PhD, O. Rechun[1]
[1] Lutsk National Technical University, Lutsk, Ukraine
[2] State Agrarian University of Moldova, Chisinau, Republic of Moldova
ljeratkachuk@gmail.com, iu.melnic@uasm.md,

Abstract. The article is devoted to the study of performance indicators of diesel fuel with the addition of rapeseed oil ether. To do this, the study used diesel fuel of Euro 5 grade "L" and the following dietary supplements: rapeseed oil methyl ester and rapeseed oil isopropyl ester. In the resulting biofuels the corresponding physical and chemical properties were determined. Based on the results of research, it was found that the complex of quality indicators of diesel fuel of petroleum origin and samples of rapeseed oil esters slightly differs from the indicators of petroleum diesel fuel, and, also, number of indicators of environmental properties are better than those of fuel of petroleum origin.

KEY WORDS: *OIL REFINING INDUSTRY, DIESEL FUEL, DIETARY SUPPLEMENTS, OPERATIONAL PROPERTIES.*

Introduction

Diesel fuel (DF) is one of the most popular types of fuel used for internal combustion engines. It is more economical than gasoline, and it is also cheaper [1,2].

However, when diesel fuel is burned, the exhaust gases of cars with diesel engines contain carbon oxides, sulphur, nitrogen, soot, hydrocarbons and carcinogenic polycyclic hydrocarbons. During the combustion of fuel containing sulphur impurities, mainly sulphur dioxide is formed. When ash elements (for example, metal-containing additives) are retained, some of the sulphur is converted to sulphates and released as solid particles. Sulphur dioxide irritates the respiratory system, participates in the formation of acid rain, in corrosion processes, and destroys catalytic converters. Consequently, tougher standards for emissions of harmful substances from the exhaust gases of internal combustion engines, limiting carbon dioxide emissions, as well as saving energy carriers of petroleum origin, force most countries to look for ways to reduce the risk of heat engines affecting the environment. These problems of our time have led to tougher requirements for the environmental properties of oil refining products.

The study of diesel fuel quality indicators with the addition of rapeseed oil methyl ester (ROME) and rapeseed oil isopropyl ester (ROIE) was carried out using standard methods regulated by technical regulations [3-5].

The Euro 6 environmental standard, which came into force in 2015, provides for a halving of nitrogen dioxide emissions for diesel vehicles produced later than this deadline. One of the methods to solve this problem is to add a certain amount of environmentally friendly bio-components to diesel fuels.

Diesel biofuels have become increasingly widespread abroad in recent years. An increase in diesel fuel production from vegetable raw materials is observed in a number of Western European countries, primarily in Germany and France, as well as in the United States, Brazil, and Malaysia [6]. In European countries, the production of diesel biofuels focuses on the use of rapeseed oil, including from rapeseed grown in Ukraine. In the United States and Brazil, they prefer the production of biodiesel from soybean oil, and in Southeast Asian countries - from palm oil [7]. A mixture of complex methyl esters obtained based on rapeseed oil (ROME) is used as 100% diesel fuel in tractors that are operated in Austria. In France, a mixture of diesel fuel with 5% ROME was used. In the United States, soybean oil-based methyl esters are used as a 100% non-fuel or as a 20% supplement to petroleum fuel. Unfortunately, in Ukraine, this problem is more theoretical in nature in the absence of data on the results of a study of the mass use of bio-components for diesel fuel. The quality of diesel fuels made from vegetable raw materials differs from oil, which is due to the difference in chemical composition. The methyl and isopropyl esters of rapeseed and soybean oils closest to diesel fuel, and methyl esters based on palm oil differ significantly in their properties [8, 9].

Materials and Methods

Standards for biodiesel mixtures are constantly being revised ASTM International (American society for testing and materials) for adopting biodiesel mixtures by manufacturers of components for cars (Original Equipment manufacturer – OEM). The EU regulates the requirements for biodiesel EN 14214:2003 «Automotive fuels – Fatty acid methyl esters (FAME) for diesel engines – Requirements and test methods», in the USA – ASTM D 6751 «Standard Specification for Biodiesel Fuel Blend Stock (B100) for middle Distillate Fuels».

In Ukraine, the quality of biodiesel fuel is regulated by DSTU 6081:2009 "Motor fuel. Esters of methyl fatty acids of oils and fats for diesel engines. Technical specifications", DSTU 7178:2010 "Alternative fuel. Ethyl esters of fatty acids of oils and fats for diesel engines. Technical requirements and control methods, DSTU 7688:2015 "Euro diesel fuel. Technical requirements", DSTU 8695:2016 "Alternative fuel for diesel engines. Technical requirements". According to the technical regulations on requirements for automobile, diesel, marine and boiler fuels and DSTU 7688:2015, the use of methyl or ethyl esters of fatty acids up to 7% is provided. The process of obtaining rapeseed oil esters is based on the reaction of transesterification of rapeseed oil with isopropyl or methyl alcohols using an alkaline catalyst – potassium alcoholate. The transesterification reaction consists of adding alcohol to triglyceride in the presence of an alkaline catalyst, and esters and glycerol are formed. The latter practically does not mix with esters.

Transesterification was performed in a glass reactor with the separation of the glycerol fraction from below. The reaction mixture was stirred at a temperature of 60 °C with a glass agitator using an electric motor. The temperature was maintained by a temperature-controlled water bath. At the end of the reaction, the mixture is gravitationally separated into two layers: biodiesel and glycerol, which settles on the bottom of the flask. By chemical composition, the new biodiesel fuel is isopropyl esters of rapeseed oil and is a yellow-lemon-collared liquid with a pungent alcohol smell [10-13].

Rezults and discussions

At the next stage of the work, the physical and chemical properties of L-grade diesel fuel of petroleum origin, which is produced at PJSC Ukrtatnafta, as well as its biocomponents - ROME and ROIE - were studied.

Table 1 shows the characteristics that are most important for comparing petroleum fuel and rapeseed oil acid esters and are determined according to standard methods. As can be seen from the table, all the properties of biocomponents are somewhat different from fuels of petroleum origin. The cetane number is the main indicator of the flammability of diesel fuel. It determines engine start, working process stiffness (pressure build-up rate), fuel consumption, and exhaust gas smokiness. The higher the cetane number of the fuel, the lower the pressure build-up rate and the less rigid the engine runs.

As can be seen from the table, the cetane number of rapeseed oil esters is slightly higher than the cetane number of diesel fuel of petroleum origin. Viscosity and density determine the processes of evaporation and mixing in diesel.

Table 1. *Physical and chemical parameters of Euro 5 diesel fuel of the "L" brand and alternative fuels*

Indicator	Test methods	Norm for DF according to DSTU 7688:2015	Actual data		
			Diesel fuel	Rapeseed oil isopropyl Ester	Rapeseed oil methyl ester
Cetane number, not less than	DSTU ISO 5165	51	49	53	54
Density at a temperature of 15 ° C, kg/m^3, within	DSTU ENISO 3675	820-845	835	875	880
Mass fraction of polycyclic aromatic hydrocarbons,%, max	DSTU EN 12916	8	7	0	0
Sulphur content, mg / kg, no more than	DSTU ENISO 20884	10	8	4	3
Flash point in a closed crucible, ° C, not lower than	DSTU ISO 2719	55	58	62	59
Ash content, % (WT.), no more than	DSTU ENISO 6245	0,005	0,004	0,004	0,003
Lubricity: wear spot diameter at 60 ° C, microns, max	DSTU ISO 12156	460	450	420	430
Kinematic viscosity at a temperature of 40 ° C, mm2 / s, within	DSTU ГОСТ 33	2,00-4,50	3,7	12,1	5,6
Maximum filterability temperature, ° C, not higher than	DSTU EN 116	–5	–10	–3	–8

As can be seen from the table, all the properties of bio-components are somewhat different from fuels of petroleum origin. The cetane number is the main indicator of the flammability of diesel fuel. It determines engine start, working process stiffness (pressure build-up rate), fuel consumption, and exhaust gas smokiness. The higher the cetane number of the fuel, the lower the pressure build-up rate and the less rigid the engine runs. As can be seen from the table, the cetane number of rapeseed oil esters is slightly higher than the cetane number of diesel fuel of petroleum origin.

Viscosity and density determine the processes of evaporation and mixing in diesel. Lower density and viscosity provide better fuel atomization, with an increase in these quality indicators, the diameter of the droplets increases and their complete combustion decreases, as a result, the specific fuel consumption increases, and the smoke content of exhaust gases increases. Bio-components differ slightly from diesel fuel of petroleum origin in these indicators. They have a higher density at 15° C. This is due to their chemical structure. Unlike petroleum fuel hydrocarbons, which contain between 5 and 16 carbon atoms, hydrocarbon chains of Ester molecules contain an average of 14-26 carbon atoms. This leads to higher values of molecular weight, and, accordingly, density. In addition, due to the longer length of the hydrocarbon chain, the viscosity of bio-components increases compared to the viscosity of Petroleum Fuel.

As the fuel viscosity increases, the resistance of the fuel system increases, and the pump filling decreases, which can lead to interruptions in its operation. When the viscosity of diesel fuel decreases, the amount of it that seeps between the plunger and the bushing increases compared to working on more viscous fuel, as a result, the pump performance decreases.

Sulphur compounds, unsaturated hydrocarbons and metals affect carbon deposits in diesel engines and cause increased corrosion and wear. During the combustion of fuel containing unsaturated hydrocarbons, due to oxidation, resinous substances are formed in the engine cylinder, and then carbon deposits. As a result, power drops and engine parts wear increases. Fuel reduces the friction force of parts in fuel pumps and injectors, as well as the piston against the cylinder mirror, as evidenced by the lubricity of diesel fuel. Pollutants reduce this ability.

The presence of water has a particularly negative effect. It can be concluded that carbon deposits in the engine directly depend on such indicators of diesel fuel as coking, sulphur and resin content, fractional composition, the amount of aromatic and unsaturated hydrocarbons, ash content. According to these indicators, biocomponents have significantly better properties than petroleum fuel [14]. The maximum filterability temperature makes it possible to assess the low-temperature properties of fuel, namely fluidity and pumpability at low temperatures. In biocomponents, this temperature is slightly higher.

Another important property of diesel fuel is the flash point. For diesel engines (especially those with direct injection), it is very important at what temperature the fuel mixture ignites. The selection of the optimal temperature contributes to the complete combustion of diesel fuel. If the temperature is too low (or vice versa high), then some components of the substance - mainly unsaturated hydrocarbons - do not burn completely, forming carbon deposits on the surface of cylinders, spark plugs and other engine elements.

The mass fraction of polycyclic aromatic hydrocarbons in diesel fuel indicates its environmental characteristics. As the content of aromatic hydrocarbons in internal combustion engine fuels increases, the amount of benzapyrene increases. For this reason, the content of polycyclic aromatic hydrocarbons is limited by legislative acts of a number of foreign countries to the level of 6-11%.

The sulphur content is the main indicator of the environmental properties of diesel fuel. Sulphur exhaust gases form acids when interacting with water. Sulphur causes damage not only to nature, but also to the engine - its combustion products provoke metal corrosion, and when they come into contact with engine oil, solid deposits are formed (the engine is coked). It should be noted that the bio-components do not contain polycyclic aromatic hydrocarbons, and the sulphur content is very low.

According to the requirements of DSTU 7688:2015, the amount of bio-components in diesel fuel can be no more than 7%, since diesel with a higher content of bioadditives cannot be used as standard in most cars with diesel engines. A higher ratio of dietary supplements in diesel is also allowed, but in this case, it would be necessary to additionally adapt the fuel supply system, since biodiesel, in comparison with conventional diesel, is more aggressive to the components of the fuel system. The time between oil and filter changes will also be reduced. Therefore, this amount of bio-components was added to diesel fuel of petroleum origin. Mixtures of petroleum fuel and biocomponents were prepared by stirring for 10 minutes using a mechanical homogenizer.

The mixtures did not contain water and did not delaminate. As a result, two types of fuel were obtained: DP + 7% isopropyl ester of rapeseed oil and DP + 7% methyl ester of rapeseed oil.

In the resulting biofuels, the corresponding physical and chemical properties were determined, which are given in Table. 2.

When biocomponents were added to petroleum fuels, the cetane number increased. Moreover, the higher this indicator, the lower the noise level and smoke during engine operation. In addition to our research, these data are confirmed by more than twenty years of experience in using such fuel in Europe and the United States.

Table 2. *Physical and chemical parameters of alternative diesel fuel with bio-components*

Indicator	Test methods	Norm for DF according to DSTU 7688: 2015	Actual data	
			DF + 7% rapeseed oil isopropyl Ester	DF + 7 % rapeseed oil methyl ester
Cetane number, not less than	DSTU ISO 5165	51	51	51
Density at a temperature of 15 °C, kg/m^3, within	DSTU ENISO 3675	820-845	842	839
Mass fraction of polycyclic aromatic hydrocarbons,%, max	DSTU EN 12916	8	7	7
Sulphur content, mg / kg, no more than	DSTU ENISO 20884	10	7,2	7,1
Flash point in a closed crucible, °C, not lower than	DSTU ISO 2719	55	60	59
Ash content, % (WT.), no more than	DSTU ENISO 6245	0,005	0,004	0,004
Lubricity: wear spot diameter at 60 °C, microns, max	DSTU ISO 12156	460	430	438
Kinematic viscosity at a temperature of 40 °C, mm2 / s, within	DSTU GOST 33	2,00-4,50	4,3	3,9
Maximum filterability temperature, ° C, not higher than	DSTU EN 116	–5	–6	–9

The density and viscosity due to bio-components have slightly increased, but the new values meet the requirements of the regulatory document. This will ensure the pumping of fuel through the vehicle's fuel system and ensure its anti-wear properties. This is also confirmed by the fact that the area of the lubricating film covering the surface increases when using biocomponents.

In terms of sulphur content, ash content and mass fraction of polycyclic aromatic hydrocarbons, the new biofuel has significantly better performance compared to petroleum, which improves its environmental properties.

Another advantage is that fuel with the addition of methyl and isopropyl esters of rapeseed oil has improved cleaning properties. The remaining indicators are within the requirements of DSTU 7688:2015.

Conclusions

1. Based on the results of research, it was found that the complex of quality indicators of diesel fuel of petroleum origin and samples of rapeseed oil esters differs slightly from the indicators of petroleum diesel fuel, and a number of indicators of environmental properties are better than those of fuel of petroleum origin.

2. As a result, it was found that when biocomponents are added to petroleum diesel fuel in the amount of 7%, the indicators of environmental properties improve first of all: sulphur content, mass fraction of aromatic hydrocarbons, ash content. It also increases the cetane number and significantly improves the lubricity, which increases the service life of the car engine. In addition, biodiesel saves fuel costs because it is cheaper than petroleum diesel fuel.

References

1. V.G. Spirkin, I.R. Tatur, B.P. Tonkonogov and others; Edited by Spirkin V.G., Tatur I.R. Chemmotology. Properties and application of fuels, lubricants and special materials: Textbook: in 2 hours - Part 1. Properties and application of fuels and special materials (2014). M.: Gubkin I. M. Russian State University of Oil and Gas. 246 p.

2. C.V. Boichenko, A.P. Pushak, P.I. Topilnytskyi, K.Leida Motor fuels: properties and quality. Textbook (2017). K.: Center for educational literature. 324 p.

3. Topilnytskyi P.I., Hrynyshyn O.B., Machynskyi O.Ya. Technology of primary oil and gas refining: textbook (2014). Lviv: Lviv Polytechnic Publishing House. 468 p.

4. Pichugin V.F., Ivanova L.V. Burov Ye.A. Improving the tribotechnical characteristics of metal vapors in diesel fuel when introducing an additive (2013). In: Chemistry and Technology of Fuels and Oils, vol. 4 (578), P.20-22.

5. Technical regulations on requirements for automobile gasoline, diesel, marine and boiler fuels. Access mode:https://zakon.rada.gov.ua/laws/show/927-2013-%D0%BF

6. A.B. Vipper, A.Yu. Yevdokimov Diesel fuels based on vegetable raw materials abroad (2004). In: Oil Refining and Petrochemistry, vol 6, 2004. P.11-14.

7. B. Prebo, A.Thurlo Pearson Improving the production of biodiesel in the United States (2011). In: Oil and Gas Technologies, vol. 3. P.85-87.

8. Pankin K.E., Ivanova Yu.V., Kuzmina R.I., Shtykov S.N. Comparison of liquid biofuels with petroleum fuels by operational characteristics (2011). In: Chemistry and Technology of Fuels and Oils, vol. 2. P. 23-25.

9. Pankin K.E., Ivanova Yu.V., Kuzmina R.I., Shtykov S.N. Comparison of liquid biofuels with petroleum fuels by environmental characteristics (2011). In: Chemistry and Technology of Fuels and Oils, vol. 3, P. 3-6.

10. Tkachuk V.V, Zakharchuk V.I. Production technology and operational characteristics of rapeseed oil isopropyl ether (2012). In: Chemistry and Technology of Fuels and Oils, vol. 6, P. 3-6.

11. Tkachuk V.V. Commodity science aspect of biodiesel production and consumption: monograph (2011). Lutsk: Editorial and Publishing Department of LNTU, 137 p.

12. Tkachuk V.V. Technical and economic calculation of biodiesel production [monograph] / collective of authors edited by K. Leidu (2019). Rzeszow: Rzeszow Polytechnic named after I. Lukasevich, 2019-Section 9. Technical and economic calculation of production, P. 83-89.

13. Iu. Melnic., V. Tkachuk, O. Rechun, Study of operational properties of motor biofuels (2019). In: Mechanization in agriculture & converving of the resources (International scientific journal). Issue 2. Bulgaria. P. 70-71.

14. Peng Deshin. Biodiesel for improving the lubricating properties of diesel fuels with low sulfur content (2016). In: Chemistry and Technology of Fuels and Oils, vol. 6, P.46-48.

Evaluation of the tire cross-section shape in relation with the traction force and traction efficiency of an agricultural tire

Radu Rosca[1,*], Petru Cârlescu[1], Ioan Țenu[1]
University of Agricultural Sciences and Veterinary Medicine "Ion Ionescu de la Brad" Iași, Romania[1]
*rrosca@uaiasi.ro

Abstract: *In this paper the traction force and traction efficiency of an agricultural type tire were evaluated, using a semi-empirical traction model of the driving wheel of a Romanian tractor; the model is based on Bekker's pressure-sinkage relationship and on the ASAE equations for traction force and traction efficiency.*

Tire deformation under vertical load was taken into account by the means of tire volume stiffness; three variants were considered in terms of tire cross-section: elliptical shape, spherical segment shape and toroidal shape.

Experimental data, obtained when ploughing operations were performed, were used in order to validate the results predicted by the models, using goodness-of-fit analysis.

It was concluded that the model based on the spherical segment shape of the tire cross section provided acceptable results for both traction force and traction efficiency in comparison with the experimental values; the other two models were more accurate in relation with the traction force, but proved to be less precise when referring to traction efficiency.

Keywords*: TRACTION MODEL, TRACTION FORCE, TRACTION EFFICICENCY, AGRICULTURAL TIRE, TIRE CROSS-SECTION*

1. Introduction

The agricultural tractor is rather a heavy machine and is used for a variety of operations, from tillage to haulage, under diverse conditions. The understanding and prediction of tractor performance has been a major goal of many researchers as it is necessary to understand the traction process in order to predict tractor performance in the field. In this context, computer models and simulation programs for predicting tractor performance help researchers to determine the relative importance of many factors affecting field performance of tractors, without conducting expensive and time consuming field tests.

The traction process has a significant effect over fuel consumption, yield and soil compaction [1].

Soil compaction is one of the main dangers threatening the agricultural land [2] and one of the most importance processes affection crop production [3]. This is why accurate prediction of tire traction may be an important tool for the management and control of soil compaction.

The models concerning tire-soil interaction may be divided into three main categories [1, 4]:

- empirical models, which relate vehicle and terrain characteristics by the means of experimental tests; these are simple models, but their predictions are difficult to extrapolate for other conditions then the ones in which the respective model was developed.
- numerical models, which take into account the mutual deformation of tire and soil in order to predict the traction parameters; these models use the Finite Element Method (FEM) in order to describe the tire-ground interaction and are expected to provide the most accurate results, but they require accurate values for a great number of tire and soil parameters. Moreover, the high variability of the soil material makes the accurate measurement of its parameters difficult. Other models, like the ones based on Artificial Neural Networks (ANNs) require a large number of experimental data for the formulation, training and validation of the respective model; in the meantime, there is no certainty that the model is adequate for other field conditions than the initial ones.
- semi-empirical models improve the empirical models by modelling some of the physical processes connected to tire-soil interaction. The basis for this type of models was laid by Bekker in 1956 [5]; the pressure-sinkage relationship that he developed describes soil properties.

Semi-empirical models are a reasonable compromise between the simpler empirical models, for which the range of applicability is limited to the cases having similar conditions to the ones from which the models were derived, and the analytical models, which require in situ evaluation of a large number of soil and tire properties [6].

Although many semi-empirical models for the estimation of models tire-soil contact process were developed, they generally do not take into account tire volume and tire stiffness [2].

In this study a semi-empirical model for predicting the traction force and traction efficiency for a 2WD agricultural tractor was considered, assuming that the shape of the tyre–ground contact area is a super ellipse; tire deformation under vertical load was taken into account by the means of tire volume stiffness; three variants were considered in terms of tire cross-section geometry: elliptical shape, spherical segment shape and toroidal shape.

2. Basic model

The model is based on the one presented in a previous paper [6] – fig. 1; it is assumed that, under the vertical load G, the wheel sinks into the soil, reaching the depth z_c and the load induces tyre deflection z_p.

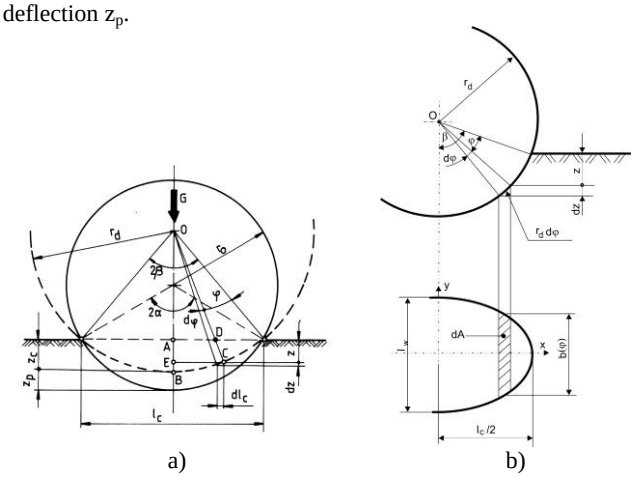


Fig. 1 *Wheel soil interaction model*
a) wheel and soil deformation; b) contact surface

The basic equation of the model is:

(1) $G = p \cdot A = q_p \cdot \Delta V_p$,

where p is the tire-ground contact pressure, A is the area of the contact patch, q_p is the tire volume stiffness and ΔV_p is the volume change of the tire in the contact area.

The tire-ground pressure was connected to the sinkage depth (z_c) using the Bekker pressure-sinkage relationship:

(2) $p = k \cdot z^n$,

where k and n are soil constants.

Tire deflection z_p is affected by the volume change ΔV_p, which

will be addressed in the next section.

The traction force was calculated assuming that it is limited only by the soil shear strength, based on the Mohr– Coulomb equation (Maclaurin, 2007) for the maximum shear stress:

(3) $\tau_{max} = c + p \cdot tg\varphi$

where c is soil cohesion [kPa], p is the vertical pressure [kPa] and φ is the internal friction angle.

The traction force and traction efficiency were calculated using the formulae given in the ASAE S296 standard [7]:

(4) $F_{t,ef} = F_t - R_r$

(5) $R_r = G \cdot \left(\frac{1}{B_n} + 0.04 + \frac{0.5 \cdot s}{\sqrt{B_n}} \right)$

(6) $\eta_{tr} = (1-s) \cdot \left(1 - \frac{R_r}{F_t} \right)$

where F_t is the traction force due to the shear stress at the tire-soil interface, R_r is the rolling resistance of the wheel, B_n is the wheel numeric and s is the wheel slip.

3. Tire deformation

In order to evaluate the volume change of the tire in the contact area, due to vertical load, three cases were taken into account:

- elliptical shape of the tire cross-section;
- spherical segment shape of the tire;
- toroidal shape of the tire.

3.1. Elliptical shape of the tire cross-section

For this variant the shape of the tire cross-section was considered to be an ellipse [8]; under vertical load, the cross-section is deformed (Fig. 2), with the minor axis decreasing from h to h-z_p and the major axis increasing from b to l_w.

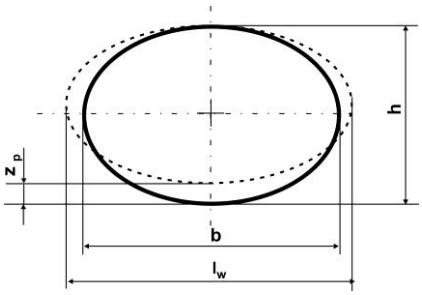


Fig. 2. *Elliptical shape of tire cross-section*

b-tire width (unloaded state);
h – tire section height (unloaded state).

The major axis of the ellipse was calculated assuming that the perimeter remained the same:

(7) $l_w = \sqrt{b^2 + 2 \cdot h \cdot z_p - z_p^2}$

The tire volume change ΔV_p was calculated as the cross-section area multiplied by the length of the contact patch:

(8) $\Delta V_p = 0{,}5 \cdot \pi \cdot \left[\alpha \cdot r_0 \cdot b \cdot h - \beta \cdot r_d \cdot l_w \cdot (h - z_p) \right]$,

with the terms of the equation defined according to Fig. 1 and Fig. 2.

3.2. Tire as a spherical segment

In this variant the tire was considered as a spherical segment, delimited by two symmetrical vertical planes and by the rim (Fig. 3).

The tire volume change due to vertical load was calculated with the formula:

(9) $$\Delta V_p = \alpha \cdot b \cdot \left[0{,}5 \cdot \left(\frac{d_i}{2} + x \right)^2 + 0{,}5 \cdot r_0^{\,2} + \frac{b^2}{24} - \frac{d_i^2}{4} \right] - \beta \cdot b \cdot \left[0{,}5 \cdot \left(\frac{d_i}{2} + x_d \right)^2 + 0{,}5 \cdot r_d^{\,2} + \frac{b^2}{24} - \frac{d_i^2}{4} \right] \cdot$$

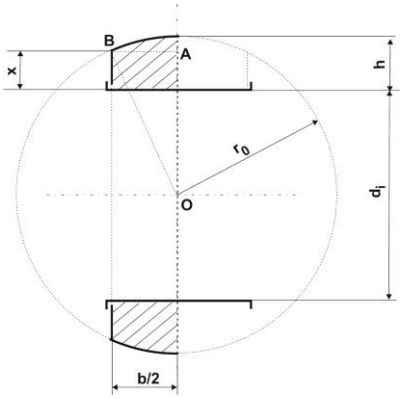


Fig. 3. *Tire as a spherical segment (unloaded state)*

d_i – rim diameter;
b-tire width;
h – tire section height;
r_0 – tire free radius.

3.3. Tire as a toroid

In this case the tire was considered to be a toroid, as shown in Fig. 4; in the loaded condition, the tire section height has decreased from h to h-z_p and tire radius in the contact area has increased from r_0 to r_d (see also Fig. 1). This assumption was also addressed by other authors [9].

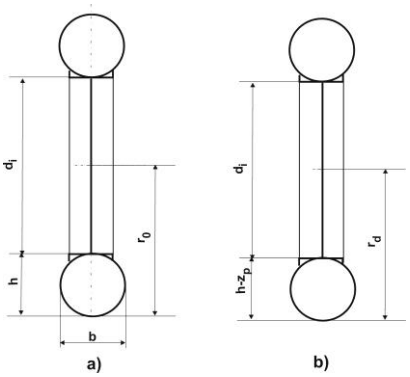


Fig. 4. *Tire as a toroid*

a) unloaded state dimensions;
b) loaded state dimensions.

The tire volume change for this case was given by the formula:

(10) $$\Delta V_p = \frac{\alpha \cdot \pi \cdot h^2}{2} \cdot \left(r_0 - \frac{h}{2} \right) - \frac{\beta \cdot \pi \cdot (h - z_p)^2}{2} \cdot \left(r_d - \frac{r_d - 0{,}5 \cdot d_i}{2} \right)$$

4. Experimental data and goodness-of-fit analysis

Experimental tests were performed in order to obtain data regarding the traction force and traction efficiency; the values predicted by the models were then compared with the experimental data based on a goodness-of-fit analysis.

The traction tests were performed during ploughing with the P2V variable width plough, using the Romanian 2WD tractor U-650; the tractor was fitted with a dynamometric frame and an electronic dynamometer. The main characteristics of the tractor, and drive tyre are summarized in Table 1.

Soil characteristics on the test field are shown in Table 2.

Table 1: *Characteristics of the U-650 tractor and drive wheels*

Item	Value
Load on the drive tire [kN]	11.75
Type of drive tire	14.00 – 38
Overall diameter of tire [m]	1.58
Tire width [m]	0.367
Lug width [m]	0.04
Lug length [m]	0.24
Lug height [m]	0.025
Distance between lugs [m]	0.195
Transversal radius of the under tread [m]	0.3

In order to evaluate the goodness-of-fit between model and

experimental data the following criteria were considered [10]:

- mean absolute deviation (MAD) – represents the mean of the absolute value of the deviation between each model prediction and its corresponding data point:

Table 2: Characteristics of the test soil

Item		Value
Soil deformation modulus, K [m]		0.05
Coefficients for the sinkage equation	k	55
	n	1.3
Soil cohesion, c [kPa]		25
Angle of internal friction, γ [^{0}]		32
Average cone penetrometer index, CI [kPa]		970

$$MAD = \frac{\sum_{i=1}^{n} |m_i - d_i|}{n} \quad (11)$$

where m_i is the model mean for point i, d_i is the data mean for each point i and n is the number of points being compared;

- root mean squared deviation (RMSD):

$$RMSD = \sqrt{\frac{\sum_{i=1}^{n} (m_i - d_i)^2}{n}} \quad (12)$$

- mean scaled absolute deviation (MSAD):

$$MSAD = \sum_{i=1}^{n} \frac{|m_i - d_i| \cdot \sqrt{m_i}}{n \cdot s_i} \quad (13)$$

where m_i is the number of values contributing to each experimental data mean d_i (in our case $m_i = 4$) and s_i is the standard deviation for each data mean. A MSAD value of 1.5 shows that, on average, the model was 1.5 standard errors off from the experimental data.

- Pearson correlation coefficient r^2;
- percentage of points within 95% confidence interval of data (Pw95CI) – represents the percentage of model predictions that lie within the 95% confidence interval of each corresponding experimental data point

The analysis was applied to both traction force and traction efficiency data.

5. Results and discussion

Fig. 5 and 6 present the results concerning the traction force and traction efficiency of the tire, for the three variants taken into account; the experimental data is also shown in the respective charts.

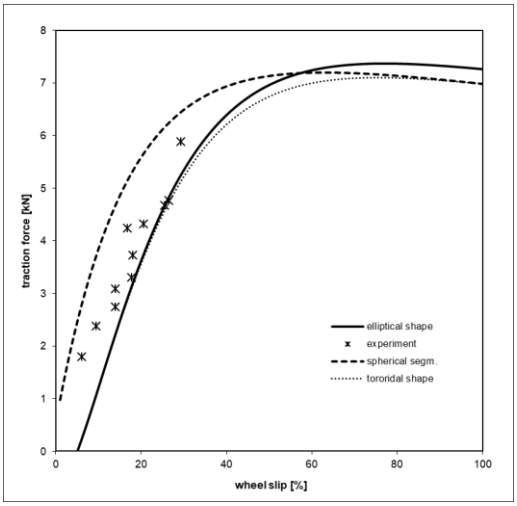


Fig. 5. *Model and experimental results for traction force*

The data in Fig. 5 shows that the variants for the elliptical shape of the tire cross-section and the toroidal shape of the tire predicted quite similar values for the traction force for wheel longitudinal slip lower that 30%; the values provided by the respective models were generally lower than the ones obtained during field tests.

On the other hand, the model based on the spherical segment shape of the tire has provided significantly higher values for the traction force in comparison with experimental data.

Table 3 presents the results of the goodness-of-fit a between the experimental data and the model data; from this point of view the best goodness-of-fit is achieved for the first and third model. Nevertheless, the Pearson correlation coefficient r^2 is only 5.6% lower for the spherical segment model in comparison with the other two models.

Table 3: Goodness-of-fit analysis for traction force

Item	Model		
	elliptical cross-section	spherical segment shape	toroidal shape
r^2	0.952	0.897	0.951
MAD	0.6927	1.3617	0.7502
MSAD	4.195	6.785	4.391
Pw95CI [%]	66.7	22.2	66.7
RMSD	0.8613	1.4163	0.8899

Fig. 6 presents the results concerning the traction efficiency data; the chart clearly shows that the model based on the spherical segment shape of the tire best fits with the experimental results. This assumption was confirmed by the results of the goodness-of-fit analysis, which are summarized in Table 4.

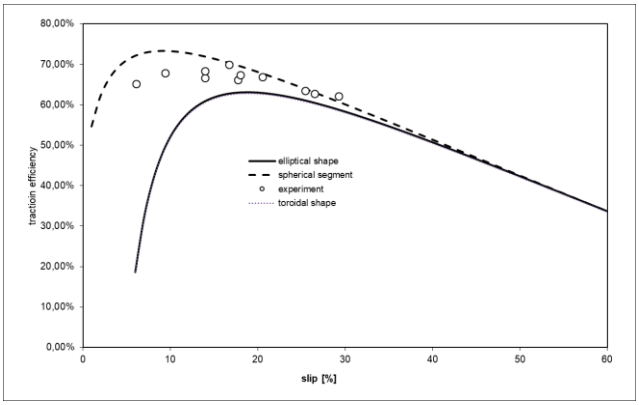


Fig. 6. *Model and experimental results for traction efficiency*

Table 4: Goodness-of-fit analysis for traction efficiency

Item	Model		
	elliptical cross-section	spherical segment shape	toroidal shape
r^2	0.013	0.657	0.013
MAD	0.1087	0.0241	0.1104
MSAD	1.861	0.454	1.888
Pw95CI [%]	77.8	100	77.8
RMSD	0.1746	0.0333	0.1742

Thus, for the above mentioned model, all the items addressed by the goodness-of-fit analysis were more favourable in comparison with the other two models (higher r^2, lower MAD, MSAD and RMSD, all the model points within the 95% confidence interval of the experimental data).

6. Conclusions

A modified semi-empirical model for the prediction of traction performance of a tractor driving wheel is presented in this study. The model took into account three variants for the shape of the tire:

- elliptical shape of the tire cross-section;
- spherical segment shape of the tire;
- toroidal shape of the tire.

Each of the above mentioned variants led to a different equation for calculation the volume changes of the tire in the contact area,

due to vertical load.

Experimental results from ploughing tests were used in order to validate and verify the applicability of the model, by the means of a goodness-of-fit analysis.

The goodness-of-fit analysis showed that, when considering the traction force data, the Pearson coefficient r^2 was comprised between 0.897 and 0.952, depending on the model taken into account; when referring to traction efficiency, only the model based on the spherical segment shape of the tire provided reliable results (r^2=0,657, compared to 0.013 for the other two models.

Overall, it was concluded that the model based on the spherical segment shape of the tire could be considered as the best compromise for predicting reliable data for both the traction force and traction efficiency.

However, it should be mentioned that the models were confronted with experimental data collected for one type of soil and a certain soil condition; further tests, performed on different soils and in different conditions, have the potential to improve the accuracy of the model.

7. References

1. K. Pentos, K. Pieczarka, K. Lejman, "Application of Soft Computing Techniques for the Analysis of Tractive Properties of a Low-Power Agricultural Tractor under Various Soil Conditions", Complexity, **2020**, Article ID 7607545, (2020) https://doi.org/10.1155/2020/7607545
2. E. Diserens, P. Défossez, A. Duboisset, A. Alaoui, "Prediction of the contact area of agricultural tractor tyres on firm soil", Biosystems Engineering, **110**, 73-82 (2011)
3. A. Mohsenimanesh, S.W. Ward, P.O.M. Owende, A. Javadi, "Modelling of pneumatic tractor tyre interaction with multi-layered soil", Biosystems Engineering, **104**, 191-198 (2009)
4. J. Dallas, M.P. Cole, P. Jayakumar, T. Ersal, "Neural network based terramechanics modelling and estimation for deformable terrains", Technical Report , US ARMY CCDC GVSC WARREN United States, Defense Technical Information Center (2019), on-line at: https://apps.dtic.mil/dtic/tr/fulltext/u2/1080945.pdf
5. M. Schreiber, H.D.Kutzbach, "Influence of soil and tire parameters on traction", Research in Agricultural Engineering, **54**, 43-49 (2008)
6. R. Rosca, P. Cârlescu, I. Tenu, "A semi-empirical traction prediction model for an agricultural tyre, based on the super ellipse shape of the contact surface", Soil&Tillage Research, **141**, 10-18 (2014)
7. ASAE D497.7, *Agricultural Machinery Management Data* (St. Joseph, Michigan, U.S.A., 2011)
8. Koutný F., *Geometry and mechanics of pneumatic tires* (Zlin, CZE, 2007), on-line at: http://wanderlodgegurus.com/database/Theory/TireGeometry.pdf
9. F. Ziani, J. Biarez, " Pressure sinkage relationship for tyres on very loose sand", Journal of terramechanics, **27** (3), 167-177 (1990)
10. C.D. Schunn, D. Wallach D., *Evaluating goodness-of-fit in comparison of models to data*, in Psychologie der Kognition: Reden and Vorträge anlässlich der Emeritierung (University of Saarland Press, Saarbrueken, Germany, 2005), 115-154

Study of the influence of the irrigation regime on the yield of short-fruited cucumbers grown in open areas under drip irrigation

Rumiana Kireva, Miho Mihov
Institute of Soil Science, AgroTechnology and Plant Protection "Nikola Pushkarov", Sofia, Bulgaria

Email: R.Kireva@abv.bg ; M.Mihov@abv.bg

Summary: *In order to establish the irrigation regime of short-fruited cucumbers in open areas in the soil-meteorological conditions of the area of the village of Chelopechene - Sofia, researches were carried out in drip irrigation of cucumbers variety "Levina", testing different regimes - from full satisfaction of daily needs the culture from water to irrigation with reduction by 30% of the irrigation norm. A variant with a 30% increase in the irrigation rate was also tested.*

The obtained results show that the cultivation of short-fruited cucumbers for fresh consumption in open areas requires 15 waterings with an average irrigation rate of 18.3 mm, which is realized at different intervals depending on plant development and the stress of metrological factors and irrigation rate 280 mm.

The realized irrigation regimes have influenced the formation of yields of short-fruited cucumbers. The yields during the three years of the experiment varied from 2368 to 5404 kg / dka, with the highest yields being obtained in the first and second years. Yields in the third year were lower by 30% as a result of adverse weather conditions, which led to a shortening of the growing season of the crop.

KEY WORDS: *IRRIGATION REGIME, DRIP IRRIGATION, YIELDS, SHORT-FRUITED CUCUMBERS, IRRIGATION RATE, VEGETABLE CROPS*

Introduction

Climate change due to global warming has a significant impact on water resources, including groundwater and surface water (Ziad A. M. and S. A. Jamous, 2010). Drought periods vary in duration and time of onset.

Under the new conditions of agricultural development, water appears as a limiting factor and becomes extremely important from an ecological and economic point of view. It is also a decisive factor for the manifestation of the maximum productive possibilities of agricultural crops with the optimal supply of plants with water.

The saving of irrigation water can be achieved by using efficient methods, such as optimizing the parameters of the applied irrigation regime, and applying water-saving irrigation technologies.

It has been experimentally found that vegetable crops, including cucumbers, respond very well to drip irrigation, both in terms of quantity and quality of production and in terms of irrigation water productivity. This is due to its relatively underdeveloped root system and the structure of its leaf apparatus with poorly developed cuticle (Shaban, N, et al., 2014).

For their normal development and fruiting it is necessary for the soil moisture to be over 80% of WHC (Murtazov et al., 1975), as the best results in terms of water use by plants are obtained by drip irrigation, and the increase in yields reaches from 15% to 18% relative to sprinkling and gravity irrigation (Clark, 1979)

In connection with the cultivation of vegetable crops in the Sofia region, the following more important conclusions can be made regarding its natural resources.

The area is suitable for growing vegetable crops, as the temperature conditions meet their requirements. The duration of the period with stable retention of the average daily air temperatures above 10^0C is 180 - 200 days. The temperature sum for this period is 3300 - 3500^{0}C. This temperature amount is sufficient for the development of basic vegetable crops. (Hershkovich and Stefanov, 1982).

The aim of the present study is to establish the irrigation regime and its influence on the yields of cucumbers grown on irrigated areas under drip irrigation.

Material and method

The studies for establishing the irrigation regime of short-selling cucumbers, Levina variety grown in open areas under drip irrigation were conducted in the experimental field of the N. Pushkarov Institute in Chelopechene, Sofia region, Bulgaria.

The following irrigation options were tested:

Pre-irrigation humidity - 85% of WHC

- 130% implementation of irrigation rate / variant M_{130} /;
- 100% implementation of irrigation rate / variant M_{100} /;
- 70% realization of the irrigation rate / variant M_{70} /;

Irrigation rates are calculated by the formula:

$$m = \left[10.Ha.\ \left(ППВ - \delta_T пр.вл.\right)\right].K$$

where: m is the magnitude of the irrigation rate, mm;

α - the bulk density of the soil in gr / cm3;

H - the depth of the active soil layer in m (in the experiment H = 0.5 m);

ППВ - the maximum field moisture content in% relative to the absolutely dry weight of the soil;

δт пр. вл - the pre-irrigation soil moisture in% in relation to the absolutely dry weight of the soil;

K - the coefficient of reduction of the irrigation rate, taking into account the area occupied by the plants in 1 da. In the experiment K = 0.67, i.e. 67% of the area is irrigated.

In the case of drip irrigation, the amount of the entire irrigation rate is not given, as in the case of other watering methods. Reduction is required at the expense of the non-irrigated area. For this purpose, the formula of (Ferckman, Grazoli, 1980) was used, taking into account the planting scheme. After calculating the irrigation norm for variant M_{100}, the norms of the other variants are established according to its size.

The experiment was performed on leached cinnamon forest soil, which is characterized by the following water - physical properties: WHC - 20.2 relative to the absolute weight of the soil, bulk density at WHC 1.54

Results

The meteorological conditions under which the field experiments with the crop were carried out in relation to the amounts of

precipitation for the period April - September in the first two years are characterized in the multiannual period as humid with a security of 15.3% and 19.2%, and the third - as dry with a security of 84%. The period July - August for the first year has a security of 47.0% and is characterized as average. Despite the temporary drought in July, the year is characterized by good natural water supply, and the second year of experience during this period is dry with 67% security, which has necessitated the implementation of irrigation with a higher irrigation rate. For the third experimental year, this period was humid with a security of 15.3%. (Table 1)

Table 1. *Precipitation during the growing season of short-fruited cucumbers*

Periods	Sum of precipitation, mm			Security of the precipitation factor, %		
Years	1-st	2-nd	3-rd	1-st	2-nd	3-rd
April - September	423		360	15,3	19,2	84,7
Average multiannual	360		365			
July-August	100		132	38,0	67,0	15,3
Average multiannual	107	107	107			

The results of the realized irrigations show that in order to maintain the soil moisture in the range between 85 - 100% of WHC in short-fruited cucumbers, 15 irrigations with an average irrigation rate of 18.3 mm and irrigation 280 mm were realized average for the study period. For the conditions of the Sofia field they have been realized for the period from the beginning of May to the end of July. in open areas. The longer growth period has led to a larger number of waterings. Unfavorable for the growth, development and fruiting of the crop in terms of weather conditions is the 3rd year, due to the dry and warm period in July. During this month, some of the plants withered, despite the planned and submitted waterings, which led to a shortening of the vegetation period of the crop, (Table 1).

The different number of irrigations in the different years had an impact in the three groups of variants on the size of the irrigation norms, which vary by years from 12.4 to 24.8 mm, and the irrigation from 186 to 397 mm. (Table 2).

The maximum irrigation norms in the individual years in the period of the greatest water consumption can be submitted every 3-4 days and satisfy the needs of the plants. At 1.5 atmospheres pressure they are realized in 2-3 hours.

Table 2. *Number of waterings, irrigation and irrigation norms of short-fruited cucumbers in open areas*

Years	1-st	2-nd	3-rd	1-st	2-nd	3-rd	Number of waterings	Irrigation rate, mm	Applied water, mm
Variants	number of waterings			Irrigation rate, mm			Average for the three years		
M_{130}	15	16	15	23,9	24,8	22,8	15,3	23,8	366
M_{100}	15	16	15	18,4	19,0	17,6	15,3	18,3	280
M_{70}	15	16	15	12,9	13,3	12,4	15,3	12,8	196

The realized irrigation regimes have influenced the formation of yields of short-fruited cucumbers. The yields in the individual years vary from 2368 to 5404 kg / dka, with the highest yields being obtained in the 1st and 2nd years. Yields in the 3rd decreased by 30% as a result of adverse weather conditions, which led to a shortening of the growing season of the crop.

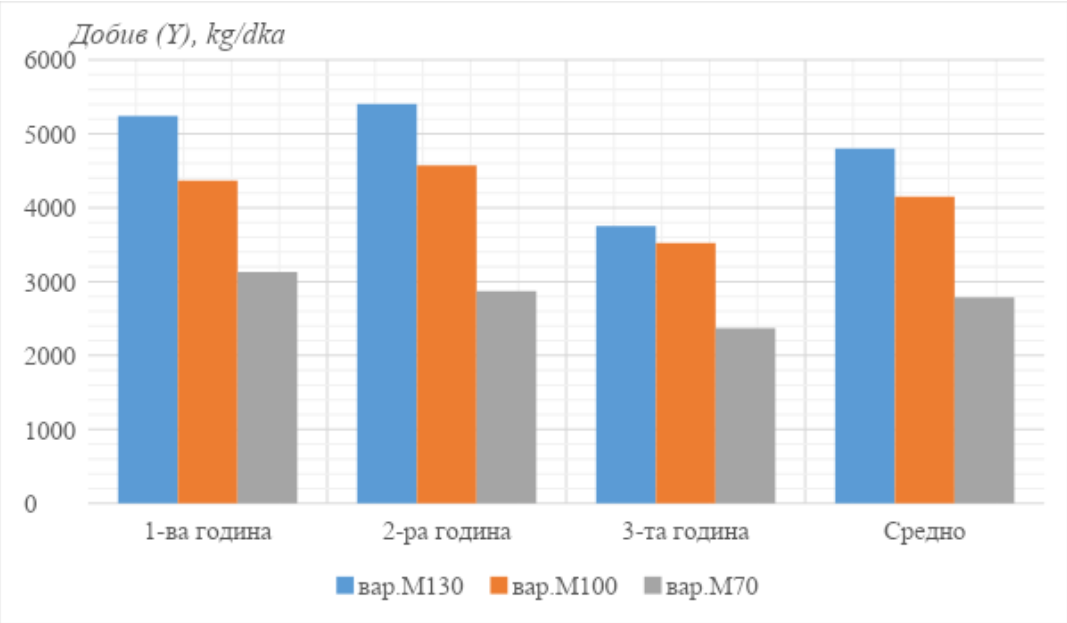


Figure 1. *Yield (Y), kg / dka of short-fruited cucumbers obtained in the experimental field Chelopechene, Sofia*

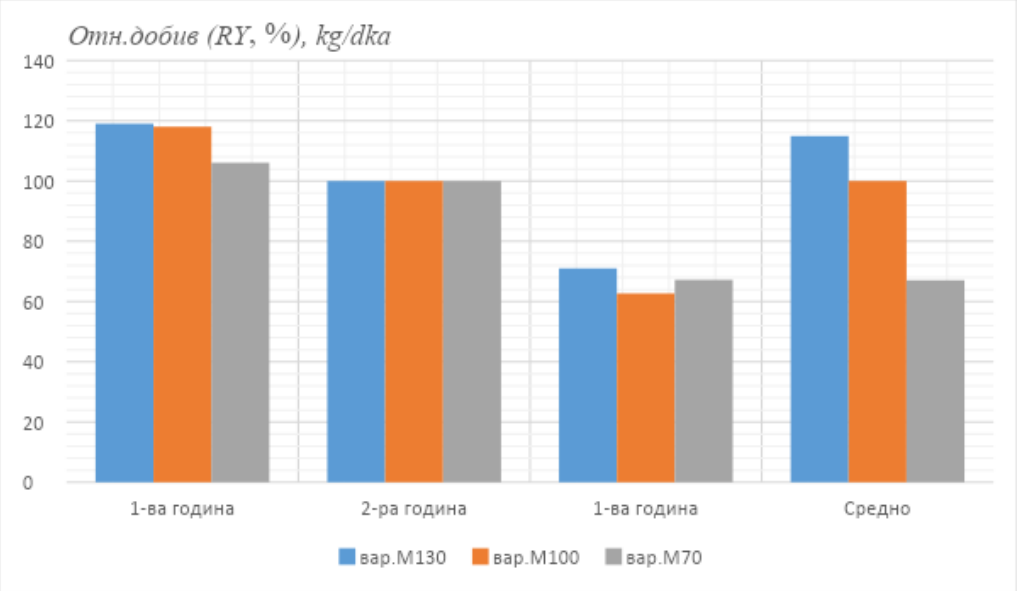


Fig.2 *Relative yield (RY,%) of short-fruited cucumbers obtained in the experimental field Chelopechene, Sofia*

The highest yield of short-fruited cucumbers grown under soil and meteorological conditions for the Sofia field in open areas is formed in the variant with 130% realization of the irrigation norm - 4978 kg / dka, followed by the variant with 100% irrigation norm - 4152 kg/ dka on average. for the research period. The lowest yields were obtained in the variant with a 30% reduction of the rate –2789 kg / dka. The increase of the irrigation norm by 30% has led to an increase of the yields up to 15%, and with a decrease of the irrigation norm by 30%, the yield has decreased by 33%. (Fig.1 and fig.2)

Conclusions

When growing short-fruited cucumbers for fresh consumption in open areas (field production), 15 irrigations with an average irrigation rate of 18.3 mm are needed, which is realized at different intervals depending on the development of plants and the tension of meteorological factors and irrigation. norm 280 mm.

The highest yield of short-fruited cucumbers grown under soil meteorological conditions for the Sofia field in open areas is formed in the variant with 130% realization of the irrigation rate - 4978 kg / dka followed by the variant with 100% irrigation rate - 4152 kg / dka on average for the period of research.

The increase of the irrigation rate by 30% has led to an increase of the yields to 15%, and with a decrease of the irrigation rate by 30%, the yield is lower by 33%.

References

1. Murtazov et al., 1975, Greenhouse Vegetable Production Plovdiv, published by Hristo Danov, p.79

2. Hershkovich, Stefanov, 1982, Agroclimatic Atlas of Bulgaria, Sofia, p.117

3. Shaban.N, et al., 2014, Vegetable Production, Sofia, p. 181, Publishing House at LTU Sofia, ISBN 978-954-332-116-2, P.490

4-.Klark 1979, Furow, sprinkler and drip irrigations in the Corn, Pepir №70-2111, presented at the summer meeting of ASEA and CSAE, Univ of Monitiba, Winipag, Canada

5. Fretsman, B., Garzoli, M.R. - Localized Irrigation FAO, Irrigation and Drainage Paper, N 36, 1980.

6-.Ziad A. M. and S. A. Jamous, 2010. Climate change and agricultural water demand: Impacts and adaptations. African Journal of Environmental Science and Technology Vol. 4 (4), pp. 183-191.

Energy consumption and emissions of agricultural machinery for different arable land types

Šimun Lončarević[1,*], Petar Ilinčić[2], Goran Šagi[2], Zoran Lulić[2]
Energy Institute Hrvoje Požar, Zagreb, Croatia [1]
University of Zagreb, Faculty of Mechanical Engineering and Naval Architecture, Zagreb, Croatia[2]
sloncarevic@eihp.hr

Abstract: *In this research, a survey was conducted in the Republic of Croatia in order to determine energy consumption in agriculture. The survey included collecting data on agricultural machinery based on machine type, fuel used, type of business and arable land type. There were more than 9,000 participants in the survey, of which more than 6,000 family farms. Results are shown on a national level for four land types: arable land, meadows and pastures, olive plantations and vineyards, as well as for three groups of participants: enterprises, family farms, and eco-producers. The last was found to have the lowest energy consumption and emissions on most land types, except on arable land, where all three groups have similar results. Vineyards had the highest emissions per hectare, while meadows and pastures had the lowest.*

Keywords*: MOBILE MACHINERY, AGRICULTURAL MACHINERY, EMISSIONS, LAND TYPE*

1. Introduction

Since global emissions are continually growing, there is a need for additional policies and measures which will help in their decrease [1]. For this to be achieved, all sources of emissions must be further researched. Among these emissions, non-road mobile machinery (NRMM) has not been researched adequately, and much less is known about their emissions in comparison to emissions from road vehicles [2]. This is partly due to a lack of a designated institution that would collect his data, as well as a lack of infrastructure and procedures for this data collecting process [3].

In Europe, the Regulation (EU) 2016/1628 introduced more stringent restrictions on emissions from NRMM [4]. It is expected to help in further decreasing of NRMM emissions by installing emission reduction technologies on new NRMM or retrofitting older models [5]. Unfortunately, there is little research regarding NRMM emission inventories and most countries do not research NRMM emissions. Without those inventories, little is known about the proportion of NRMM emissions in overall emissions and how this proportion compares with regard to overall NRMM energy consumption. Due to large differences between various models of internal combustion engine installed in NRMM, and large differences concerning NRMM working conditions, even the latest legal restrictions do not follow the ones for road vehicles [6].

There has been little research on agricultural machinery emissions. Since construction machinery and agriculture machinery have the largest proportions in overall NRMM emissions [7, 8], it is important to emphasize their emissions, considering that their emission reduction would result in the largest overall NRMM emission reduction. Unfortunately, there is no data on emission from agricultural machinery based on different arable land types. This information would enable the regulatory bodies to implement optimal measures, which would target machinery that operates on arable land types with the largest emissions per area unit. Furthermore, it would enable them to provide incentives for agricultural work, which results in the lowest emissions.

When researching emissions, the proven method of collecting data is to conduct a survey. It gives a good insight into real work conditions and fuel consumption of different machinery, which is a precondition to estimate emissions [9, 10]. Such approach provide results which accurately represent emissions per type of arable land.

2. Methods

Data on fuel consumption of agricultural machinery was collected as a part of a larger survey on energy consumption in agriculture. Data collection was conducted through a web application and field surveys. Administrative data was provided by the Croatian Bureau of Statistics (CBS), and data collection was conducted from December 2017 to April 2018. A total of 9710 participants were included in the survey, and data on fuel consumption based on fuel type, machine type and agricultural land type were collected.

Concerning land types, data collection was divided into four land types: arable land, meadows and pastures, olive plantations and vineyards. Concerning the type of business, the participants were divided into one of the following three groups: enterprises, family farms, and eco-producers. Data on fuel consumption was collected for diesel and gasoline fuel. Machinery was divided by type, which is shown in Table 1.

Each participant was assigned a unique identification number from the CBS database in order for the results to be linked with the existing CBS data. Results were controlled for their plausibility using certain identifiers. For example, average fuel consumption for tractors was determined in order to single out the outlying answers (e.g., using the wrong fuel based on machinery type or wrong order of magnitude). Following this control, the results were shown on national levels using weight factors provided by the CBS. When calculating weight factor, the CBS took into account individual properties for each survey participant, e.g. type of machinery used, geographic properties, end-use of machinery as per national occupational classification etc.

Table 1. *Total number of NRMM used in agriculture in Croatia in 2016 by ownership and machinery type*

	Number of machines-owned	**Number of machines-rented**
Single-axle tractors	56 039	682
Two-axle tractors	111 113	2 602
up to 40 kW	57 184	1 755
from 41 to 60 kW	31 579	292
from 61 to 100 kW	16 598	401
more than 100 kW	5 752	153
Combine harvesters	8 604	537
Machinery for potatoes and sugar beet	654	4
Machinery for fodder plants	5 203	127
Other harvesting machinery	258 745	875
Balers	51 515	1 090
Other	73 232	1 231
TOTAL	**565 105**	**7 147**

In order to calculate energy consumption from the fuel consumption data collected in the survey, fuel consumption was converted to megajoules to represent the results in megajoules per hectare (MJ/ha). The conversion factors used were obtained from the national energy report, "Energy in Croatia", which is published annually by the Ministry of Economy and Sustainable Development. For diesel, a density of 0.832 kg/L and an energy density of 42.71 MJ/kg was used. For gasoline fuel, a density of 0.737 kg/L and an energy density of 44.59 MJ/kg was used [11].

Since only data on fuel consumption could be collected, Tier 1 method as specified in the EMEP/EEA air pollutant emission inventory guidebook for 2019 was used for calculating the emissions [12]:

$$E_{pollu} = \sum_{fuel\ type} FC_{fuel\ type} \times EF_{pollu,fuel\ type}$$

where E_{pollu} is the emission of the specified pollutant; $FC_{fuel\ type}$ is the fuel consumption of each fuel for the source category; $EF_{pollu,\ fuel\ type}$ is the emission factor for a specific pollutant for each fuel type. The emission factors for forestry machinery based on fuel type and pollutant type in g/tonnes of fuels are shown in Table 2. In agriculture in Croatia, diesel and gasoline fuel are used, and emission factors are shown for CO_2, CO, NO_X, HC and PM.

Table 2. *Emission factors for different pollutants and fuel types for NRMM used in agriculture*

	Emission factors [g/tonnes of fuel]	
Pollutant	**Diesel**	**Gasoline**
CO_2	3 160 000	3 197 000
CO	11 469	770 368
NO_X	34 457	7 117
HC	87	665
PM	1 913	157

3. Results

Based on data from the survey and from the EMEP/EEA air pollutant emission inventory guidebook for 2019, energy consumption and emissions were calculated for different types of business and arable land types. Energy consumption for all types of businesses, types of fuel and arable land types are shown in Table 3 and Figure 1.

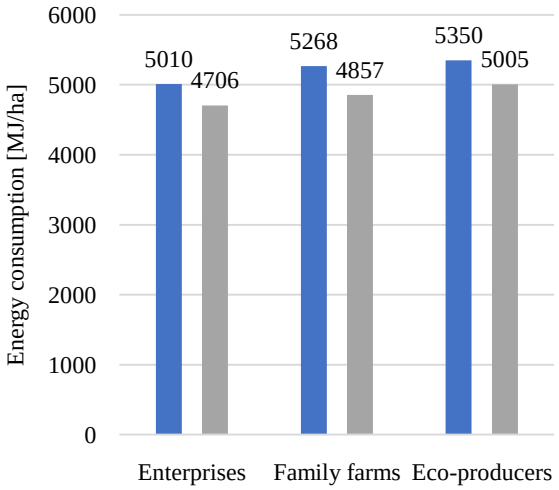
Table 3. *Energy consumption per hectare for types of businesses, types of fuel and arable land types*

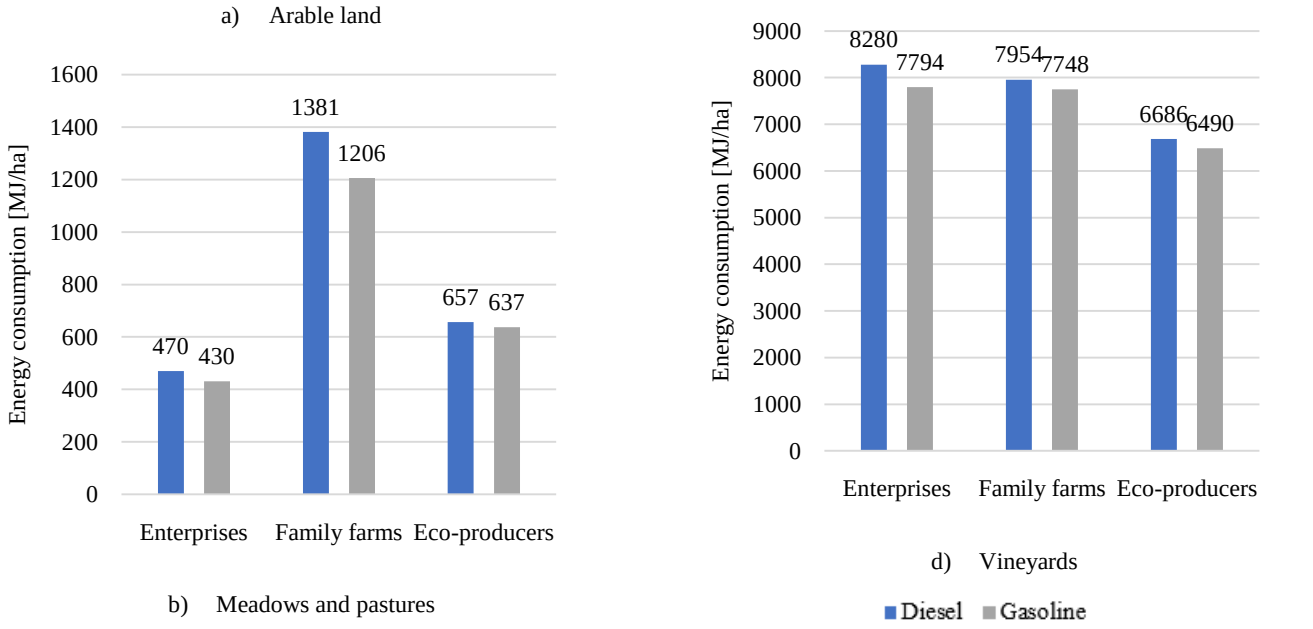
	Average consumption (MJ/ha)	
	Diesel	**Gasoline**
Arable land		
Enterprises	5 010	4 706
Family farms	5 268	4 857
EKO producers	5 350	5 005
Average arable land	5 104	4 738
Meadows and pastures		
Enterprises	470	430
Family farms	1 381	1 206
EKO producers	657	637
Average meadows and pastures	956	858
Olive plantations		
Enterprises	5 112	4 771
Family farms	6 543	6 135
EKO producers	2 647	2 471
Average olive plantations	4 941	4 610
Vineyards		
Enterprises	8 280	7 794
Family farms	7 954	7 748
EKO producers	6 686	6 490
Average vineyards	8 213	7 762

Since there is significantly more machinery that uses diesel fuel than machinery which uses gasoline fuel, the total energy consumption in Croatia is much larger for machinery which uses diesel fuel. Therefore, comparing total energy consumption would make it difficult to compare data between different types of businesses and different arable land types. For the purpose of better comparison of data, the results are shown not for total energy consumption, but in average energy consumption per hectare in megajoules per hectare. This enables data to be adequately compared between different types of businesses and different arable land types.

Concerning energy consumption, results show that vineyards had the highest energy consumption and emissions per hectare of land for both diesel and gasoline fuels. For diesel fuel, energy consumption was 8280 MJ/ha for enterprises, 7954 MJ/ha for family farms, and 6685 MJ/ha for eco-producers. For gasoline fuel, energy consumption was 7794 MJ/ha for enterprises, 7748 MJ/ha for family farms, and 6489 MJ/ha for eco-producers.

The lowest fuel consumption was on meadows and pastures for both fuels. For diesel fuel, energy consumption was 469 MJ/ha for enterprises, 1381 MJ/ha for family farms, and 656 MJ/ha for eco-producers. For gasoline fuel, energy consumption was 430 MJ/ha for enterprises, 1205 MJ/ha for family farms, and 637 MJ/ha for eco-producers.





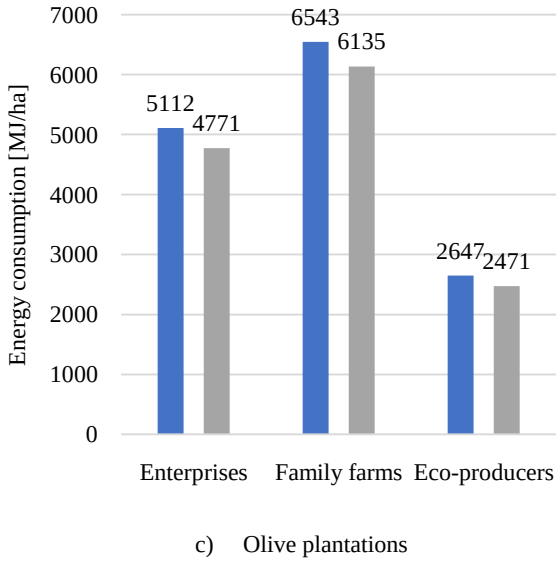


Fig. 1 *Energy consumption of agricultural machinery per hectare based on types of businesses, fuel types and arable land types*

Emissions per hectare for each business and land type were also calculated and shown in Table 4 for diesel and gasoline fuel. The highest emissions were from machinery working in vineyards. Different types of emissions were highest for different fuels. Concerning diesel fuel, the highest emissions were 616.38 kg CO_2/ha, 6.72 kg NO_X/ha and 0.37 kg PM/ha for enterprises. The highest CO and HC emissions were from machinery in enterprises using gasoline fuel, with 135.95 kg CO/ha and 0.12 kg HC/ha. As with fuel consumption, the lowest emissions per hectare were from machinery working in meadows and pastures. The lowest emissions for gasoline fuel were in enterprises and were 31.16 kg CO_2/ha, 0.07 kg NO_X/ha and 0.002 kg PM/ha. For diesel fuel, emissions were lowest in enterprises and were 0.13 kg CO/ha and 0.001 kg HC/ha.

As expected, when comparing the same business types and land types, CO_2, NO_X and PM emissions were higher from machinery using diesel fuel than those using gasoline fuel. For machinery using gasoline fuel, it was vice versa, with CO and HC emissions being higher compared to emissions from machinery using diesel fuel. Furthermore, eco-producers had the least emissions on every type of land, except on arable land, where they had similar emissions to family farms and enterprises.

Table 4. *Emissions per hectare for types of businesses, types of fuel and arable land types*

	Diesel emissions [kg/ha]					**Gasoline emissions [kg/ha]**				
	CO_2	CO	NO_X	HC	PM	CO_2	CO	NO_X	HC	PM
Arable land										
Enterprises	372.93	1.35	4.07	0.01	0.23	340.61	82.08	0.76	0.07	0.02
Family farms	392.15	1.42	4.28	0.01	0.24	351.55	84.71	0.78	0.07	0.02
Eco-producers	398.28	1.45	4.34	0.01	0.24	362.26	87.29	0.81	0.08	0.02
TOTAL	379.96	1.38	4.14	0.01	0.23	342.99	82.65	0.76	0.07	0.02
Meadows and pastures										
Enterprises	34.96	0.13	0.38	0.001	0.02	31.16	7.51	0.07	0.01	0.002
Family farms	102.82	0.37	1.12	0.001	0.06	87.29	21.03	0.19	0.02	0.004
Eco-producers	48.89	0.18	0.53	0.001	0.03	46.14	11.12	0.10	0.01	0.002
TOTAL	71.16	0.26	0.78	0.001	0.04	62.08	14.96	0.14	0.01	0.003
Olive plantations										

	Diesel emissions [kg/ha]					Gasoline emissions [kg/ha]				
	CO_2	CO	NO_X	HC	PM	CO_2	CO	NO_X	HC	PM
Enterprises	380.52	1.38	4.15	0.01	0.23	345.37	83.22	0.77	0.07	0.02
Family farms	487.07	1.77	5.31	0.01	0.29	444.08	107.01	0.99	0.09	0.02
Eco-producers	197.02	0.72	2.15	0.01	0.12	178.87	43.10	0.40	0.04	0.01
TOTAL	367.84	1.34	4.01	0.01	0.22	333.71	80.41	0.74	0.07	0.02
Vineyards										
Enterprises	616.38	2.24	6.72	0.02	0.37	564.20	135.95	1.26	0.12	0.03
Family farms	592.14	2.15	6.46	0.02	0.36	560.87	135.15	1.25	0.12	0.03
Eco-producers	497.70	1.81	5.43	0.01	0.30	469.77	113.20	1.05	0.10	0.02
TOTAL	611.37	2.22	6.67	0.02	0.37	561.82	135.38	1.25	0.12	0.03

4. Conclusion and recommendations

Unlike emissions from road transport, which are extensively researched and in the focus of public debate and policies, much less is known about emissions from non-road mobile machinery. Although they significantly contribute to overall emissions, they are often neglected in emission reduction policies and rarely peak research interest. In addition to contributing to overall emissions, agricultural machinery emission more directly affects both the workers operating this machinery and the final product, i.e., the food which the final consumers eat. Like any other emission from internal combustion engines, agricultural machinery emission affects the environment, especially the workers operating this machinery and the final product, i.e., the food which the final consumers eat.

The results of this paper, which show emissions based on land type and business type, provide data that can help policymakers develop policies to create optimal measures for emission reduction. Vineyards, with the largest emissions per hectare, are most suitable for policies aiming at emission reduction. A policy of incentivizing eco-production would result in emission reduction in vineyards and olive plantations and meadows and pastures. For arable land, additional policies could further reduce emissions and protect both the workers operating agricultural machinery and the end consumers.

3. References

[1] U. N. Environment, "Emissions Gap Report 2019," *UNEP - UN Environment Programme* (2019). Available: http://www.unenvironment.org/resources/emissions-gap-report-2019.

[2] J. Brodny and M. Tutak, "Analysis of the diversity in emissions of selected gaseous and particulate pollutants in the European Union countries," *Journal of Environmental Management*, **vol. 231**, pp. 582–595 (2019), doi: 10.1016/j.jenvman.2018.10.045.

[3] T. S. Poulsen, "Market Analysis for Non-road Mobile Machinery Sector," Scandinavian GPP Alliance (2017). Available: https://www.gate21.dk/wp-content/uploads/2017/06/Market-Analysis-for-Non-Road-Mobile-Machinery-Sector_FINAL.pdf.

[4] Regulation 2016/1628, "On requirements relating to gaseous and particulate pollutant emission limits and type-approval for internal combustion engines for non-road mobile machinery, amending Regulations (EU) No 1024/2012 and (EU) No 167/2013, and amending and repealing Directive 97/68/EC (Text with EEA relevance)." European Parliament (2016),Available: http://data.europa.eu/eli/reg/2016/1628/oj/eng.

[5] K. J. Walus, L. Wargula, P. Krawiec, and J. M. Adamiec, "Legal regulations of restrictions of air pollution made by non-road mobile machinery-the case study for Europe: a review," Environ. Sci. Pollut. Res., **vol. 25**, no. 4, pp. 3243–3259 (2018), doi: 10.1007/s11356-017-0847-8.

[6] N. Szymlet, P. Lijewski, P. Fuć, B. Sokolnicka, and M. Siedlecki, "Comparative analysis of passenger car and non-road machinery specific emission in real operating conditions," in *2018 International Interdisciplinary PhD Workshop (IIPhDW)* (2018), pp. 226–230, doi: 10.1109/IIPHDW.2018.8388362.

[7] B. Notter, P. Wüthrich, and J. Heldstab, "An emissions inventory for non-road mobile machinery (NRMM) in Switzerland," Journal of Earth Sciences and Geotechnical Engineering, **vol. 6**, no. 4, pp. 273–292 (2016).

[8] M. Winther, "Danish emission inventories for road transport and other mobile sources," p. 136 (2020).

[9] P. Lijewski, J. Merkisz, P. Fuć, A. Ziółkowski, Ł. Rymaniak, and W. Kusiak, "Fuel consumption and exhaust emissions in the process of mechanized timber extraction and transport," Eur J Forest Res, **vol. 136**, no. 1, pp. 153–160 (2017), doi: 10.1007/s10342-016-1015-2.

[10] J. Lang *et al.*, "A high temporal-spatial resolution air pollutant emission inventory for agricultural machinery in China," J. Clean Prod., **vol. 183**, pp. 1110–1121 (2018), doi: 10.1016/j.jclepro.2018.02.120.

[11] "Energy in Croatia," Ministry of Economy and Sustainable Development, Zagreb (2020). Available: http://www.eihp.hr/wp-content/uploads/2021/01/1_Energija_u_Hrvatskoj_2019-2_compressed-1.pdf.

[12] EEA, "EMEP/EEA air pollutant emission inventory guidebook 2019." European Environment Agency (2019). Available: https://www.eea.europa.eu/publications/emep-eea-guidebook-2019.

Balkan endemic plants of Shutman Strict Nature Reserve in Kosovo - an inventory with chorological and life-form analyses

Haxhi Halilaj[1], Lirika Kupe[1,*], Xhavit Mala[2]
Agricultural University of Tirana, Albania [1]
Ministry of Environment and Spatial Planning, Kosovo[2]
lkupe@ubt.edu.al

Abstract: *Balkan endemic taxa are those whose distribution is restricted exclusively to the Balkan Peninsula. The aim of the present study is to determine the number of the Balkan endemic taxa in Shutman Strict Nature Reserve in Kosovo and to presented chorological groups and life-form categories of this flora. In the investigated area are recorded 67 Balkan endemic and sub-endemic species and subspecies. The most important contributors at family rank in the Balkan endemic taxa are Asteraceae, Caryophyllaceae, Brassicaceae, Campanulaceae and Rosaceae, while the richest genuses are Silene, Achillea and Campanula. In the chorological structure of the of the Balkan endemics the largest numbers are from the Balkan, S European and C European chorological groups, while in the life-form spectrum of the flora hemicryptophytes and chamaephytes are the most abundant. The data of the study showed that Reserve of Shutman has a very high level of endemic species. This fact shows that Shutman Reserve is an important center of the Balkan endemic flora in the Kosovo and the Balkan Peninsula and the existence of a rich endemic flora is of great importance in the conservation of biodiversity in this area.*
Keywords*: BALKAN PENINSULA, KOSOVO, FLORA, ENDEMIC TAXA, CHOROLOGY, LIFE FORM.*

1. Introduction

Sharr Mountains in southern Kosovo and western North Macedonia is one of the largest and highest mountain ranges and one of the most rugged and impassable in the Balkan Peninsula. The Sharr National Park in Kosovo that located in southeastern part of Kosovo is one the most important Balkan and European centers and one of the most qualitative endemism (Halilaj et al., 2019; Tomović et al., 2014). On the territory of the Sharr National Park there are 15 strict natural protected areas, one of which is the Shutman protected area with 5057.39 ha and an altitude ranging from 1600-2536 m above sea level. This strict reserve is dominated by alpine and sub-alpine pastures, cliffs and rocky creeps, on the limestone or siliceous substrate. The subalpine zone extends above the upper forest belt from 1600 to 2100 m (rare to 2200 m.) above sea level (Abdii & Xhulaj, 2016) and at high altitudes is found the alpine zone. The average annual rainfall is 1370 mm, and the annual average temperature is 8.6° C. with a summer temperature average of 18.1° C, and winter annual temperature average of -0.4° C (MMPH, 2013).

The great floristic diversity of the studied area cannot only be explained by the by the alpine and continental climate, at times influenced by a moderate continental climate (MMPH, 2013) and the specific geographical location, hydrological characteristics, different rock substrata and soil types but also by habitat diversity formed as a result of extensive anthropogenic influence.

The endemic plants are among the plant groups important for understanding the florogenetic tendencies and phytogeographic characteristics of each region (Ranđelović et al., 2008). Endemism is one of the most important concepts in biogeography and is of high relevance for conservation biology (Casagranda & de Grosso, 2013; Norrozi et al., 2019). The number of endemic species in a biogeographic region is a first step for assessing the conservation situation of that region, and also for understanding the evolutionary and ecological processes that have shaped the biodiversity hotspots in general and areas of endemism in particular (Norrozi et al., 2019).

The phenomenon of endemism characterizes those taxa whose distribution is restricted to a certain area. Balkan endemic plants are those species whose distribution is restricted exclusively to the territory of the Balkan Peninsula (Tomović et al., 2014; Millaku et al., 2017), whereas sub-endemic are restricted to a narrow area that is marginally shared with only one or two neighbouring countries (Gavrilović et al., 2017; Shuka et al., 2018), e.g. Kosovo, Albania and North Macedonia. The aim of this study was to inventor the Balkan endemic and sub-endemic plant species and to analyse chorological groups, life form and biological types for each species.

2. Materials and Methods

The list of endemic taxa of the Shutman Reserve is based on the continuous field observations carried out between 2018 and 2019, applying stationary and routes methods of research. Identification of the collected plants is made according to Flora of Albania (Paparisto et al., 1988; Qosja et al., 1992, 1996; Vangjeli et al., 2000), Atlas of Kosovo Plants (Berisha et al., 2012), Excursion Flora of Albania (Demiri, 1983) and Flora Albanica Atlas (Vangjeli, 2017). The nomenclature used is according to Barina et al. (2018) and the databases of the Plant List (theplantlist.org).

Classification of endemics was done according to Millaku et al. (2008; 2017), Mustafa et al. (2015), Mahmutaj (2015), Petrova & Vladimirov (2010), Tomović et al. (2014), Vuksanović et al. (2016) and Zahariev (2016). Floristic elements, life forms and biological types are given for each taxon. For the attribution of life forms the criteria proposed by Raunkiaer (1934) and Mueller-Dombois & Ellenberg (1974) were followed. Taxa were classified as chamaephytes (Ch), hemicryptophytes (H) and geophytes (G). Biological types were defined by Flora of Albania (Paparisto et al. 1988; Qosja et al. 1992, 1996; Vangjeli et al. 2000) and Berisha et al. (2012). Each endemic taxon was relegated to a chorological group corresponding to the floristic regions of Assyov & Petrova (2012), complemented with data from Vangjeli (2003, 2015, 2017). The floristic list (Table 1) is provided in alphabetical order by species.

3. Results and Discussions

The endemic taxa of the Shutman Reserve are represented by 67 endemic taxa (58 species and 9 subspecies). Of these, 57 species are Balkan endemics (85% of all species) and 10 species are Balkan sub- endemic (15% of all species). They belong to 21 families and 46 genera. Richest in endemics are the families Asteraceae (16), Caryophyllaceae (11), Brasicaceae (9), and Campanulaceae and Rosaceae both with 4 species. Seven families, Crassulaceae, Iridaceae, Liliaceae, Ranunculaceae, Saxifragaceae, Scrophylariaceae and Violaceae are presented with 2 species, while 9 others families are presented only with 1 species. Most species belong to the following genera: Silene (4), Achillea, Campanula, Cerastium and Dianthus all with 3 species, 10 genera are presented with 2 species and 31 other genera are presented only with one species. The established taxonomically diversity can be explained by the variety of combinations of terrain, hydrological, climatic and soil conditions as a prerequisite for the variety of biodiversity within the territory of the Shutman Mountain.

Table 1: *List of endemic and sub-endemic species of the Shutman Natural Strict Reserve*

Nr	Species	Family	Life forms	Chorological group	Biological type
Balkan endemic taxa					
1.	*Achillea abrotanoides* (Vis.) Vis.	Asteraceae	H	Bal	p
2.	*Achillea chrysocoma* Friv.	Asteraceae	H	Bal	p
3.	*Achillea pindicola* subsp. *corabensis* (Heimerl) Greuter	Asteraceae	Ch	Bal	p
4.	*Aconitum pentheri* Hayek.	Ranunculaceae	H	Bal	p
5.	*Alkanna scardica* Griseb.	Boraginaceae	H	SEur	p
6.	*Alyssum scardicum* Wettst.	Brassicaceae	Ch	Eur-Med	p
7.	*Arabis bryoides* Boiss.	Brassicaceae	H	Bal	p
8.	*Asperula doerfleri* Wettst.	Rubiaceae	H	Bal	p
9.	*Aubrieta gracilis* ssp. *scardica* (Wettst.)	Brassicaceae	Ch	Bal	p
10.	*Barbarea balcana* Panc.	Brassicaceae	H	Bal	p
11.	*Campanula albanica* Witasek	Campanulaceae	H	Bal	p
12.	*Campanula spathulata* Sibth. et Sm.	Campanulaceae	G	Bal	p
13.	*Cardamine carnosa* Waldst. & Kit.	Brassicaceae	H	Bal	p
14.	*Carduus ramosissimus* Pančić	Asteraceae	H	Bal	b-p
15.	*Carduus scardicus* (Griseb.) Wettst.	Asteraceae	H	Bal	p
16.	*Cerastium decalvans* Schlosser & Vuk.	Caryophyllaceae	H	Bal	p
17.	*Cerastium eriophorum* Kit.	Caryophyllaceae	Ch	Bal	p
18.	*Cerastium grandiflorum* Waldst. & Kit.	Caryophyllaceae	Ch	Bal	p
19.	*Cicerbita pancicii* (Vis.) Beauverd	Asteraceae	H	Bal	p
20.	*Cirsium appendiculatum* Griseb.	Asteraceae	H	Bal	p
21.	*Cirsium tymphaeum* Hausskn.	Asteraceae	H	Bal	b-p
22.	*Colchicum macedonicum* Košanin	Liliaceae	G	Bal	p
23.	*Crepis baldaccii* Halacsy subsp. *albanica* Jav.	Asteraceae	H	Bal	p
24.	*Crocus veluchensis* Herb.	Iridaceae	G	Bal	p
25.	*Dianthus integer* Vis.	Caryophyllaceae	H	Bal	p
26.	*Dianthus tristis* Velen.	Caryophyllaceae	H	Bal	p
27.	*Digitalis viridiflora* Lindl.	Scrophylariaceae	H	Bal	p
28.	*Draba korabensis* Kummerle & Degen ex Jav.	Brassicaceae	H	Bal	p
29.	*Edraianthus montenegrinus* Horák	Campanulaceae	Ch	Bal	p
30.	*Erigeron epiroticus* (Vierh) Halacsy.	Asteraceae	H	Sub Bal	p
31.	*Erysimum pectinatum* Bory & Chaub.	Brassicaceae	H	Bal	p
32.	*Geum coccineum* Sibth. & Sm.	Rosaceae	H	SubMed	p
33.	*Geum reptans* L.	Rosaceae	H	Alp-Carp-Bal	p
34.	*Heliosperma pusilla* subsp. *albanica* (K.Maly) Greuter & Burdet.	Asteraceae	Ch	Bal	p
35.	*Hieracium waldsteinii* Tausch	Asteraceae	H	Bal	p
36.	*Laserpitium siler* subsp. *zernyi* (Hayek) Tutin	Apiaceae	H	Bal	p
37.	*Lilium albanicum* Griseb.	Liliaceae	G	Bal	p
38.	*Linaria peloponnesiaca* Boiss. & Heldr.	Plantaginaceae	H	Bal	p
39.	*Lunaria telekiana* Jáv.	Brassicaceae	H	CEur	p
40.	*Narthecium scardicum* Kosanin	Nartheciaceae	Ch	Bal	p
41.	*Onobrychis montana* subsp. scardica (Griseb.) P.W.Ball	Fabaceae	H	Eur-Med	p
42.	*Pinguicula balcanica* Casper	Lentibulariaceae	H	Bal	p
43.	*Potentilla speciosa* Willd. subsp. *illyrica* Soják	Rosaceae	Ch	SEEur	p
44.	*Saxifraga scardica* Griseb.	Saxifragaceae	Ch	Bal	p
45.	*Saxifraga taygetea* Boiss et Helder.	Saxifragaceae	H	Bal	p
46.	*Schivereckia doerfleri* (Wettst.) Bornm.	Brasicaceae	H	Bal	p
47.	*Senecio procerus* (*Gris*.) Boiss.	Asteraceae	H	Bal	p
48.	*Senecio wagneri* Degen	Asteraceae	H	Carp-Bal	p
49.	*Silene asterias* Griseb.	Caryophyllaceae	H	Bal	ssh
50.	*Silene pusilla* subsp. *albanica* Greuter et Burdet.	Caryophyllaceae	H	Alp-Med	p
51.	*Silene waldsteinii* Griseb.	Caryophyllaceae	H	Bal	p
52.	*Soldanella pindicola* Hausskn.	Primulaceae	Ch	Bal	p
53.	*Tephroseris papposa* subsp. *wagneri* (Degen) B. Nord.	Asteraceae	H	Bal	p
54.	*Verbascum scardicolicum* Bornm.	Scrophylariaceae	H	Bal	p
55.	*Vincetoxicum huteri* Vis. et Asch.	Apocynaceae	H	Bal	p
56.	*Viola gracilis* Sm.	Violaceae	H	Bal-Anat	p
57.	*Viola schariensis* Erben	Violaceae	H	Bal	p
Balkan sub- endemic taxa					
58.	*Campanula lingulata* Waldst et Kit	Campanulace	Ch	Ap-Bal	p
59.	*Crepis macedonica* Kitanov	Asteraceae	H	Bal	p
60.	*Crocus scardicus* Košanin	Iridaceae	G	Bal	p
61.	*Dianthus scardicus* Wettst.	Caryophyllaceae	H	Bal	p

62.	*Petrorhagia illyrica* (Ard.) P.W. Ball & Heywood	Caryophyllaceae	H	Pont-Med	p
63.	*Potentilla doerfleri* Wettst.	Rosaceae	Ch	SEEur	p
64.	*Ranunculus degenii* Kümmerle & Jav.	Ranunculaceae	H	Bal	p
65.	*Sempervivum kosanini* Praeger	Crassulaceae	H	Bal	p
66.	*Sempervivum macedonicum* Praeger	Crassulaceae	H	Bal	p
67.	*Silene lerchenfeldiana* Baumg.	Caryophyllaceae	H	Carp-Bal	p

All taxa at the subspecies levels are Balkan endemics: Achillea pindicola subsp. corabensis, Aubrieta gracilis ssp. scardica, Crepis baldaccii subsp. albanica, Heliosperma pusilla subsp. albanica, Laserpitium siler subsp. zernyi, Onobrychis montana subsp. scardica, Potentilla speciosa Willd. subsp. illyrica Soják, Silene pusilla subsp. albanica and Tephroseris papposa subsp. wagneri.

The Balkan endemic plants, Potentilla doerfleri and Dianthus scardicus, should be considered simultaneously as stenoendemic species of Sharr Mountain, meaning it has restricted distribution only in Mt. Sharr, part of North Macedonia, of Kosovo and Albania. The occurrence of some Balkan endemic species, such as Ranunculus degenii Kümmerle & Jav. and Sempervivum macedonicum Praeger confirms floristic connection of Shar Mountain with North Albania and other parts of the Balkans as Dinaric Alps and Scardo-Pindhic mountain systems. Therefore, Shutman region is an important distribution corridor for orophytes from Sharr Mountain towards Dinaric Alps, Albanids and Pindhos, as well as vice-versa, from the other side.

According to some authors (Morrone, 2008; Fattorini, 2017; Crispi et al., 2001; Casagranda & de Grosso (2013), an area of endemism must have at least two endemic species. The degree of endemism (number of endemic species) in the Shutman Reserve is extremely high and this makes it an important centre of endemism in Sharri National Park as well as in Kosovo and Balkan Peninsula. Identifying centres of plant endemism may greatly aid plant conservation efforts by allowing specific regions to be actively conserved.

The biological spectrum (Fig. 1) shows a pronounced hemicryptophyte character of the endemic flora of the Shutman. Hemicryptophytes represent 73.14 % of the total number of endemics (49 species), followed by chamaephytes (19.40 % or 13 species) and geophytes (7.468 % or 5 species). This distribution of floristic elements can be explained with the geographic location of the studied area. The domination of hemicryptophytes in the biological spectrum reflected better the climate of the research area – a cold mountain climate and may be related to the fact that Balkan flora is dominated by hemicryptophytes (Goranova et al., 2013).

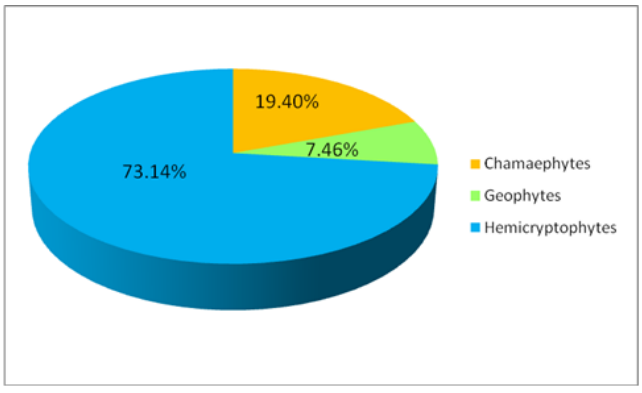


Fig. 1 *Life-form -form spectrum of the endemic flora of the Shutman Natural Strict Reserve.*

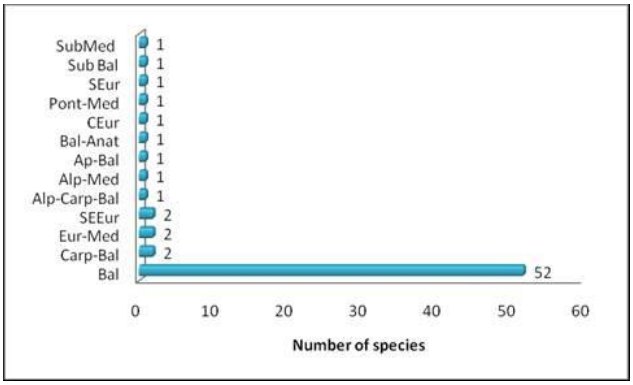


Fig. 2 *Chorological spectrum of endemic flora of the Shutman Mountain.*

Analysis of the chorological groups gives an idea of the phytogeographic characteristics of the investigated flora. The specific physical and geographic conditions determine the diversity of chorological groups. The identified plant species in the investigated territory belong to 13 chorological groups (Fig. 2). Most of the species are Balkan chorological (77.6%, 52 species), followed by European-Mediterranean, Carpathian-Balkan and Southeast European chorological groups, all with 2 species (2.99%). The remaining groups of floristic elements are presented by one species: Alpine-Carpathian-Balkan, Alpine- Mediterranean, Alpine-Balkan, Balkan-Anatolian, Central European, Pontic-Mediterranean, South European mountainous, sub-Balkan and sub-Mediterranean. The dominance of Balkan floristic elements is decisive for the genesis of the endemic flora on Shutman area. Most endemics are herbaceous perennials (64 species). Transitional forms between the main biological types of biennial and perennial species are represented by two species. The dominant presence of perennial herbaceous plants can be explained by the wide variety of plant communities and habitats on the territory of Shutman Reserve.

4. Conclusions

The endemic flora of Shutman Natural Strict Reserve includes 67 taxa (58 species and 9 subspecies) Balkan endemics and sub-endemics, represented by 46 genera and 21 families. The largest number of endemics (52 species, 77.6%) belongs to Balkan chorological group. The endemic flora of the Shutman Reserve can be divided into three types of life forms. Hemicryptophytes are represented by 73.14 % of the total number of endemic species, expressing the influence of the cold mountain climate. The high number of endemics species recorded in Shutman Strict Nature Reserve establishes this area as a one of the most important centre of diversity of endemic flora in Kosovo and Balkan Peninsula. The obtained results can be used for comparison with the data on the endemic species of different strict protect area in Sharri National Park, as well as in the other protect areas.

3. References

1. Abdii, N. & Xhulaj, M., (2016). Alpine and subalpine flora of Sharr Mountain - (Macedonian Part). International Journal Advanced Research, 4(9), p. 2238-2249.

2. Assyov, B. & Petrova, A. (eds.) 2012: Conspectus of the Bulgarian vascular flora. Distribution maps and floristic elements. Ed. 4. Bulgarian Biodiversity Foundation, Sofia.
3. Barina, Z., Somogyi, G., Pifkó, D., Rakaj, M. (2018). Checklist of vascular plants of Albania. Phytotaxa 378 (1): 001–339.
4. Berisha, B., Mala, Xh., Rexhepi, F., Millaku. F. (2012). Atllasi i Bimëve të Kosovës –I, Siprint.
5. Casagranda, D. D., de Grosso, D. M. L. (2013). Areas of endemism: Methodological and applied biogeographic bontributions from South America. Current Progress in Biological Research, Marina Silva-Opps, IntechOpen.
6. Crisp, M. D., Laffan, S., Linder, H. P., Monro, A. (2001). Endemism in the Australian flora. Journal of Biogeography, 28: 183-198.
7. Demiri, M., (1983). Flora ekskursioniste e Shqiperisë, Shtëpia Botuese e Librit Shkollor, Tiranë.
8. Fattorini, S. (2017). Endemism in historical biogeography and conservation biology: concepts and implications. Biogeographia 32: 47–75.
9. Gavrilović, B., Tomović, G., Niketić, M., Milenković, M., Simić, S. & Radovanović, M. (2017). Geoecological characteristics of plant endemism in the Balkan part of Serbia, Botanica Serbica, 41 (2): 177-197.
10. Goranova, V., Vassilev, K., Pedashenko, H. (2013). Vascular flora of the Valley of Mesta River floristic region, SW Bulgaria. Phytologia Balcanica 19 (1): 89-114.
11. Halilaj, H., Kupe, L., Bajrami,A., Mala, Xh. (2019). The endemic and relic alpine–subalpine plant species in Shutman natural reserve of Kosovo and their conservation status. Albanian j. agric. sci., Special edition: 101-108.
12. Mahmutaj, E., (2015). Studimi dhe kartografimi i habitateve dhe florës së Parkut Kombëtar Tomorr-Kulmak, me fokus kryesor ata prioritarë (sipas Natura 2000), të rrallë e të kërcënuar. Disertacion, Universiteti i Tiranës, Fakulteti i Shkencave të Natyrës, Tiranë.
13. Millaku, F. Heiselmayer, P., Rexhepi, F., Krasniqi, E., Eichberger, C. Haziri, A. (2008). Endemie, steno-endemic and relict plants in serpentines of Kosova. Sauteria 16: 149-162.
14. Millaku, F., Krasniqi, E., Berisha, N. & Rexhepi, F., (2017). Conservation assessment of the endemic plants from Kosovo. Hacquetia 16/1: 35–47.
15. MMPH (2013). Spatial Plan - National Park "Sharri", Prishtina.
16. Morrone, J. J., 2008: Endemism, in SVEN ERIK JØRGENSEN AND BRIAN D. FATH (Editor-in- Chief), Evolutionary Ecology, Vol. 2 of Encyclopedia of Ecology, 5 vols. p. 1254-1259. Oxford, Elsevier.
17. Mueller-Dombois, D., Ellenberg, H. (1974). Aims and Methods of Vegetation Ecology. John Wiley & Sons, New York.
18. Mustafa, B., Hajdari, A., Mala, Xh., Veselaj, Z., Pulaj, B., Mustafa, N. (2015). The Pashtrik Mountain, a potential protected landscape area. Biologija. Vol. 61. No. 2: 73–82.
19. Noroozi, J., Talebi, A., Doostmohammadi, M., Manafzadeh, S., Asgarpour, Z., Schneeweiss, G. M. (2019). Endemic diversity and distribucion of the Iranian vascular flora across phytogeographical regions, biodiversity hotspots and areas of endemism. Scientific Reports, 9:12991, https://doi.org/10.1038/s41598-019-49417-1.
20. Paparisto, K., Demiri, M., Mitrushi, I. & Qosja, Xh. (1988). Flora e Shqipërisë, 1. Tiranë.
21. Petrova, A., Vladimirov, V. (2010). Balkan endemics in the Bulgarian flora. Phytologia Balcanica, 16 (2): 293-311.
22. Qosja, Xh., Paparisto, K., Demiri, I., Vangjeli, J. & Balza, E. (1992). Flora e Shqipërisë, 2. Tiranë.
23. Qosja, Xh., Vangelji, J. & Ruci, B. (1996). Flora e Shqipërisë, 3. Tiranë.
24. Ranđelović, V.N., Zlatković, B.K., Milosavljević, V.N., Ranđelović, N.V. (2008). The endemic flora of Bosilegrad surroundings (Krajište region) in SE Serbia. Phytologia Balcanica, 14 (3), p. 367-375.
25. Raunkiaer, C. (1934). The Life forms of plants and statistical plant geography, Oxford, Clarendon Press.
26. Shuka, L., Mullaj, A., Hoda, P., Kashta, L., Miho, A. (2018). Overview of the flora and vegetation of the Albanian Alps - the degree of conservation and threats. 37th EADSVE Meeting - Prizren (Kosovo), 13–16 July, Book of Abstracts, p. 18.
27. Tomović, G., Niketić, M., Lakušić, D., Randelović, V., Stevanović, V. (2014). Balkan endemic plants in Central Serbia and Kosovo regions: distribution patterns, ecological characteristics, and centres of diversity. Botanical Journal of the Linnean Society, 2014, 176: 173–202.
28. Vangjeli, J. (2003). Udhëheqës fushor i florës së Shqipërisë, Akademia e Shkencave, Tiranë.
29. Vangjeli, J. (2015). Excursion flora of Albania, Koeltz Scientific Books, Königstein.
30. Vangjeli, J. (2017). Flora Albanica Atlas. Vol. 1, Pteridophyta-Apiaceae, Koeltz Botanical Books, Schmitten-Obereifenberg.
31. Vangjeli, J., Ruci, B., Mullaj, A., Paparisto, K., Qosja, XH. (2000). Flora e Shqipërisë, 4. Tiranë.
32. Vuksanović, S., Tomović, G., Niketić, M., Stevanović, V. (2016). Balkan endemic vascular plants of Montenegro – critical inventory with chorological and life-form analyses. Willdenowia 46, p. 387 – 397.
33. Zahariev, D. (2016). Biodiversity of Relict Vascular Plants in Bulgaria. International Journal of Research Studies in Biosciences, Volume 4, Issue 1, p. 38-51.